NASA CONTRACTOR REPORT 145249

AERONAUTICAL REPORT 77-2

AN ANALYTICAL MODEL FOR HIGHLY SEPARATED FLOW ON AIRFOILS AT LOW SPEEDS

GLEN W. ZUMWALT AND SHARAD N. NAIK
DEPARTMENT OF AERONAUTICAL ENGINEERING
WICHITA STATE UNIVERSITY
WICHITA, KANSAS

FINAL REPORT
TO
NATIONAL AERONAUTICS AND SPACE ADMINISTRATION
LANGLEY RESEARCH CENTER
HAMPTON, VIRGINIA
GRANT NSG 1192
MAY 1, 1977

ACKNOWLEDGEMENTS

This work consists largely of the doctoral dissertation of Mr. Sharad N. Naik at Wichita State University. This was carried out under the guidance of Prof. Glen W. Zumwalt, who proposed the basic model. Financial support was provided by the National Aeronautics and Space Administration on Grant NSG 1192. The Grant was monitored by Dr. Harry L. Morgan of the NASA Langley Research Center. Mr. P. K. Pierpont of the Langley Center aided in the oversight and procurement of the Grant.

Parallel NASA-supported work at WSU under the direction of Dr. William H. Wentz and Dr. H. C. Seetharam provided experimental data for testing the accuracy of the model and its computed results. Their assistance and suggestions are acknowledged with thanks. Prof. John O'Loughlin of the WSU Computing Center provided much appreciated council and assistance.

Mr. Lloyd Gross of the McDonnell-Douglas Aircraft Company, St. Louis, was instrumental in obtaining permission for the MDAC Mixed Boundary Condition computer program to be made available for this work. His help and the willingness of the McDonnell-Douglas company to share this resource are gratefully acknowledged.

ABSTRACT

A computer program has been developed to solve the low speed flow around airfoils with highly separated flow. A new flow model, which was suggested by Zumwalt , included all of the major physical features in the separated region. It was suggested by experimental airfoil studies made in the WSU low speed wind tunnel. Flow visualization tests also were made which gave substantiation to the validity of the model.

The computation involves the matching of the potential flow, boundary layer and flows in the separated regions.

The potential flow program was available from the McDonnell-Douglas company. Head's entrainment theory was used for boundary layer calculations and Korst's jet mixing analysis was used in the separated regions. A free stagnation point aft of the airfoil and a standing vortex in the separated region were modelled and computed. The separation location and pressure were found iteratively without a priori specification.

A GA(W)-1, 17% thick airfoil, at three angles of attack and two Reynold's numbers, was used for the analysis since experimental data were available. The surface pressures resulting from the computation matched very well with experimental data. In particular, separation locations and pressures were nearly identical with experimental values.

TABLE OF CONTENTS

LIST OF SYMBOLS

b	Refers to the actual separating streamline in jet mixing analysis
C_F	Local skin friction coefficient
C_p	$\frac{P-P_\infty}{q_\infty}$, pressure coefficient
Cp_R	Pressure coefficient of rear stagnation point
C	$\frac{u_e}{2Cp_pT_o}$, Crocco number
F	Entrainment parameter (Head's boundary layer analysis)
H	$\frac{\delta^*}{\theta}$, boundary layer shape factor for two-dimensional flow
H_1	$\frac{(\delta-\delta^*)}{\theta}$, modified shape factor
I_{1S}	Mass flow integral for S streamline
I_{1R}	Mass flow integral for R streamline
ℓ	Distance from separation point in free shear layer
M	Mach number
$\dot{M}$	Mass flow rate
P	Pressure
Q	Height for the reverse mass flow in separation bubble
q	$\frac{1}{2}\rho_\infty u_\infty^2$, dynamic pressure
RN	Reynolds number
R_θ	Reynolds number based on boundary
R	Streamline stagnating at the rear stagnation point in the bubble
S	Discriminating streamline of the jet mixing theory
u	Velocity
x	streamwise coordinate in % chord

z Transverse coordinate in % chord

Δ Mass flow thickness (boundary layer analysis)

δ Boundary layer thickness

δ^* $\int_0^\delta (1 - \frac{u}{u_e})dz$, boundary layer displacement thickness

η $\frac{z\sigma}{x}$, dimensionless height in the jet mixing region

θ $\int_0^\delta \frac{u}{u_e} (1 - \frac{u}{u_e})dz$, boundary layer momentum thickness

ρ Density

σ Goëtler's spreading rate parameter

ϕ $\frac{u}{u_e}$, dimensionless velocity in the jet mixing region

Subscripts

C Camber of airfoil

e Flow at outer edge of boundary layer or shear layer

L Lower surface of airfoil

o Virtual origin

r The reverse flow condition in the bubble

s The discriminating streamline

T.E. Trailing edge

T Thickness of airfoil

U Upper surface of airfoil

SEP Separation point

Superscripts

' Indicates conditions on the lower side of the airfoil

LIST OF FIGURES

22. Typical Plot Showing Bubble Mass Flow Convergence (Convergence 4).

23. Separation C_p Variation and Convergence.

24. Velocity Profile in the Separation Bubble on the Upper Surface.

25. GA(W)-1 Airfoil at $\alpha = 18.4°$ Showing Separation Streamlines, $M_\infty = 0.16$, $RN = 2.5 \times 10^6$.

26. Pressure Distributions, GA(W)-1 Airfoil, $\alpha = 18.4°$, $RN = 2.5 \times 10^6$, $M_\infty = 0.16$.

27. Pressure Distributions, GA(W)-1 Airfoil, $\alpha = 16.4°$, $RN = 2.5 \times 10^6$, $M_\infty = 0.16$.

28. Pressure Distributions, GA(W)-1 Airfoil, $\alpha = 14.4°$, $RN = 2.5 \times 10^6$, $M_\infty = 0.16$.

29. Typical H-distribution on upper surface, GA(W)-1 airfoil $\alpha = 18.4$, RN=2.5x10, M=0.16.

30. Typical displacement thickness distribution, GA(W)-1 airfoil $\alpha = 18.4$, RN=2.5x10, M=0.16.

Table 1: Results of present analysis and available experimental data.

Table 2: Typical convergence history.

I. INTRODUCTION

Separated flow behind wings has been of interest to researchers from the time it was first discovered that it causes stalling of aircraft. The complex nature of the problem hindered the analysts in obtaining a solution to the problem of separation because solving the Navier Stokes Equation was an insurmountable task before high speed computers were available. As technology improved, making possible short take offs and landings, separated flow research gained more importance. Research in the past has been mainly experimental due to the complexity involved in theoretical analysis. However, with the advent of modern computers it has been possible in principle to solve Navier Stokes Equations, but with the available memory and speed the cost of analysis has been prohibitive. Several mathematical models have been proposed and solved by computers which did not involve a complete solution of the Navier Stokes Equation, but used simplified boundary layer methods for the viscous flow, some empirical relations, and a few assumptions. Most of the models hitherto proposed have considered the separated region either as extending to infinity or as a bulbous region. The specific details in the separated region have not been considered. Axisymmetric separated flow analysis is available but is not applicable to the highly unsymmetric separated region behind an airfoil at high angles of attack.

The present separated flow model was suggested by Zumwalt (Ref. 1) based on experimental measurements of separated flow on a GA(W)-1 airfoil in the WSU 7' x 10' subsonic wind tunnel. It takes into account the details in the separated region. The velocity field pattern predicted by this model closely matched the experimental measurements thus

providing a basis for the validity of the model. Flow visualization studies of the separated flow behind an airfoil gave qualitative substantiation.

The analysis involves a computer solution for low velocity flow around and behind an airfoil with massive separation. It required first an invisicid flow analysis, and second a matching with all possible viscous interactions.

Typical of successful computation programs for attached flow on airfoils are References 6 and 7. Ref. 6 is the direct method where specified geometry produces pressure distribution, and Ref. 7 is the inverse method where specified pressure distribution gives geometry. The McDonnell-Douglas Mixed Boundary Condition (Ref. 3) program will permit one to either (a) supply the surface profile and obtain the adjacent flow conditions or (b) supply the pressure of a streamline and obtain the streamline location. This provides a single method for treating both attached and separated flows.

Separated flow occurs when the flow leaves the surface of the airfoil due to an adverse pressure gradient. The location of the separation point plays the important role of dividing the flow regimes. It is a point of zero surface shear and is dependent on the pressure gradient, angle of attack and the nature of the boundary layer.

Several investigators have developed criteria to predict the separation point using analytical and empirical methods. Reference (4) has described some of these methods and evaluated the methods by comparison with experiment. There is no agreement among the different methods and all of them draw from experimental data in order to be able to predict the separation point. Predictions were also dependent on

the method used for boundary layer calculations and the method of using experimental data for the empirical evaluation. Thus it is clear that there is still some confusion in the empirical methods for predicting separation.

The shape factor H ($H = \delta^*/\theta$) has been used as a guide for determining the separation point. Earlier investigators have successfully used this method for prescribing separation, and in the present analysis, separation is specified by prescribing a value of the shape factor, H.

The existence of two kinds of flow, namely laminar and turbulent, necessitates the distinction between laminar separation and turbulent separation. Airfoil separation has been classified into three categories by McCullough and Gault (Ref. 5).

(1) Trailing edge separation. This is essentially a turbulent separation at the trailing edge moving upstream with angle of attack increase. The turbulent separation can either be preceded by transition from laminar to turbulent or by a laminar separation and with turbulent reattachment. The latter is the case of a short bubble with transition.

(2) Leading edge separation: laminar flow separation near the leading edge without any reattachment.

(3) Thin airfoil separation: laminar flow separation near the leading edge with flow reattachment (long bubble) at a point which moves downstream with increase of angle of attack.

The present analysis assumes that the flow is turbulent very near the leading edge and thus considers only turbulent separation. Laminar separation is not included since it makes the analysis more complicated

and is unlikely in practical low speed aircraft wings. Also, the main object was to analyze the flow model with attention to the details in the separated region. The flow is assumed to be steady, incompressible and two-dimensional.

Head's entrainment method was adopted to calculate the turbulent boundary layer characteristics and the separation point and was used in an iterative interaction with the inviscid flow solution, until convergence was achieved.

Korst's separated flow analysis was used to map the flow from separation point to the trailing edge station of the airfoil for the upper surface. Mass flows into and out of the separated region behind the airfoil is also determined by the above analysis and from boundary layer theory.

The two separated flows, namely the top surface separated flow and the bottom surface separated flow, and the free stagnation point at which they meet formed the separation bubble behind the airfoil.

The free stagnation point behind the airfoil was located at a distance of a third of the distance between the separation point and the trailing edge from the trailing edge. This was an assumption based on the WSU experimental measurements (Ref. 2). The vertical position of the free stagnation point was not fixed.

The details of flow in the separation bubble circulatory flow was determined by velocity distributions of Korst's model and an assumed profile for the reversed flow based on experimental data.

A computer program has been developed to solve the separated flow model on a two dimensional airfoil for incompressible subsonic flow. It determines the pressure distributions on the airfoil and maps the separated

flow region. It uses the McDonnell-Douglas potential flow program for the inviscid analysis, Head's entrainment method and Korst's separated flow model for the viscous flow and the separated region respectively. The conditions to be satisfied for a valid solution are discussed in detail in Chapter III.

Flow visualization experiments were made for a qualitative observation of the flow details in the separated region and they generally indicated that the assumptions in the flow model were realistic.

The computer program was used to calculate the pressure distribution around a 17% thick GA(W)-1 wing (Fig. 1) at three angles of attack. The results were compared to experimental data to verify the model and computational method.

This research was conducted under a grant from NASA Langley Research Center; Grant No. NSG 1192.

II. PREVIOUS RELATED WORK

The analysis of separated flow on airfoils has been approached in two ways: one, by a numerical solution of the complete Navier Stokes equations, and the other by assuming a physical model for the separated region and then solving for the mathematical solution.

Numerical solution of Navier Stokes equations for separated flow has been attempted by Thames et al (Refs. 8) on arbitrary airfoils. The analysis reported is only for laminar flow and for very low Reynolds number. Fig. 2 shows a typical streamline pattern obtained by this method of separated flow on an airfoil. Higher Reynolds number analysis will require prohibitive length of computer times. Turbulent modelling in separated regions is the most important aspect of separated flow and this is not achieved in this method.

Jacob's (Refs. 9,10,12) idea (Fig. 3) of using a source or source distribution in the aft region of the airfoil to form the separated region has been adopted by a number of researchers with modifications. Hahn et al, Bhately and Mcwhirter, Farn et al, are some who have reported analyses based on this idea (Refs. 4, 11,13). The main differences in all these models are in their methods of finding the source distributions which satisfies the boundary conditions and of choosing the location of the separation point and pressure.

In all these models the separated region is considered to extend to infinity which is quite contrary to experimental observations. Jacob (1975) proposed a model recently which closes the region by using a sink at a point downstream of the trailing edge (see Fig. 6). The details and some of the results are shown in Figs. 4 and 5.

Extension of a conventional boundary layer analysis into the separated region has also been attempted (Refs. 14,15) for the representation of separated flow. But, as one can see, the credibility of the boundary layer assumptions are lost when the boundary layer thickness becomes very large.

In addition, the available methods for separated flow analyses have not considered the effect of reverse flow on the pressure distribution of the airfoil. The separation pressure or its location has been assumed.

Based on experimental investigations (Figs. 7,8,9,10) in the 7' x 10' WSU low speed wind tunnel (Ref. 2), a model will now be presented which takes into account more details in the separated region. One of the key factors not considered in the earlier models is the mass recirculated in the separation bubble.

III. DESCRIPTION OF THE FLOW MODEL

A sketch of the flow model is shown in Fig. 11. The flow has separated from the upper surface and leaves the lower surface at the trailing edge. The jet mixing sheets starting from the two airfoil separation points coalesce to form the separation bubble behind the airfoil. These two jets entrain air from the dead air region (near-wake). The entrained air has to be replaced by backflow of air which must be supplied from somewhere. If S and S' (Fig. 11) are the two separation streamlines, it can be seen that the amount and width of flow entrained are growing in the downstream direction, consequently, the space for backflow decreases and the demand for it increases. Since this cannot continue very far, a termination is required of the near wake recirculation region, and a stagnation point is formed. At this point the two streams rejoin defining the end of the separation bubble. This near wake free stagnation point is termed a "saddle point" since pressure distribution resembles a saddle.

The entrained masses of the two jets are not the same since their lengths and velocities are different. Generally, the upper one will entrain a larger mass. Therefore the stagnating streamlines are not necessarily S and S' at the saddle point.

Details of the separated regions are shown in Fig. 12. It shows two other streamlines R and R' stagnating at the saddle point providing passages for the flow to enter and leave the separation bubble. The mass flow through the corridor between R and S should be the same as between R' and S'. Further, R and R' do not terminate at the saddle point but must continue upstream and downstream. The required mass

conservation in the region requires the formation of two bubbles and an S-shaped corridor. Based on experimental data, constant pressure is assumed in the whole region except in the neighborhood of the saddle point, where a high pressure wedge will form along the RR' line and extend into the recirculating regions, turning back the low velocity flows.

Analysis of flow in the separated region would require a nearly constant pressure along S and S' in order to be able to apply turbulent jet mixing analyses for constant pressure regions. Experimental data have indicated that this is true on the upper surface but not in the vicinity of the saddle point.

Viscous effects can be ignored in the neighborhood of the saddle point and all velocity changes considered as being due to the pressure gradients. Thus the region is divided into viscous dominated and pressure dominated regions. This follows the classical approach originated by Prandtl for boundary layers and more recently applied successfully to separated and reattaching flows in the Chapman-Korst (Ref. 12) mixing models.

The jet mixing theory is required for computation of turbulent mixing entrainment rates. The Göertler exchange coefficient model, as adapted by Korst, was considered to be best for a first attempt due to its successful application to other plane flow problems and the availability of mass and momentum integral tables for these flows.

The trailing edge plane is assumed to divide the constant pressure region of the separated flow and the region of pressure rise to the near stagnation point. This plane is also the location for satisfying the mass continuity.

Fig. 18 shows a schematic diagram of the velocity profile at the trailing edge of the airfoil. The velocity profile consists of three segments:

(1) The error function profile of the upper high velocity flow.

(2) A constant velocity reverse flow region.

(3) A third degree parabola to join (1) and (2).

The Korst profile is adopted until the point where the velocity is half the value at the outer edge of the shear flow. The parabola matches slopes and velocity at the other two flow segments. The matching location for the reversed flow is chosen from experimental data, as will be explained in Chapter V.

The complete solution of a wing requires the mating of the separated region to the potential flow and boundary layer flow.

IV. EXPLORATORY EXPERIMENTS

A. ELECTRICAL ANALOGY

An electric conducting table analogy experiment was attempted initially in the hope that it would indicate the conditions required for the formation of the separated region with a potential flow model and that it would also aid parameter selection for the computer program. A GA(W)-1, 13% thick, 10 inch chord airfoil was used for this purpose. Fig. 13 shows the apparatus. It consists of the conducting paper laid flat on a table with the silver-paint airfoil in the center of the paper. The ends of the paper are firmly held by conducting rods or angle sections. The airfoil is oriented on the paper such that the streamlines are parallel to the conducting rods. Electrical leads buried in the paint are connected to a potentiometer to vary the voltage of the airfoil.

The model simulation was attempted by placing circular brass discs of ¼ inch diameter at positions where the vortices were predicted. The voltages in the airfoil and the two discs were varied to represent various values of circulation. The flow was simulated by reducing the voltage of the airfoil so that the trailing edge stagnation streamline was displaced and formed on the upper surface of the airfoil. This corresponds to the reduction of circulation on the airfoil. The voltage of the disc near the airfoil was then adjusted so that the streamlines very near the lower surface were diverted to form the S-shape as represented in the model. Fig. 14 shows the streamline shapes resulting in the electric analog. This indicated that vortices can be used in the computer

program to form the separated region but the separation cannot be simulated satisfactorily for the potential flow model, but rather a boundary layer must be included in the attached flow program. The usable result from this experiment turned out to be the fact that small movements of the downstream saddle point did not change the flow pattern appreciably. This was an important assumption made in the computer program since the vertical position of the saddle point is not specified. The idea of using vortices to form the separated region was abandoned after it was known that the potential flow program to be used in the analysis could provide the displacement surface of the separated flow.

B. FLOW VISUALIZATION STUDIES

Flow visualization experiments were conducted in a small, 6" x 14", low speed wind tunnel at a Reynolds number of 0.3×10^6. A 10 inch chord, two-dimensional, GA(W)-1 wing was used. The wing was held at a fixed angle of attack, supported by the sides of the tunnel. A thin aluminum plate was mounted vertically on the wing at midspan so that it was parallel to the flow. The plate was smeared with a mixture of lampblack and kerosene. A few flow photographs are shown in Figs. 15 and 16. The main observations are as follows:

(1) The wake closes behind the airfoil to form a bubble shaped region with the free stagnation point very close to the trailing edge as the earlier measurements of Ref. 2 had indicated.

(2) The recirculating flow in the near wake forms a fairly large unsymmetric vortex which is clearly seen in the photographs.

(3) There is an upward flow from the lower wake of the airfoil flowing upstream in separation bubble and turning back to join the

main stream. This S-shaped, lower-to-upper flow may not be clearly visible in the photographs, but was easily detected during the tests.

The flow visualization tests confirmed that the assumed features in the model were present and thus substantiated the validity of the present model.

V. DESCRIPTION OF ANALYSIS OF THE FLOW

The analysis of separated flow over an airfoil has been divided into two sections, an outside problem and an inside problem, each of which is solved separately, then matched for a complete solution. Fig. 17 shows the geometry of the outside problem. Velocities and pressures along the attached-flow surfaces of the airfoil were calculated by a computer program adapted from the McDonnell-Douglas Mixed Boundary Condition program. A boundary layer computation was made along the surface to indicate the separation point and provide the displacement thickness. These were iterated until the solutions became stable. The pressure of the separated region was assumed to be equal to separation point pressure from the separation point to the airfoil trailing edge. A parabolic increase to the free stagnation point pressure from the trailing edge pressure was assumed.

The separation point location was determined by the boundary layer routine. Fig. 18 shows the inside problem. The Korst jet mixing analysis was used to determine the mass entrained from the separated region by the upper surface jet sheet. The two stagnating streamlines, R' and R, and the rear free stagnation point pressure were determined from a balance of the mass inflow and mass outflow of the separation bubble. The mass inflow into the separation bubble from the lower surface of the airfoil was calculated by using a power law velocity profile for the turbulent boundary layer at the trailing edge station.

A. POTENTIAL FLOW SOLUTION

The Mixed Boundary Condition flow program of McDonnell-Douglas Company (MCAIR) (Ref. 3) is a modification of the wing body analysis

program developed by Woodward (Ref. 18). The configuration of the airfoil is divided into a number of panels on the chordline. The effects of thickness, camber and the angle of attack are represented by planar source and vortex singularities. The boundary condition, the Neuman and the Kutta conditions determine the strengths of the source and vortex singularities. They form a system of linear equations which are then solved for the singularity strengths. The program allows the specified boundary conditions to be given either as surface geometry or surface pressure distributions. The equations are solved by a routine using Gauss elimination to obtain the pressure distributions and surface configuration of the airfoil and the separation bubble. The present analyses are made on a GA(W)-1 general aviation airfoil (Ref. 19).

The geometry conditions required by the program are the slope of the camberline and the slope of the airfoil thickness distribution. In the present case, the airfoil geometry was known. In a more general case only the airfoil thickness distribution and the camberline are specified at a number of points on the chordline. A subroutine in the program prepares the geometric boundary conditions in the required form and at required stages of the program. The Neuman condition requires that the velocity be tangent to the surface, implying no flow across the physical boundaries. The Kutta condition determines the unique circulation around the airfoil. This is satisfied by specifying upper and lower pressures to be equal at the trailing edge. This enables Kutta condition to be satisfied for airfoils with blunt trailing edges as in the present case. However, when separation is present, the point at which the Kutta condition is to be applied is generally not clear. In the present case it is satisfied by specifying the same pressures for

the separation point and the lower surface trailing edge point. The points at which the singularities are applied are important since when discrete singularities are applied on finite sized panels there is a mathematical singularity at each edge of the panels and the velocity or pressure calculated is erroneous. This problem is avoided by applying the boundary conditions for the vortex singularity at an intermediate point and choosing this "control point" in such a way that the resulting solution at this point is as near as possible to the correct one. The optimum control point in the present case is at 85% of the panel length, as suggested in Ref. 3. The accuracy of the overall solution will depend upon the size and number of panels. An improvement is seen if the control point corresponds as closely to the trailing edge as possible. But on account of numerical instability there can be no sharp disparity in adjacent panels. Hence, a trade-off is established between the accuracy and the cost of calculation. Similarly, the nose region should also be represented by a larger number of smaller panels on account of its high curvature. The panel length, in the leading and trailing edge portions were chosen to be 1% of the chord, and the lengths increased to 5% in the center of the airfoil. The panels in the near wake were also 1% long.

B. BOUNDARY LAYER ANALYSIS

Viscous flow interactions are introduced by adding the displacement thickness of the boundary layer to the original airfoil shape. The new pressure distribution on the augmented airfoil is then determined by the potential flow program. The boundary layer characteristics of the augmented airfoil give a new value of displacement thickness.

This is again added to the original airfoil and the iterative process is continued until the pressure distribution settles down to within 0.01.

When separation occurs on the top surface, the iterations are continued only up to the separation point. Since the potential flow program also provides the separation streamline, the displacement thickness at the separation point is added to the ordinates of the separation streamline up to the trailing edge to obtain the displacement surface. A parabolic pressure distribution was assumed for the region after the trailing edge up to the rear stagnation point for both the upper and lower surfaces. To start the iteration, a value for the rear stagnation pressure was assumed.

Since the objective of the project was to show the feasibility of the mathematical model, sophisticated boundary layer analysis was not used. Instead, the flow was assumed to be turbulent from the leading edge. The momentum integral method was used because of its simplicity and adaptability to iterative calculations.

Head's entrainment method (Ref. 20) of calculating the turbulent boundary layer characteristics was chosen as being sufficiently accurate without undue complexity.

The momentum integral equation for incompressible, two-dimensional flow in the integral form is:

$$\frac{d\theta}{dx} = \frac{C_f}{2} - \frac{\theta}{u_e}\frac{du_e}{dx}(H + 2) \qquad 2.1$$

where

θ = Momentum thickness of the boundary layer

C_f = Skin friction coefficient

u_e = Velocity at the edge of the boundary layer

H = Shape factor = δ^*/θ

δ^* = Displacement thickness

Head introduced the concept of the mass entrainment to the boundary layer. He argued that the rate of change of mass within the boundary layer was a unique function of the velocity defect. He derived a method for calculating simultaneously the development of the momentum thickness θ and a quantity Δ which is referred to as the mass flow thickness.

$$\Delta = \int_0^{\delta} \frac{u}{u_e}\, dy = \delta - \delta^* \qquad 2.2$$

An auxiliary equation is obtained by considering the rate at which the turbulent boundary layer entrains fluid from the free stream.

$$\frac{d\Delta}{dx} = F - \frac{\Delta}{u_e}\frac{du_e}{dx} \qquad 2.3$$

The non-dimensional entrainment parameter F is a unique function of another shape factor, $H_1 = \Delta/\theta$. Head obtained empirical relationships for F and relations between H_1 and the familiar shape factor $H = \delta^*/\theta$.

$$F = 0.0306\,(H_1 - 3.0)^{-0.653} \qquad 2.4$$

$$H_1 = \frac{2H}{H-1} \qquad 2.5$$

Green (Ref. 20) obtained a linear relation for F by cross plotting in terms of H.

$$F = 0.025H - 0.022 \qquad 2.6$$

He also considered a relation between H and H_1 which was in better agreement with experiments.

$$H_1 = 3.3 + \frac{0.9}{(H-1)^{4/3}} \qquad 2.7$$

The auxiliary equation is simplified by writing equation 2.3 as

$$H_1 \frac{d\theta}{dx} = \theta \frac{dH_1}{dx} = F - H_1 \frac{\theta}{du} \frac{du_e}{dx}$$

Using the relation between H and H_1 (Eq. 2.5), the auxiliary equation becomes:

$$-\theta \frac{dH}{dx} = H (H^2 - 1) \frac{\theta}{u_e} \frac{du_e}{dx} + \frac{H-1}{2} \left[(H-1) F - Hc_f\right] \qquad 2.8$$

The momentum integral equation, together with the auxiliary equation and relations for the local skin friction provide a step-by-step method for calculating the development of an incompressible turbulent boundary layer. Two skin friction relations were considered, those of Felsch and Ludwig-Tillman. The two expressions are:

$$C_F = 0.246\ R_\theta^{-0.268}\ 10^{-0.678H} \quad \ldots \text{ Ludwig-Tillman}$$

$$C_F = 0.058\ (0.93 - 1.95 \log H)^{1.705}\ R_\theta^{-0.268} \quad \ldots \text{ Felsch}$$

Both have wide acceptance and when used in the present program gave very similar results. However, the Ludwig-Tillman expression seemed to amplify a numerical instability tendency at one point in the computation development, while the Felsch did not. Hence, the Felsch expression was retained.

C. SEPARATED FLOW

Based on the experience of other investigators, separation was assumed to have occurred when the value of H reached about 2 on the upper surface of the airfoil. Even though H values as large as 2.6 have been measured experimentally, the higher values of H and the rapid boundary layer growth produced large induced slopes at the panels causing severe instabilities in previous analyses (see Ref. 21). Although specification of an exact value of H for separation is not possible, most of the integral methods have assumed H from 1.8 to 2.4. Even though the range of H seems large, the separation location does not vary as much since close to separation the shape factor increases quickly.

1. Jet Mixing Analysis

Separation is assumed at the end of any panel in which it occurs. Korst's theory, developed for a constant pressure, turbulent mixing of an isoenergetic free jet, was adapted for the incompressible case here to model the flow on the upper surface from the separation point to the free stagnation point.

Korst assumed similar velocity profiles in the free shear layers for fully developed flows and proposed that the velocity profile could be modelled by

$$\phi = \frac{u}{u_e} = \frac{1}{2}\left[1 + \text{erf}\ (\sigma\frac{y}{\ell})\right] = \frac{1}{2}\ (1 + \text{erf}\eta)$$

where σ is the jet spreading rate parameter. A value of $\sigma = 12$ is well established for subsonic flow. For the viscous shear layer an intrinsic system of coordinates defined by the center of the mixing region (i.e., $y = 0$ at $u = \frac{1}{2}u_e$) creates a shift y_m, between intrinsic and inviscid coordinate systems. This shift is determined by the use of the streamwise momentum equation.

Equating the momenta below the e streamline (Fig. 21) for the two sections gives the shift y_m.

$$\dot{M} = \rho_e\ u_e^2\ y_e = \int_{-\infty}^{y_e} \rho u^2 dy$$

$$= \rho_e\ u_e^2\ \frac{\ell}{\sigma}\ (1 - c_e^2) \int_{-\infty}^{\eta_e} \frac{\phi^2}{1 - c_e^2\phi}\ d\eta$$

$$= \rho_e\ u_e^2\ \frac{\ell}{\sigma}\ (1 - c_e^2) I2_e$$

where y_e = edge of the shear layer, and $\eta = \sigma\cdot\frac{y}{x}$.

$$I2_e = \int_{-\infty}^{\eta_e} \frac{\phi^2}{1 - c_e^2\phi^2}\ d\eta$$

A jet boundary streamline (Fig. 19), S, which separates the mass originally flowing at the separation point from that entrained by jet mixing from the dead air region is found by equating the mass for the given velocity profile with that of undisturbed flow.

$$\dot{M} = \rho_e u_e (y_e - y_m) = \rho_e u_e^2 \frac{\ell}{\sigma} (\eta_e - \eta_m) = \int_{y_s}^{y_e} \rho u dy$$

$$= -\rho_e u_e \frac{\ell}{\sigma} (1 - c_e^2) (I_{1_e} - I_{1_s})$$

where $I_{1_e} = \int_{-\infty}^{\eta_e} \frac{\phi d\eta}{\Lambda - c_e^2 \phi^2}$ and $I_{1_s} = \int_{-\infty}^{\eta_s} \frac{\phi d\eta}{\Lambda - c_e^2 \phi^2}$

The mass flow integrals are tabulated for various values of ϕ ($\phi = u/u_e$) and c_e (Crocco Number). Thus the mass flow between any two streamlines in the mixing region could be obtained by taking the difference between two integrals corresponding to them and multiplying it by the appropriate variables of the flow.

The boundary layer at separation can be replaced by a jet mixing profile having the similar characteristics. This is done by locating a virtual origin for the mixing which gives the resulting jet mixing profile which is the same as those of the actual boundary layer. The virtual origin is displaced upstream of the separation point by x_0 and y_0 on the intrinsic coordinate system. This method was developed by Hill (Ref. 23). The details are shown in Fig. 19.

b: the actual streamline corresponding to the displacement surface from the separation point.

I: inviscid streamline for the Korst flow starting from (x_0, y_0). Note I and b are parallel.

x: intrinsic coordinate axis corresponding to a velocity of half the value in the inviscid stream adjacent to the dissipative region

S: streamline which separates the mass originally flowing at the separation point (or more precisely at the virtual origin) from that entrained from the dead air region.

The expressions for x_0 and y_0 are

$$x_0 = \frac{\sigma\theta}{(1 - c^2_e) I_{1_S}}$$

From (Ref. 23)

$$y_0 = \theta + \delta^*$$

where δ^* and θ are the displacement thickness and momentum thickness at the separation point,

and $$I_{1_S} = \int_{-\infty}^{\eta_S} \frac{\phi}{1 - c^2_e \phi^2} \, d\eta$$

or incompressible flow: $c_e^2 \to 0$.

$$x_0 = \frac{\sigma\theta}{I_{1_e}}$$

$$I_{1_s} = \int_{-\infty}^{\eta_s} \phi d\eta = \int_{-\infty}^{\eta_s} \frac{1}{2}(1 + \text{erf}\eta)d\eta$$

$$\phi_s = 0.61632 \quad \text{for} \quad c_e^2 = 0 \qquad \text{From (Ref. 24)}$$

From the tables of I_1 integrals we obtain:

$$I_{1_s} = 0.399$$

$$x_0 = \frac{12}{0.399}\Theta \simeq 30\theta$$

and

$$y_0 = \theta + \delta^*$$

2. Stagnation Streamline Determination

Initially a value for the rear stagnation pressure is assumed, based on experimental data, to start the calculations. This enables the determination of the two displacement surfaces from the upper and lower separation points. There is an upper limit to the choice of the reattachment pressure since it is the stagnation point for the flow inside the separation bubble. Referring to Fig. 19, the S streamline

which separates the primary mass from that entrained from the separated region will have the highest possible stagnation pressure in the separation bubble.

$$C_{P_S} = \frac{P_{O_S} - P_\infty}{q_\infty} = \frac{P_S + \frac{1}{2}\rho u_S^2 - P_\infty}{q_\infty}$$

$$= \frac{P_{SEP} - P_\infty}{q_\infty} + \frac{u_S^2}{u_\infty^2}\,\frac{u_e^2}{u_\infty^2}$$

$$C_{P_S} = C_{P_{SEP}} + \phi_S^2 \left(\frac{u_e}{u_\infty}\right)^2$$

$$C_{P_R} \leq C_{P_{SEP}} + \phi_S^2 \left(\frac{u_e}{u_\infty}\right)^2$$

Alternately, the choice can be based on the experimental value from Ref. 14. The initial value of C_{P_R} was taken as 0.0 to begin the calculations.

The mass leaving the separation bubble $\dot{M}_U$ is obtained by considering the flow between the S streamline and the R streamline, which stagnates at the stagnation point. The mass entering, $\dot{M}_L$, is obtained by considering the flow at the trailing edge between the lower surface of the airfoil and the stagnating streamline R', see Fig. 18.

From Korst's analysis:

$$\dot{M}_U = \frac{u_e x_{TE}}{\sigma}\,(I1_S - I1_R)$$

$$= u_e\,(100 - x_{SEP} + x_0)\,(I1_S - I1_R)/\sigma$$

$I1_R$ and $I1_S$ can be found from the tables for known values of ϕ_R and ϕ_S. Since the proper ϕ_R is determined by iterating the mass flows entering

and leaving the separation bubble, a parabolic fit for I_{1_R} as a function of ϕ_R for a working range of n values was determined from the mass flow tables. The expression is:

$$I_{1_R} = 0.11402 - 0.20457\ \phi_R + 0.0817\ \phi_R^2$$

Values calculated by this expression matched within 0.03% for the range $n = 0$ to $n = n_S$.

$\dot{M}_L$ is calculated from boundary theory, as follows. Here, the prime indicates lower side conditions.

$$\frac{\dot{M}_L}{\rho} = \int_0^{z'_R} u'dz'. = u'_e\delta' \int_0^{z'_{R/\delta'}} \left(\frac{u'}{u'_e}\right) d\left(\frac{z'}{\delta'}\right)$$

Assuming a power law for the boundary layer profile:

$$\frac{u'}{u'_e} = \left(\frac{z'}{\delta'}\right)^{1/n}$$

$$u'\delta^{*'} = \int_0^{\delta} (u'_e - u')dz' = u'_e\delta' \int_0^1 (1 - \phi')d\left(\frac{z'}{\delta'}\right)$$

$$= u'_e\delta' \int_0^1 \left(1 - \frac{z'}{\delta'}\right)^{1/n} d\left(\frac{z'}{\delta'}\right)$$

$$\frac{\delta^*}{\delta'} = \left(1 - \frac{n}{n+1}\right) = \frac{1}{n+1}$$

Now

$$u'^2_e\theta' = \int_0^{\delta} u'(u'_e - u')dz = u_e{}^2\delta' \int_0^1 [\phi' - (\phi')^2]d\left(\frac{z'}{\delta'}\right)$$

$$\frac{\theta'}{\delta'} = \frac{n}{(n+1)(n+2)}$$

A relationship between the shape factor H' and n can be determined:

$$H' = \frac{\delta^{*'}}{\Theta'} = \frac{\frac{1}{n+1}}{\frac{n}{(n+1)(n+2)}} = \frac{n+2}{n}$$

$$n = \frac{2}{H' - 1}$$

For known values of H', n can be found.

Hence $\dot{M}_L$ is calculated as:

$$\frac{\dot{M}_L}{\rho} = u'_e \delta' \int_0^{z'_{R/\delta'}} \left(\frac{z'}{\delta'}\right)^{1/n} d\left(\frac{z'}{\delta'}\right)$$

$$\delta' = \delta'^{*}(n + 1)$$

$$u'_e(n + 1)\delta^{*'} \int_0^{z'_{R'/\delta^{*'}}} \left(\frac{z}{(n+1)\delta^{*'}}\right)^{1/n} d\left(\frac{z}{(n+1)\delta^{*'}}\right)$$

$$\frac{\dot{M}_L}{\rho} = u'_e \delta^{*'} \left(\phi'_{T.E.}\right)^{n+1} \left(\frac{n}{n+1}\right)(n+1)^{-1/n}$$

where $$n = \frac{2}{H' - 1}$$

Since the streamlines R and R' stagnate at the same point from the same static pressure, their velocities must be equal:

$$u_R = u'_R$$

The value of u_R is iterated until $\dot{M}_U = \dot{M}_L$.

3. Recirculating Mass Balance

The mass balance for the separation bubble is calculated at the 99.85% chord station, which is the control point of the last airfoil panel. The velocity profile is made up of four segments, Figure 24:

a) From the R streamline to the $u = 0.5\ u_e$ streamline, the error function jet mixing profile is used. Thus the upper half of the ordinary free jet profile is retained.

b) Experiments show a constant-velocity reverse flow, u_r, (i.e., forward on the airfoil) region. This is assumed to exist from the inside of the error function profile (defined as $u \approx 0.01$ or $\eta = -2$) to the augumented airfoil surface. The value of this reverse flow velocity will be discussed later.

c) Between (a) and (b), a third degree parabola is placed which matches values of slopes of both the (a) and (b) profiles.

d) The airfoil upper surface is augumented by the displacement thickness of the lower surface trailing edge. This pictures the boundary layer as swirling almost unchanged around a small separated bubble at the trailing edge.

Since the evidence for a constant-velocity reverse flow profile is great, no logical and simple model can be suggested to give a"core" flow from reversal of shear flows. A purely empirical choice was accepted as necessary and a value of $u_r = 0.2\ u_e$, was derived from examination of several GA(W) wing flow measurements. The sensitivity of the results to this choice will be discussed later.

$$\dot{M}_{STREAMWISE} = \frac{u_{SEP} x_{TE}}{\sigma} \left(I_{1_S} - I_{\eta=0}\right) + \int_{\eta_0}^{\eta=0} u \cdot dz$$

$$\dot{M}_{REVERSE} = \int_{\eta=-2}^{\eta_0} u\,dz + \frac{u_r}{u_{SEP}} \cdot Q \cdot u_{SEP}$$

where n_0 = value of n for $u = 0$.

The mass balance in the recirculating region was achieved by changing the value of the shape factor H for separation and iterating until convergence is reached. The pressure distribution corresponding to this condition was accepted as the solution of the analysis.

D. ASSUMPTIONS IN THE PRESENT ANALYSIS

1. The flow is assumed to be incompressible and steady
2. The boundary layer is fully turbulent.
3. The rear stagnation point location is assumed at a chordwise distance of one-third the distance from the separation point on the upper surface to the trailing edge. This was based on the experimental results of Ref. 2.
4. The rear stagnation point pressure coefficient value assumed to start the calculations. This was also based on the experimental data of Ref. 2. This value is, of course, replaced to form convergence 2.
5. A constant 'core' velocity of the reverse flow in the separation bubble equal to a value of 0.2 times that of the velocity at the edge of the shear layer.

VI. DESCRIPTION OF THE COMPUTER PROGRAM

The program is titled "SEPFLO" and is coded in fortran language to operate on the IBM 360 or other compatable models. It is divided into three main sections, namely, the potential flow, the boundary layer and the separated region.

The potential flow part was adapted from the McDonnell Douglas Aircraft Company's Mixed Boundary Condition Program (Ref. 3) developed from the earlier program of Reference 18. The McDonnell Douglas program is still a proprietary item and hence it will not be discussed in detail here. Henceforth it will be referred to as the "Potential flow program".

The main program controls all the three sections of the program . The potential flow part uses six subroutines to determine the pressure distributions and the airfoil shape, including the separated streamlines. The viscous flow routine 'BLAYR' calls for three subroutines 'CONV','AFSL' and 'LEASQ' to determine the boundary layer displacement thickness δ^*, momentum thickness and the shape factor H. It also calculates the shape of the augumented airfoil by adding the displacement to the original airfoil shape.

The separated flow region calculations are included in the main program. This part determines the rear stagnation pressure and the bubble mass flows in conjunction with 'Potential flow program' and'BLAYR'.

A. INPUTS

The program input sequence is as follows:

1. Main parameters of the program : The panel details and all the required flow parameters.

2. The station distances for the ordinates of the airfoil.

3. The airfoil thickness distribution; defined as $Z_T = \frac{(Z_U - Z_L)}{2}$

where Z_U and Z_L are the upper and lower co-ordinates from the mid-section line at the given airfoil stations.

4. The airfoil camber distributions; defined as $Z_C = \frac{(Z_U + Z_L)}{2}$

5. The panel widths for the whole range.

6. The slopes of the upper surface of the deflected airfoil at the control points, calculated by a separate program from co-ordinates and .

7. The slopes of the lower surface of the deflected airfoil at the control points, calculated as in 6.

8. Specified pressures for points after the separation point if a separation point is assumed to start the calculations.

9. The angle of attack of the airfoil.

B. OPERATION

A diagram of the computer logic flow is shown in Fig. 20. The 'Potential flow program' prepares the airfoil for the solution by locating the panels and the control points. The source distribution and the vorticies are placed on the panels and at control points respectively. The solving of the simultaneous equations to determine the vortex strengths is performed by a standard IBM subroutine 'SIMEQ', which uses the Gauss elimination method. The output from the 'Potential flow program' is in the form of pressure coefficients at the control points and the new ordinates at the panel beginning points. The velocity distribution and the airfoil coordinates are used as inputs to 'BLAYR' for the determination of the boundary layer characteristics and the augumented airfoil.

The calculations are done separately for the upper and lower surfaces. Since the ordinates of the airfoil are obtained at panel beginning points and the velocities are calculated at panel control points, subroutine 'CONV' converts the ordinates to the panel control points by a three point parabolic interpolation.

The boundary layer displacement thickness determined by Head's entrainment method is added to the previous ordinates of the airfoil at the control points.

The separation location is determined by comparing the values of H with a specified H_{SEP} value. The control point at which H first exceeds H_{SEP} is taken as the separation point at which separation will occur. The program is designed, however, to move the separation point only one panel at a time to avoid numerical instabilities. This is continued until the assumed separation point reaches the true separation point determined by the H distribution. The separation point is moved downstream if the H distribution fails to reach the specified value of H_{SEP}. This allows free movement of the separation point depending on the pressure distribution.

The separation point location determines the separation pressure, which is the value of the pressure coefficient at the separation location chosen from the previous pressure distribution on the airfoil. The pressure on the trailing edge panel control point station is also set to the separation pressure to satisfy the Kutta condition.

The boundary conditions are rearranged by specifying the separation pressure for the upper surface panels downstream of the separation panel up to the last panel on the airfoil(i.e.,trailing edge panel) and a parabolic increase from the separation pressure to the rear stagnation

pressure on panels up to the last panel of the flow field. The panels downstream of the trailing edge station on the lower surface of the airfoil are also specified by the same parabolic increase. The boundary conditions on the remaining attached flow panels are specified by the new slopes. The new slopes are calculated by the subroutine'AFSL' from the augumented airfoil surface points by matching a three point parabola.

The potential flow routine now recalculates the new pressure distribution of the modified airfoil. This is continued iteratively until convergence is reached, i.e., the variation of the pressure is within 0.01. This is denoted by 'Convergence 1' (Fig. 21).

After achieving 'Convergence 1' the program now calculates the separated region conditions. The location of the virtual origin of jet mixing flow (x_0,y_0) and the mass flows entering and leaving the bubble are determined. The two mass flows $\dot{M}_U$ and $\dot{M}_L$ should be equal. Mass flow equality is acheived by iterating for the proper stagnating streamlines, R and R', of the reattachment point (see Fig. 18). This is denoted by 'Convergence 2'. The new rear stagnation pressure is used to recalculate the pressure distribution on the airfoil and the separated region. That is, we return to the potential flow and viscous routines. After 'Convergence 1' is again reached the new stagnation pressure is found by satisfying 'Convergence 2'. This is iteratively continued until the changes in the values of the reattachment pressure coefficient are within 0.001. This is designated by 'Convergence 3.'

The last step in the program is the calculation of the recirculating mass flow in the separation bubble. The streamwise flow and the reverse flow masses are calculated and,if not equal, the value of H_{sep}

is changed so that the separation point is moved upstream to create the changes necessary for the mass balance (see Fig. 21) .

This has to be iteratively continued until convergence is reached. This iteration involves all the other convergences (see Figs. 20 and 21). When this is reached the output corresponding to this iteration is the solution of the program.

C OUTPUT

The output from the computer are the following:

1. The panel positions.
2. Pressure distributions on both the upper and lower surfaces at the control points
3. The ordinates of the airfoil and the separation bubble at the panel beginning points
4. The position of the control points
5. The slopes of the upper and lower surfaces
6. Velocity distribution on the upper and lower surfaces at the control points

D. NUMERICAL INSTABILITIES AND THEIR REMEDIES IN THE OPERATION OF THE PROGRAM

The boundary layer program exhibited numerous instabilities during its initial development. The cause of these instabilities could depend on a confluence of the various small irregularities in the different distributions of the physical parameters. The values of H on the upper surface near the leading edge were sometimes exceeding the H_{SEP} value and thus spread the instability to the downstream points. The same instability was also experienced on the lower surface near the stagnation point. An upper limit and lower limit for the H value were specified in order to damp out these oscillations. In addition to this, the comparison for the H value with the H_{SEP} value was started only after about 15% chord to guard against the indications of premature separation. The Felsch expression for skin friction caused the program to find an exponent of a real negative number beyond a value of H = 3.0. Hence the upper limit was set at this value of H.

During the development of the viscous flow program numerous instabilities were encountered. Any abnormally high values of δ^*, which caused wild variations were smoothened out by forbidding negative gradients of δ^* for the first half of the airfoil. In spite of this, variations in δ^* caused severe instabilities in the C_p distributions due to erroneous slopes. The δ^* distributions were further smoothened by averaging the values with the values of previous viscous calculation since it was noticed that the variations were subsiding very slowly as the program went through the iterations.

Satisfying the Kutta condition by forcing the separation pressure on to the trailing edge point on the lower surface of the airfoil caused fluctuations of pressure distribution in the trailing edge region. This was confined to only the last 10 points. A second order least squares fit was used to smooth the calculated slopes in that region, which cured the instability.

E. COMPUTER TIME AND COST ESTIMATES

The computer runs were made on the IBM 360/44 and 370/145. The estimates are given in the following table.

α	Computer Time	Total Number of Iterations	Amount
18.4°	40 mins.	72	$ 120.00
16.4°	21 mins.	44	$ 68.00
14.4°	14 mins.	27	$ 36.00

Initially a trial run with 69 smaller panels was attempted with the hope that the instabilities with 49 larger panels would be avoided. But the length of time required and the failure to cure the instabilities caused a return to the larger size panels.

A typical convergence pattern and history for the case α = 18.4°, M = 0.135, RN = 2.2 x 10^6 is shown in Figs. 22, 23 and Table 2.

VI. RESULTS AND DISCUSSION

The present analysis was used to find the pressure distributions on a GA(W)-1 17% airfoil at three angles of attack (18.4°, 16.4°, 14.4°) for which experimental data were available (Ref. 19). Fig. 25 shows the GA(W)-1 airfoil in the $\alpha = 18.4^{\circ}$ position with the separation streamline. The results of the pressure distributions are shown in Figs. 26, 27 and 28. It can be seen that the agreement with experimental data is good in the forward position of the airfoil and the separation pressure is predicted quite accurately. The position of the separation point is a little aft of the experimental value. The rear stagnation pressures also agree well with experiments. The values of the rear stagnation point pressure for separation and the separation pressures are given in Table 1.

The stagnation point pressures are close to the experimental data and H-separation values are also near those found in Ref. 2.

The empiricism in this method is confined to (a) the position of the rear stagnation point, which is assumed from experimental data and appears to have slight influence on the results, (b) the well-established Göertler jet spreading rate parameter σ, and (c) u_r, the reverse flow velocity in the separation bubble. The assumption of a constant pressure separated region up to the trailing edge is such a well-established result from experiments that it can be considered to be a fact.

The method does not restrict any of the separation variables. The separation point is determined by the boundary layer analysis for each of the changed pressure conditions and is allowed to move. The mixed boundary condition program retains the separation pressure at

its specified value during the potential flow calculation, but once the separation point is altered, the sepration pressure changes to the value of the pressure at the new separation point. Thus there is no restriction applied on either the position of the separation point or its pressure.

The empirical assumption of the position of the rear stagnation point is based on carefully measured experimental (Ref. 2) data, and the results of the electric analog also showed that small movements of the rear free stagnation point did not produce any change in the streamline pattern around the airfoil.

Finally, the assumption of a uniform velocity u_r for the reverse flow was also based on carefully measured experimental data. The axisymmetric separation model of Green (Ref. 15) also assumes a constant velocity reverse flow behind the base.

The potential flow program calculates high positive pressure on the panels upstream of the front stagnation point on the lower surface. The panels up to the stagnation point were not included in the viscous analysis for this reason. The lower surface δ^* was assumed to be zero for all the upstream panels since the flow is accelerating very fast in the forward direction. This avoided the problem of having pressure coefficients higher than 1 on the lower surface.

The choice of u_r, though based on experimental data, turned out to be the key parameter for the final convergence of an acceptable solution, since u_r is used to find the reverse mass flow. Values of u_r/u_e = 0.12, 0.15, 0.18, and 0.20 were tried and the ideal value for which the solutions matched well with experimental data was u_r/u_e = 0.20

for both α = 18.4° and α = 14.4°. This indicates that the value of 0.20 may be a universal term.

The convergence for α = 16.4° was not achieved at $u_r = 0.20\ u_{SEP}$, but rather at a value of $u_r = 0.22\ u_e$. From the results of measurements on GA(W)-1 wings in Ref. 2 it was noticed that α = 16.4° represents the stalling condition (i.e., the C_{Lmax} condition) and this is a highly unstable condition. Measurements of the separated region data were difficult to make due to the unsteadiness of the flow. We could perhaps attribute the present difficulty in the convergence at the same value of u_r to this unstable mode.

The MBC potential flow program used singularity distribution on the chord line to represent the airfoil. This would accurately predict results for thin airfoils, but for airfoils with large thicknesses, such as GA(W)-1, there can be significant errors in the pressure distributions. A better potential flow solution which uses the singularity distributions on the surface could improve the theoretical solution to match more accurately the experimental pressure data.

Head's boundary layer method is an integral method and thus is limited by its assumptions. A more accurate boundary layer method could also improve the present solution.

The accuracy of the method also depends upon the panel size. The pressure distributions show certain deviations from the experimental values at the points where there is a sudden change in the panel size. The choice of the panel size can greatly change this. By choosing a larger number of panel the accuracy of the method could be improved at the cost of increased computing time.

Typical H and δ^* distributions for the GA(w)-1 airfoil are shown in figures 29 and 30.

Despite these limitations, this model has been shown to include all the significant physical features of separated wing flow. A computational method has been formulated which gives good surface pressure results. The one sensitive empirical value, u_r/u_e, may be a universal value of 0.2; it is recommended that computation be performed for other wings to determine whether this is true.

RECOMMENDATIONS FOR FURTHER WORK

1. This program should be used for computing pressure distributions on other airfoils for which separated-flow data are available. If data can be obtained for the separated region velocity field, the $u_r/u_e = 0.2$ assumption can be tested directly; otherwise, the value will have to be inferred from the pressure field which results from various u_r/u_e values.

2. An extension to the present model and program should be made to permit drag estimations. This could be done by computing pressure and velocity values on a vertical plane at the trailing edge station, and carried to a distance sufficient to insure that the flow is undisturbed. The momentum deficit method could then give a drag value based on the detailed pressures and velocities at this plane.

3. An improved mixed-boundary-condition potential flow program and boundary layer calculation method should be sought and mated to the separated flow model.

4. Attempts should be made to extend this model and method to apply to multi-element airfoils, i.e., wings with flaps.

REFERENCES

1. Zumwalt, G.W.: "An Analytical Model for Separated Flow on Wings," Research proposal to Langley Research Center, NASA. January 29, 1975.

2. Seetharam, H.C.: "Experimental Investigation of Separated Flow Fields on an Airfoil at Subsonic Speeds," AR 75-1, Wichita State University.

3. Bristow, D.R.: "Computer Program to Solve the Three-Dimensional Mixed Boundary Conditions Problem for Subsonic or Supersonic Potential Flow," Report No. MDCA3190, McDonnell-Douglas Aircraft Company.

4. Hahn, M., Rubbert, P.E., and Mahal, A.S.: "Evaluation of Separated Flow Criteria and Their Application to Separated Flow Analysis," Technical Report AFFDL-TR-145, January 1973.

5. McCullough, G.B., and Gault, D.E.: "Examples of Three Representative Types of Airfoil Section Stall at Low Speeds," NASA TN 2502, 1951.

6. Stevens, W.A., Goradia, S.H., and Braden, J.A.: "Mathematical Model for Two-Dimensional Multi-Component Airfoils in Viscous Flows," NASA CR-1843, July 1971.

7. Narramore, J.C., and Beatty, T.D.: Douglas Paper 6347. Douglas Aircraft Company.

8. Thames, F.C., Thompson, J.F., and Mastin, C.W.: "Numerical Solution of the Navier Stokes Equations for Arbitrary Two-Dimensional Airfoils." NASA Sp. 347. Paper in NASA Conference at Langley Research Center, March 4-6, 1965.

9. Jacob, K.: "Computation of Separated Incompressible Flow Around Airfoil and Determination of Maximum Lift," AVA Report 67A62, Publication in Zeitschrift Fur Flugwissenschaften, Lechere at WGLR Committee Meeting for Aerodynamics, Institute of Technology, Berlin, October 1-4, 1967.

10. Jacob, K.: "Weiterentwicklung eines Verfahren zur Brechnug der abgelösten Profilströnungnich besonderer Berücksichtigung des Profilwilderstandes,: DFVLR-AVA Internal Report 251-75A16, June 1975.

11. Bhatley, I.C., McWhirter, J.S.: "Development of Theoretical Method for Two-Dimensional Multi-Element Airfoil Analysis and Design, Part I, Viscous Flow Analysis Method," AFFDL-12-96, August 1972.

12. Jacob, K., and Steinbach, D.: "A Method for Prediction of Lift for Multi-Element Airfoil Systems with Separation," Paper 12, AGARD CP-143, 1974.

13. Farn, C.L.S., Goldschmeid, F.R., and Whirlow, D.K.: "Pressure Distribution Prediction for Two-Dimensional Hydrofoils with Massive Turbulent Separation," Journal of Hydronautics, Vol. 10, No. 3, July 1976, pp. 95-101.

14. Kuhn, G.D., and Nielson, J.N.: "Prediction of Turbulent Separation Boundary Layers," AIAA Paper No. 73-6333, July 1973.

15. Green, J.E.: "Two-Dimensional Turbulent Reattachment as a Boundary Layer Problem," RAE Rep. 66059, February 1966.

16. McErlean, D.P., and Prizerembel, C.E.G.: "The Turbulent Near Wake of an Axisymmetric Body at Subsonic Speeds," AFOSR Scientific Report 70-0669TR, February 1970.

17. Korst, H.H.: "A Theory of Base Pressures in Transonic and Supersonic Flow," Journal of Applied Mechanics, Vol. 23, 1956, pp. 593-600.

18. Woodward, F.A.: "Analysis and Design of Wing Body Combinations at Subsonic and Supersonic Speeds," Journal of Aircraft, Vol. 5, No. 6, Nov.-Dec. 1968.

19. Wentz, W.H., Jr., and Seetharam, H.C.. "The Development of a Fowler Flap System for a High Performance Subsonic Flow Analysis," NASA CR-2443, December 1974.

20. Head, M.R., and Patel, V.C.: "Improved Entrainment Method for Calculating Turbulent Boundary Layer Development," British R & M 3643, March 1968.

21. Green, J.E.: "The Prediction of Turbulent Boundary Layer Development in Compressible Flow," Journal of Fluid Mechanics, Vol. 31, 1968, pp. 753-778.

22. Gross, L.W.: "Interactions of the Viscous and Inviscid Flow Fields of Wings at Near Stall Angles of Attack," Report No. MDCA32128, McDonnell-Douglas Aircraft Company.

23. Hill, W.G., Jr., and Page, R.H.: "Initial Development of Turbulent Compressible Free Shear Layer," ASME Paper No. 68 WA/FE-21, 1968.

24. Korst, H.H., and Chow, W.L.: "Non-Isoenergetic Turbulent (Pr_t = 1) Jet Mixing between Two Compressible Streams at Constant Pressure," University of Illinois, ME TN 293-2.

25. Schlichting, H.: "Boundary Layer Theory," McGraw-Hill Publications, NY, 1960.

26. Naik, S.N.: "An analytical model for the study of highly separated flow on lowspeed airfoils," Ph.D. dissertation, Wichita State University, Department of Aeronautical Engineering, 1977.

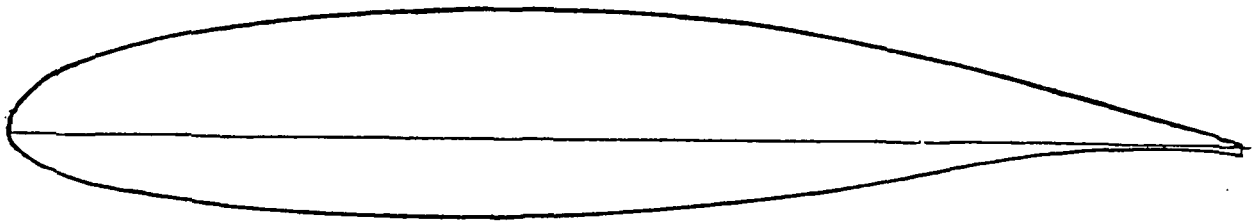

Upper Surface		Lower Surface	
X /c	Z /c	X /c	Z /c
0.00000	0.00000	0.00000	0.00000
.00200	.01300	.00200	-.00930
.00500	.02040	.00500	-.01380
.01250	.03070	.01250	-.02050
.02500	.04170	.02500	-.02690
.03750	.04965	.03750	-.03190
.05000	.05589	.05000	-.03580
.07500	.06551	.07500	-.04210
.10000	.07300	.10000	-.04700
.12500	.07900	.12500	-.05100
.15000	.08400	.15000	-.05430
.17500	.08840	.17500	-.05700
.20000	.09200	.20000	-.05930
.25000	.09770	.25000	-.06270
.30000	.10160	.30000	-.06450
.35000	.10400	.35000	-.06520
.40000	.10491	.40000	-.06490
.45000	.10445	.45000	-.06350
.50000	.10258	.50000	-.06100
.55000	.09910	.55000	-.05700
.57500	.09668	.57500	-.05400
.60000	.09371	.60000	-.05080
.62500	.09006	.62500	-.04690
.65000	.08599	.65000	-.04280
.67500	.08136	.67500	-.03840
.70000	.07634	.70000	-.03400
.72500	.07092	.72500	-.02940
.75000	.06513	.75000	-.02490
.77500	.05907	.77500	-.02040
.80000	.05286	.80000	-.01600
.82500	.04646	.82500	-.01200
.85000	.03988	.85000	-.00860
.87500	.03315	.87500	-.00580
.90000	.02639	.90000	-.00360
.92500	.01961	.92500	-.00250
.95000	.01287	.95000	-.00260
.97500	.00609	.97500	-.00400
1.00000	-.00070	1.00000	-.00800

FIGURE 1 GA(W)-1 AIRFOIL COORDINATES

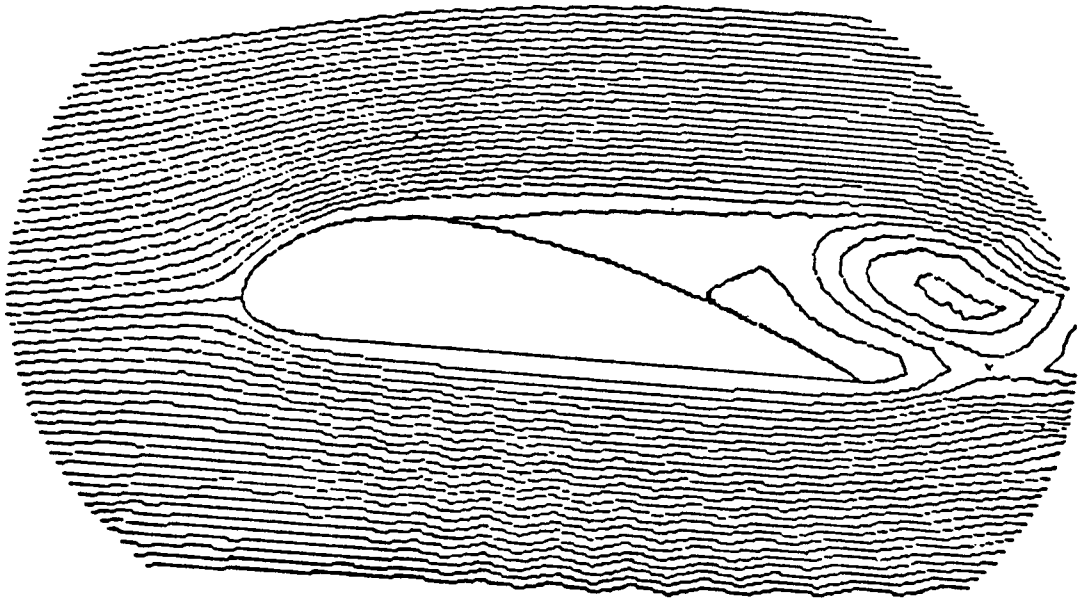

FIGURE 2 STREAMLINE PATTERN-NAVIER STOKES SOLUTION

(FROM REF. 8)

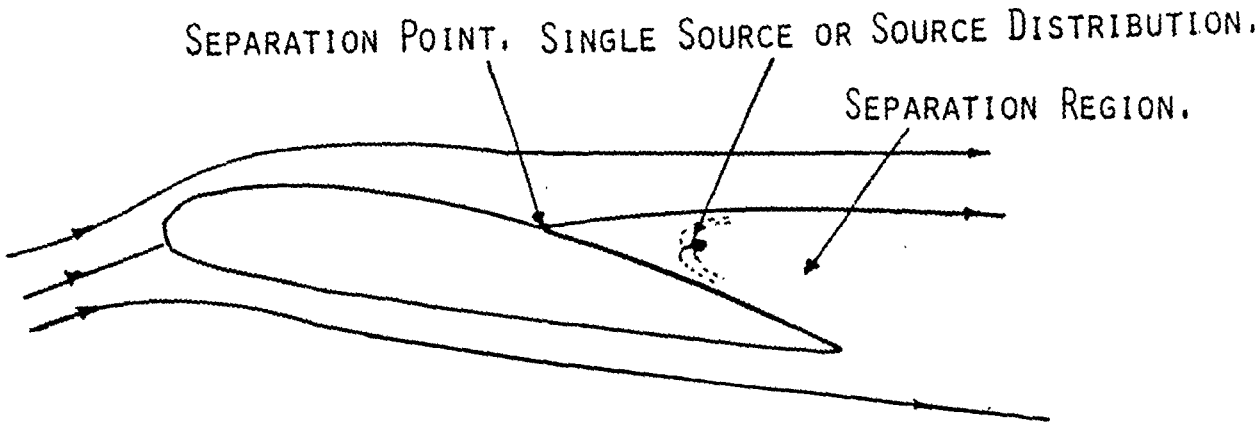

FIGURE 3 SIMULATION OF SEPARATED REGION BY SOURCES

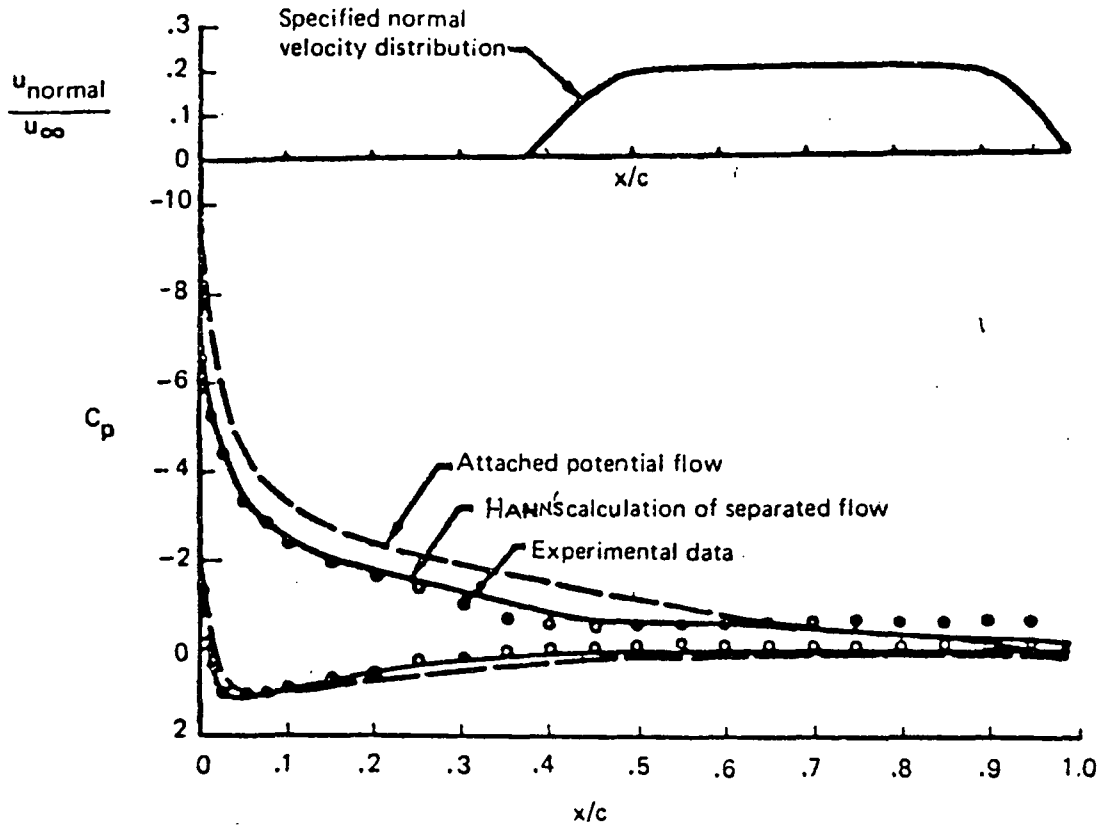

Comparison of Calculated and Experimental Data on NACA 63_3-018 at $\alpha = 16°$.

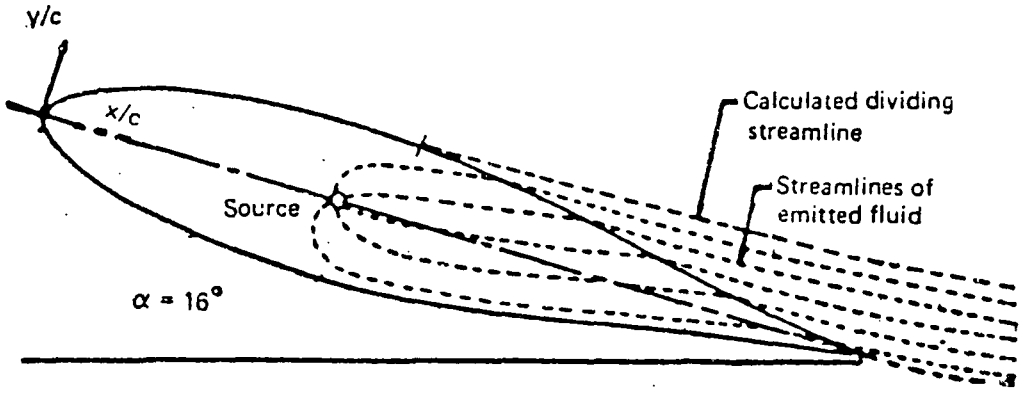

Calculated Flow Pattern of Separated Flow, NACA 63_3-018 at $\alpha = 16°$.

FIGURE 4 SOURCE DISTRIBUTION MODEL (FROM REF 4)

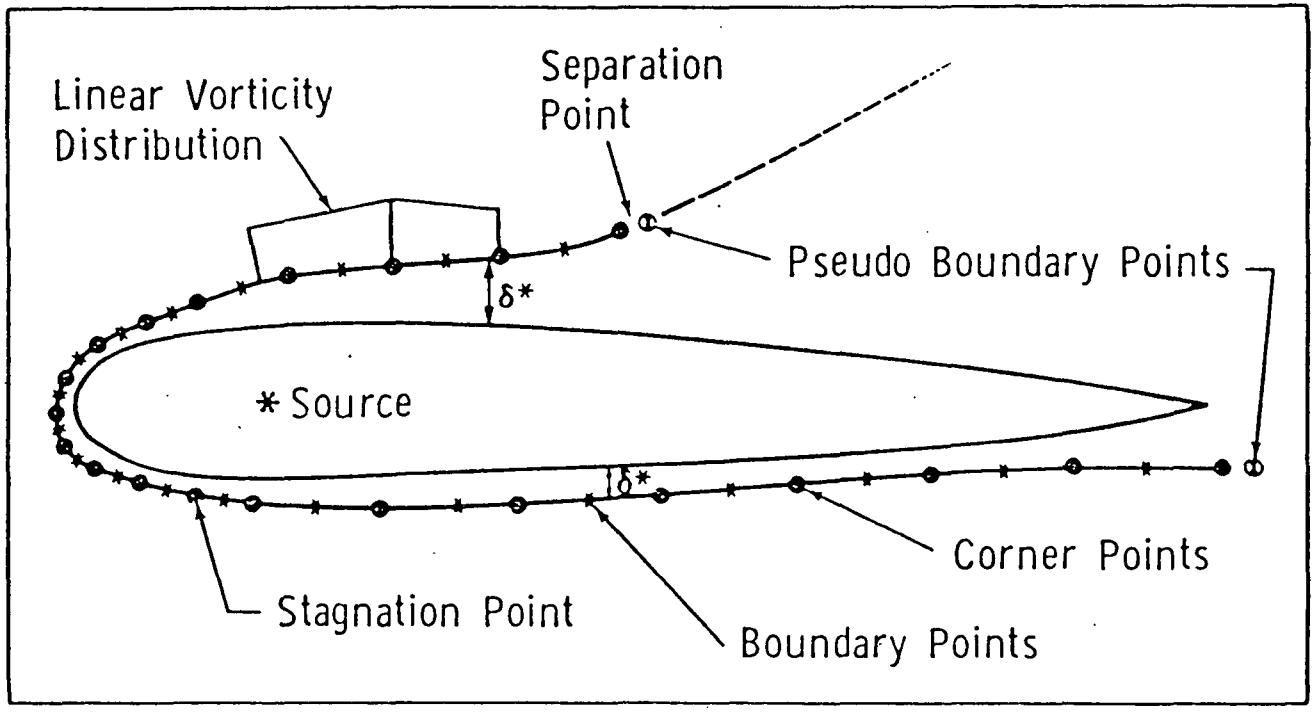

FIGURE 5 EQUIVALENT AIRFOIL MODEL FOR SEPARATED FLOW (FROM REF. 11)

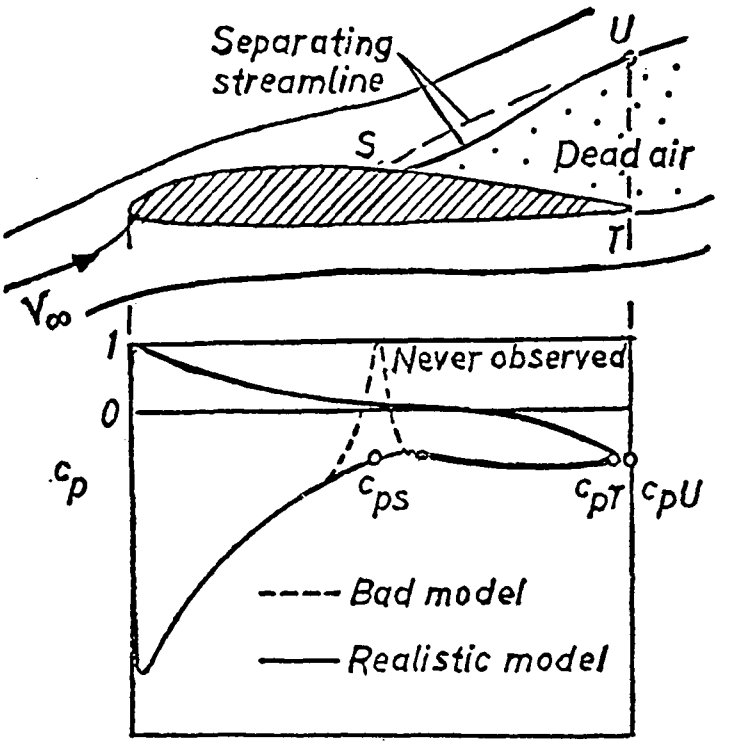

Pressure distribution for flow with a separated wake (Jacob and Steinbach, 1974).

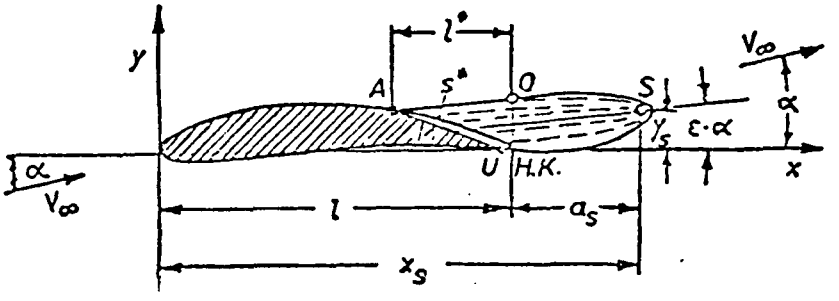

s* = Conture length between A and U

Sketch of the new Jacob dead air flow region model with unsymmetric separation (Jacob 1975).

FIGURE 6 JACOB'S MODIFIED MODEL (FROM REF. 10)

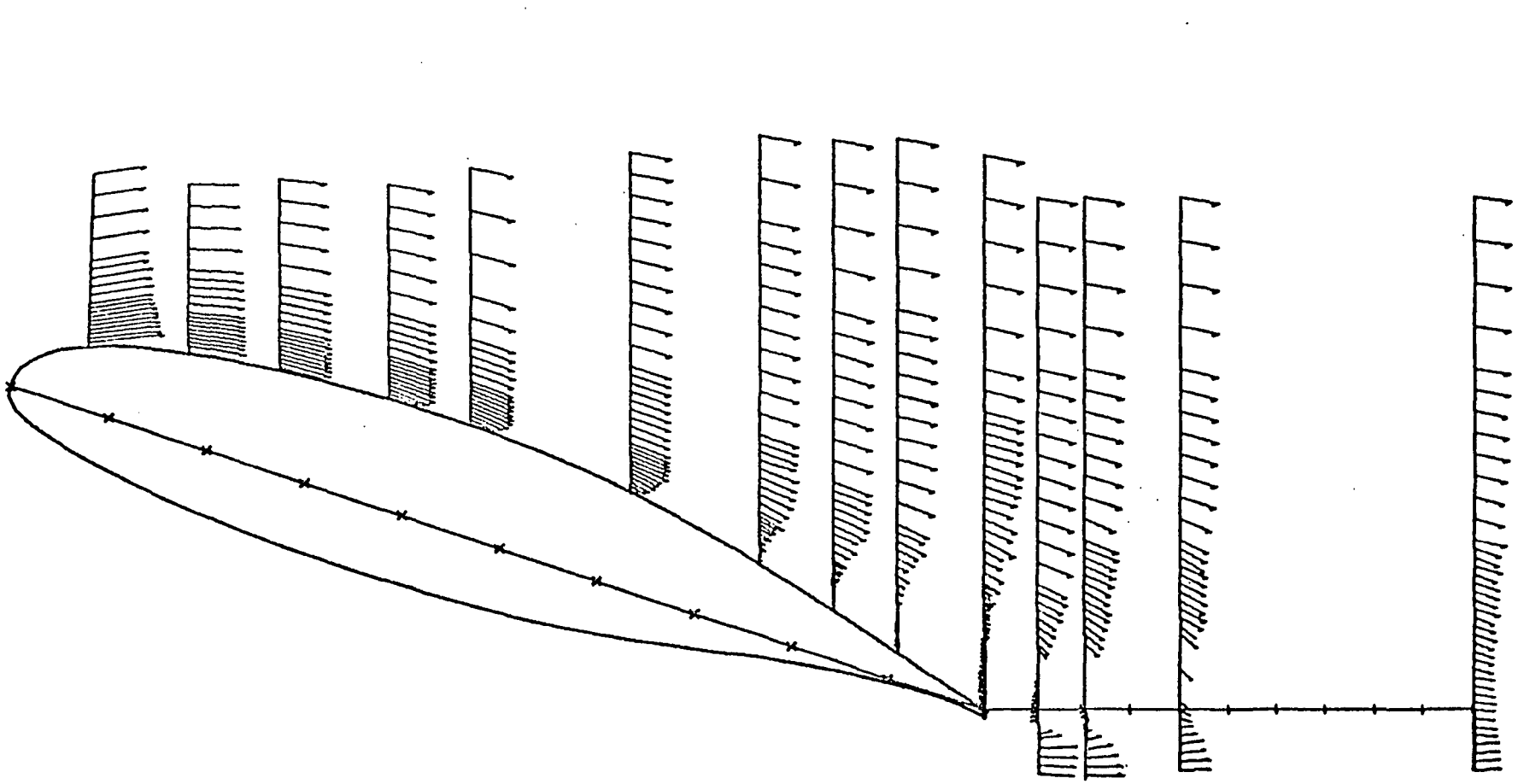

FIGURE 7 EXPERIMENTAL VELOCITY PLOT, GA(W)-1 AIRFOIL

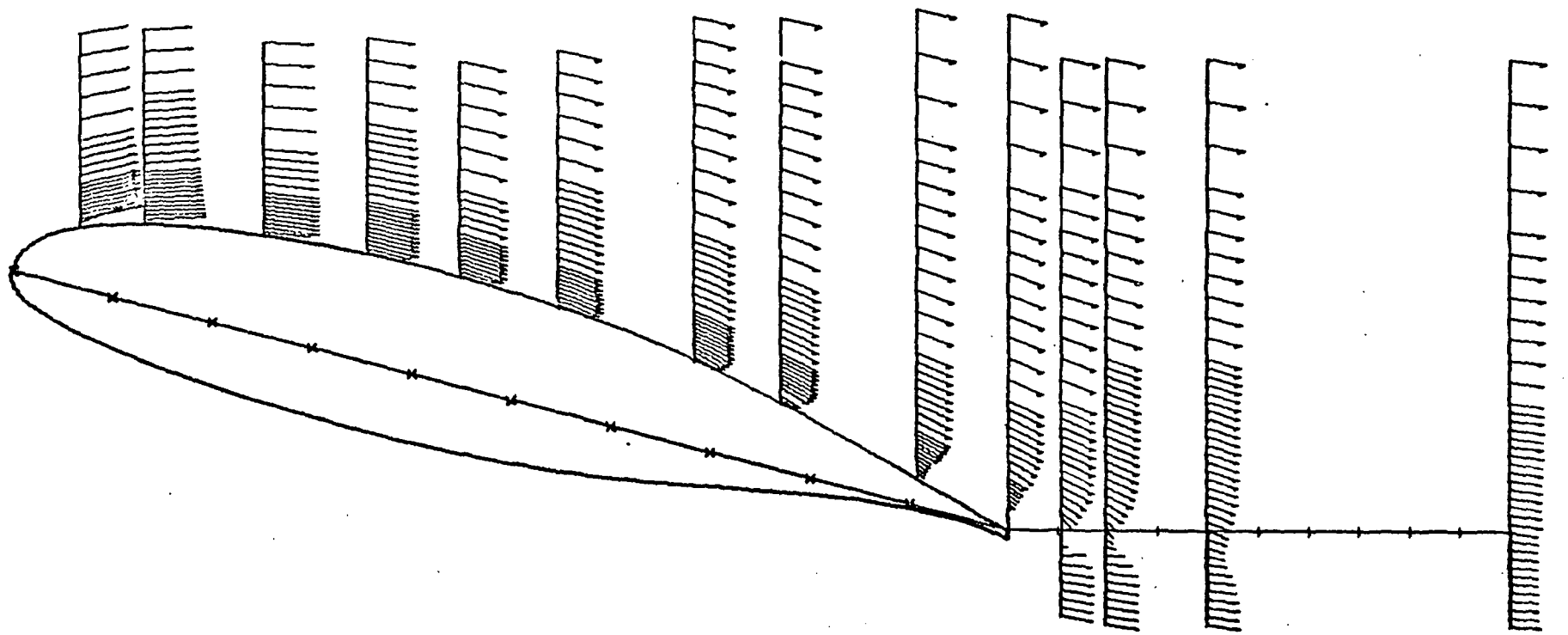

FIGURE 8 EXPERIMENTAL VELOCITY PLOT, $\alpha = 14.4^{\circ}$, RE.NO.=2.5 x 10^{6} (FROM REF 2)

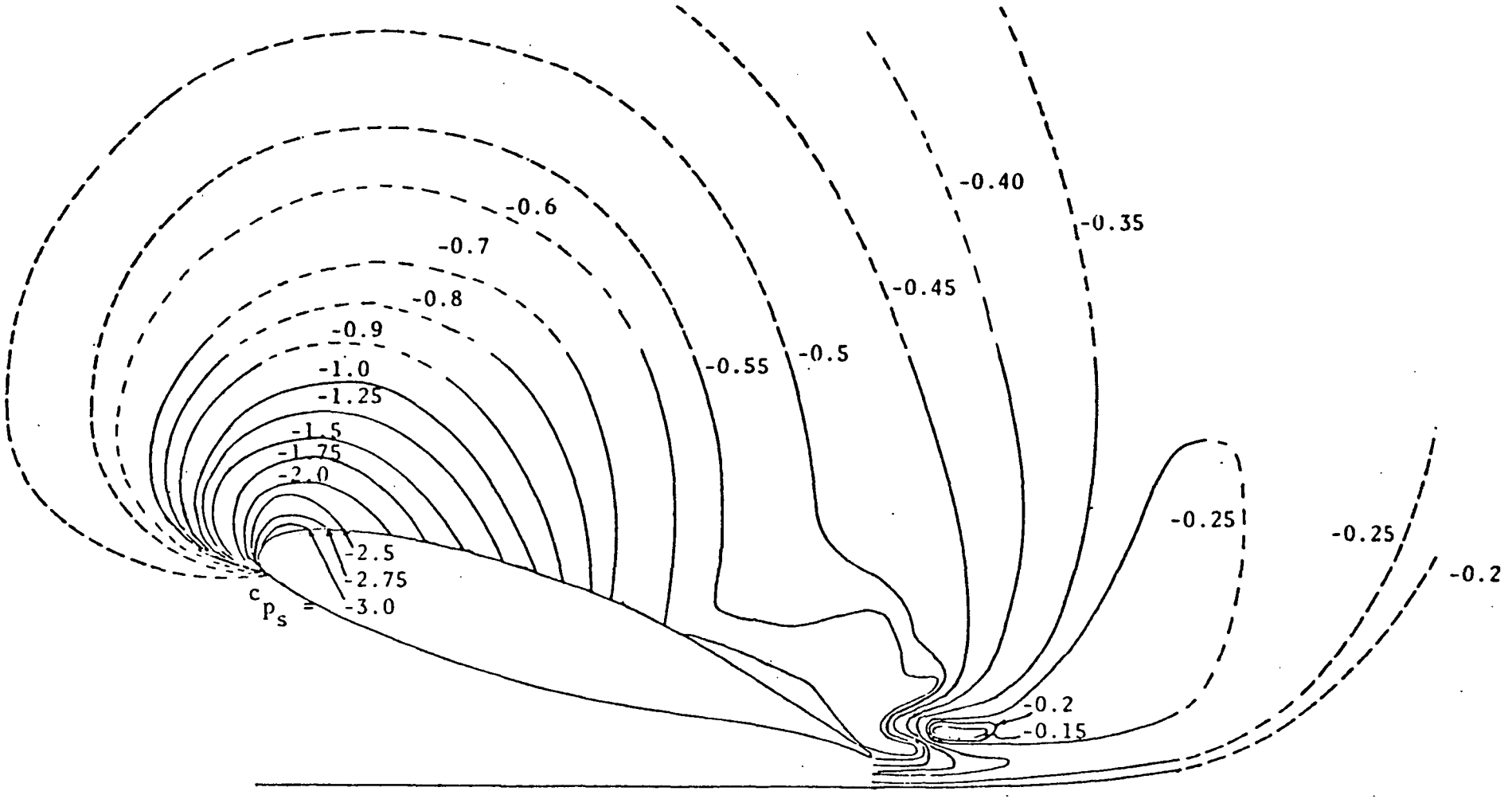

FIGURE 9 STATIC PRESSURE FIELD CONTOURS, GA(W)-1 AIRFOIL, α =18.4°, RE. NO. =2.2 x 10^6
(FROM REF 2)

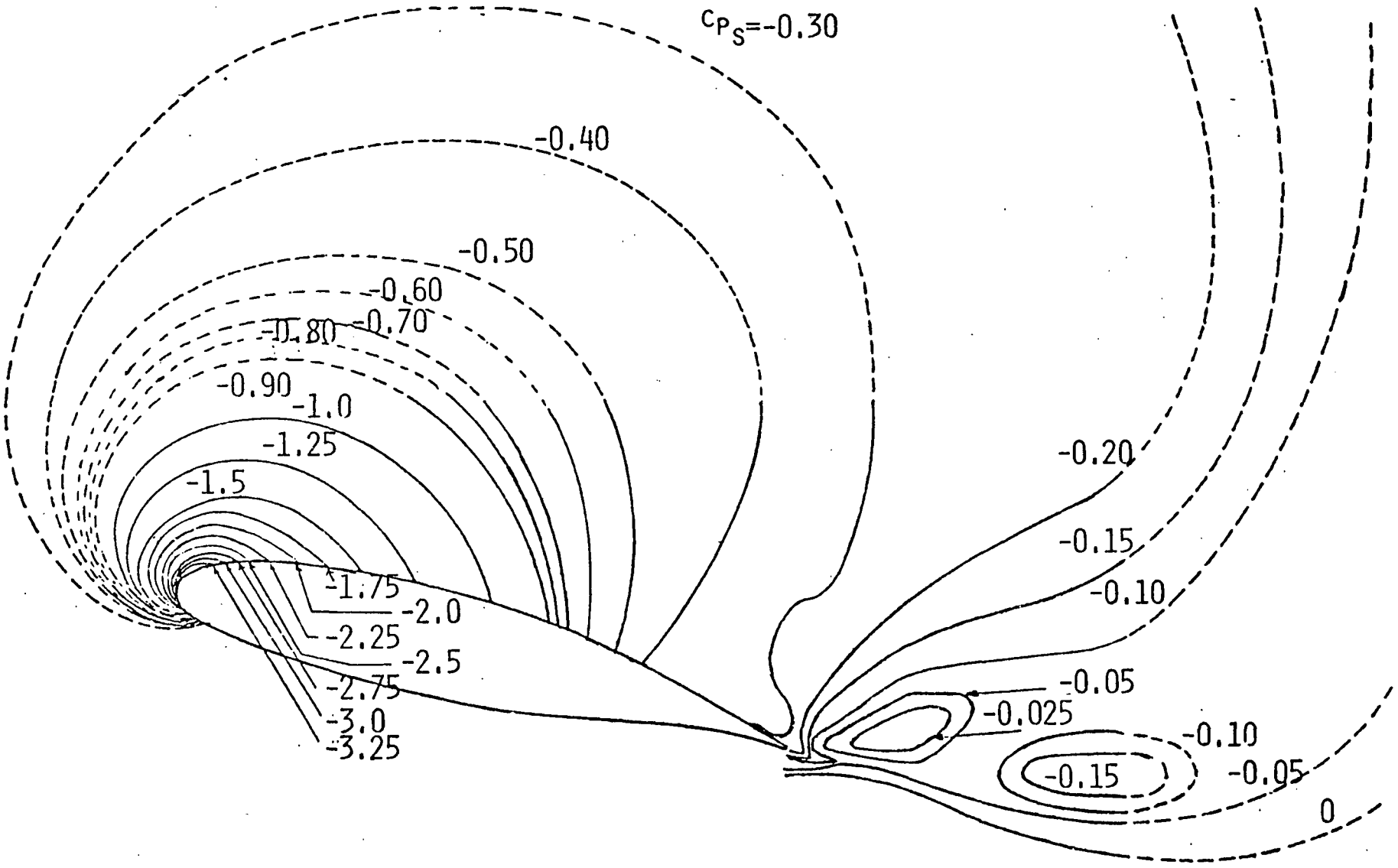

FIGURE 10 STATIC PRESSURE FIELD CONTOURS, GA(W)-1 AIRFOIL, α=14.4°, RN= 2.5x10
(FROM REF. 2)

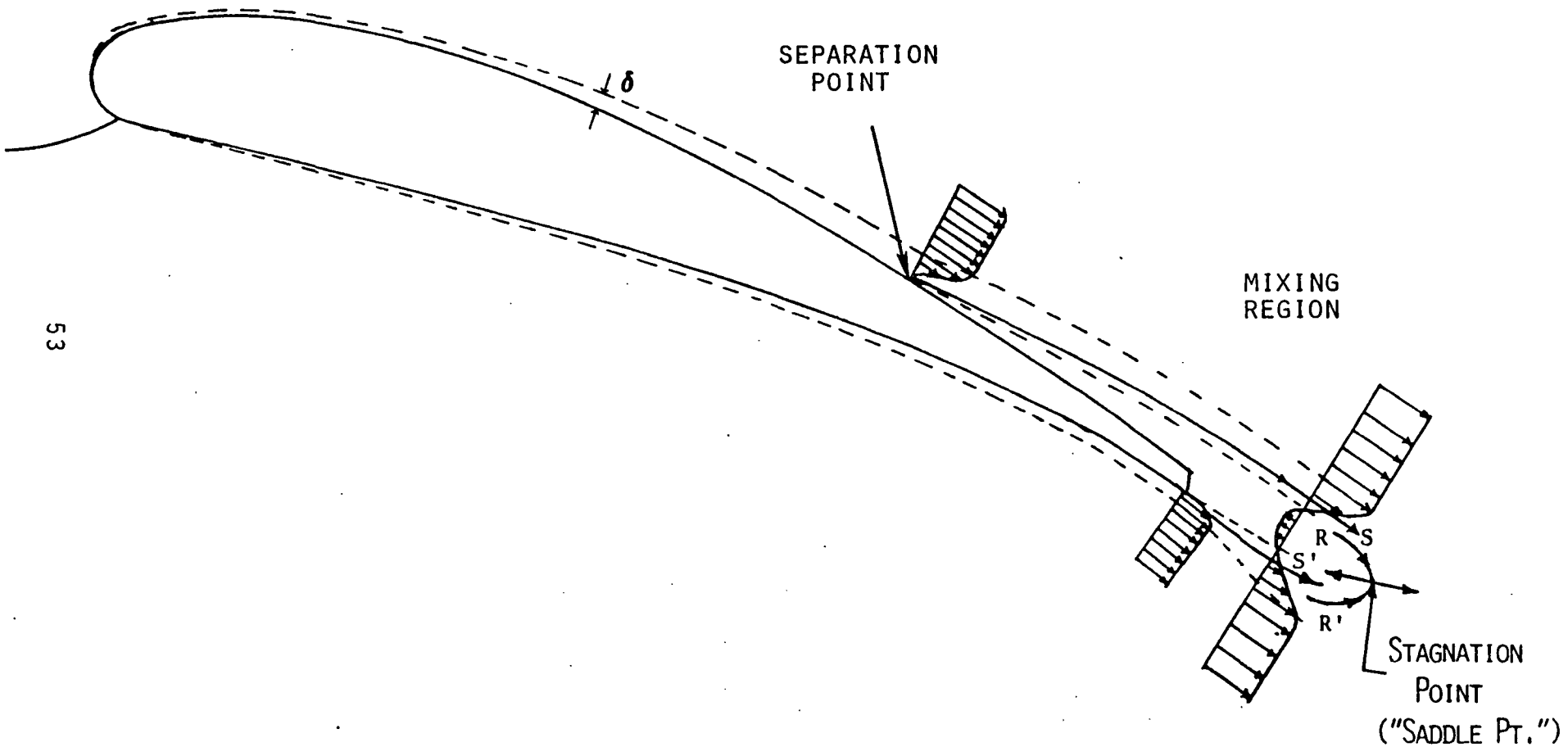

FIGURE 11 SCHEMATIC DIAGRAM OF SEPARATED FLOW MODEL

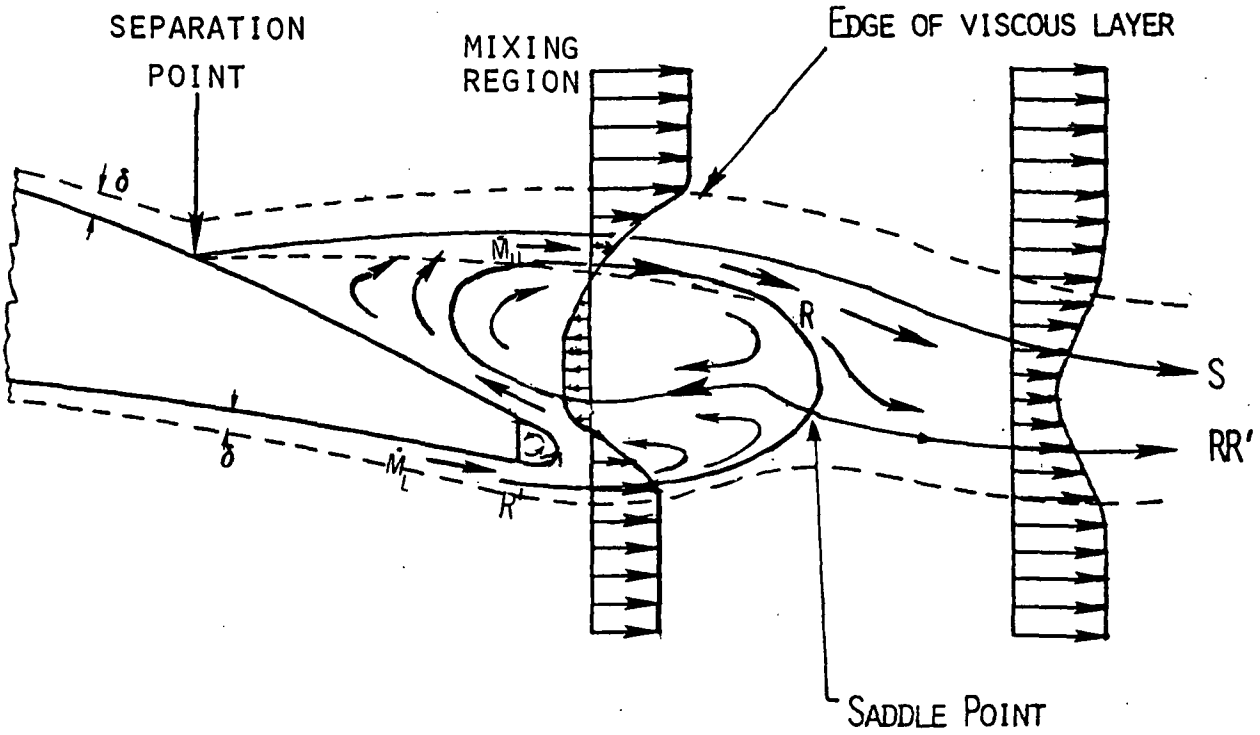

FIGURE 12. DETAILS OF THE SEPARATED REGION

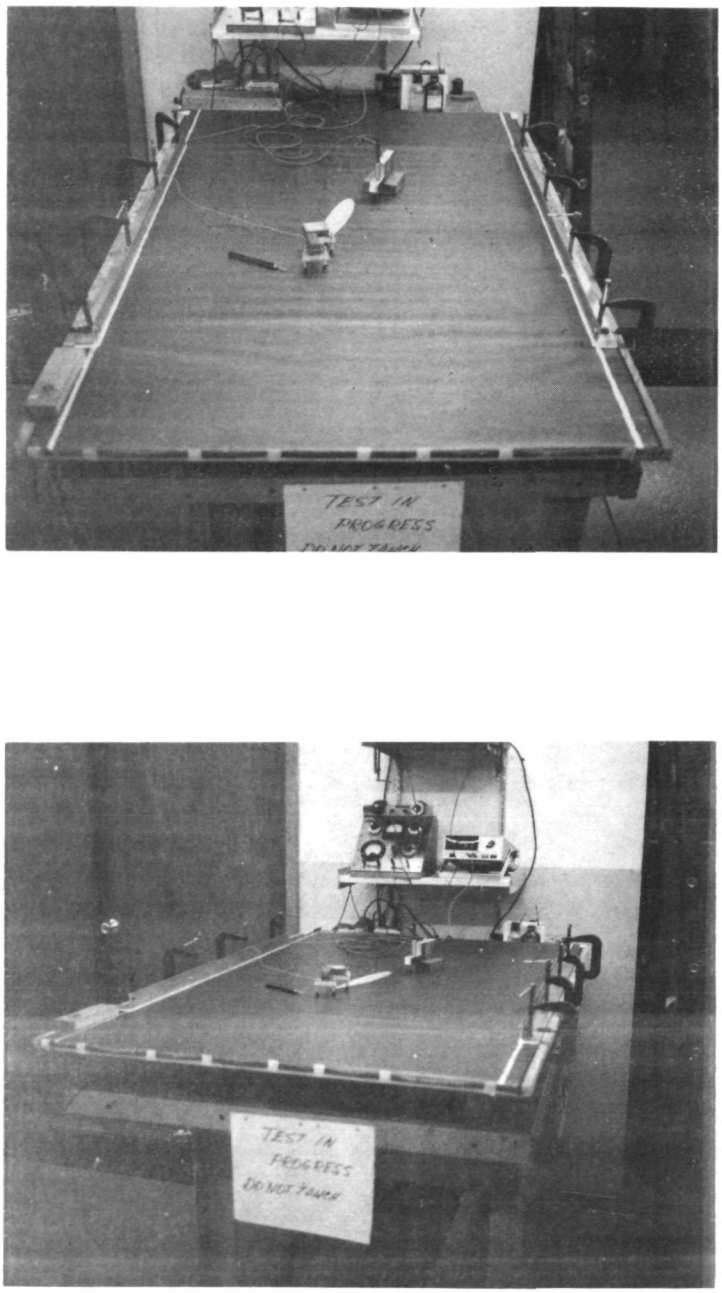

FIGURE 13 EXPERIMENTAL SETUP FOR ELECTRICAL ANALOGY

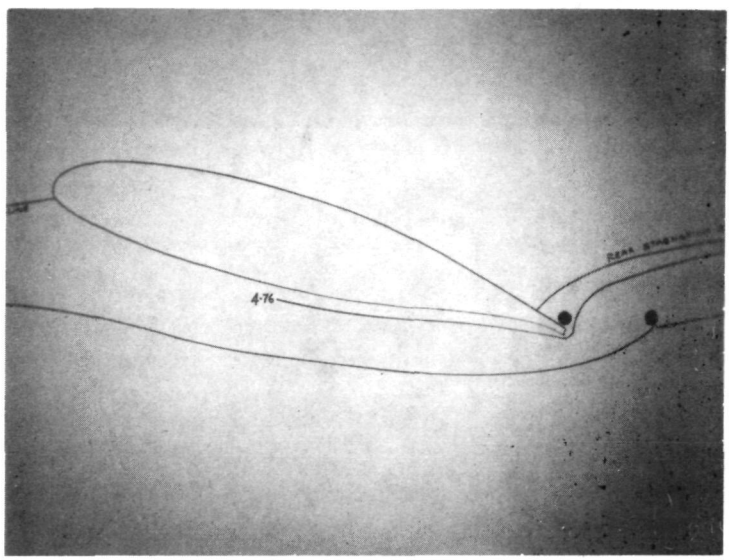

FIGURE 14 STREAMLINE PATTERN FROM ELECTRICAL ANALOGY

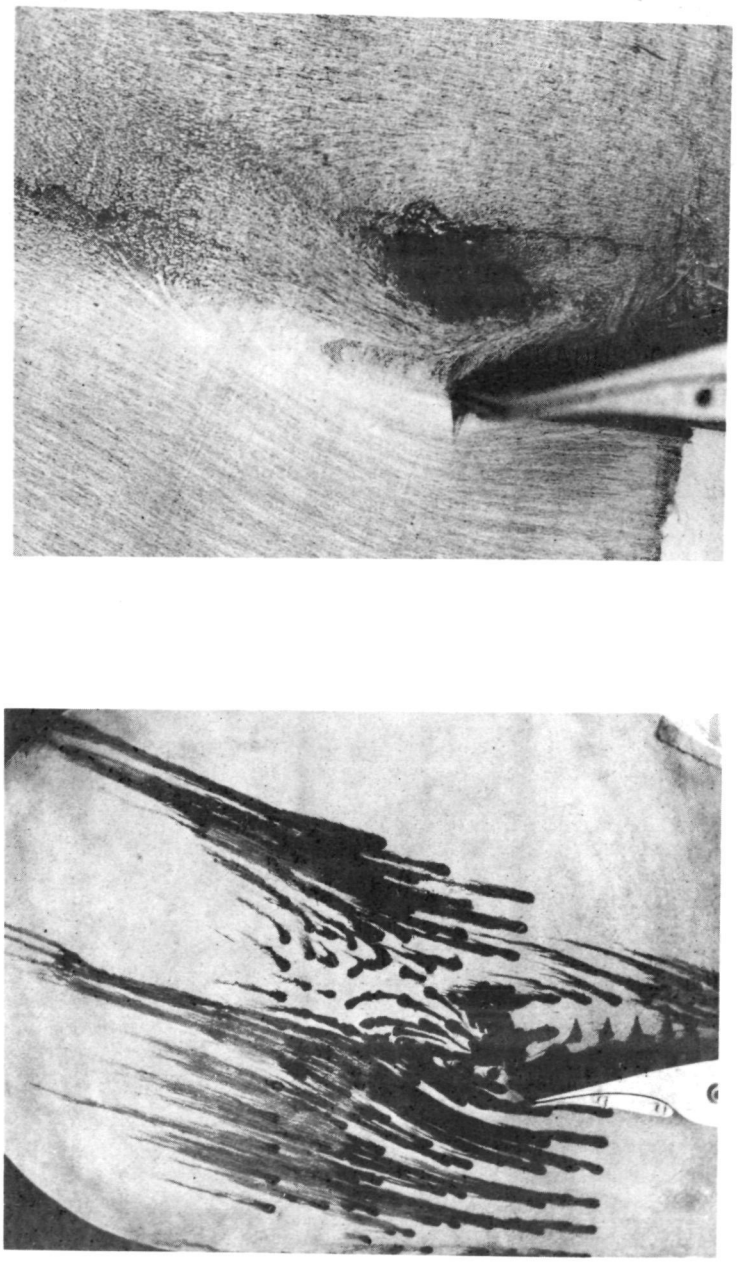

FIGURE 15 FLOW VISUALISATION PHOTOGRAPHS OF SEPARATED REGION- GA(W)-1, $\alpha = 18^{\circ}$; R.N.=0.3×10^{6}

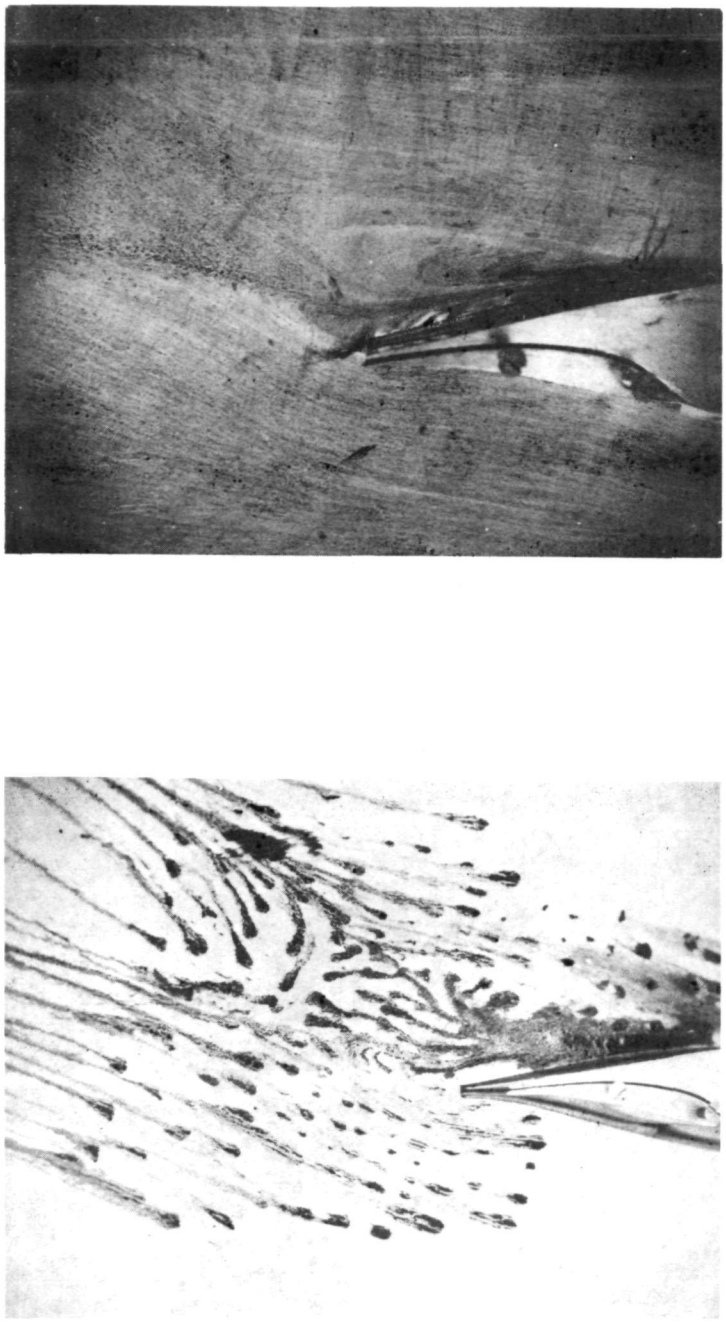

FIGURE 16 $\alpha = 16^{\circ}$, R.N.$\approx 0.3 \times 10^{6}$ (GA(W)-1 WING)

OIL FLOW PATTERNS

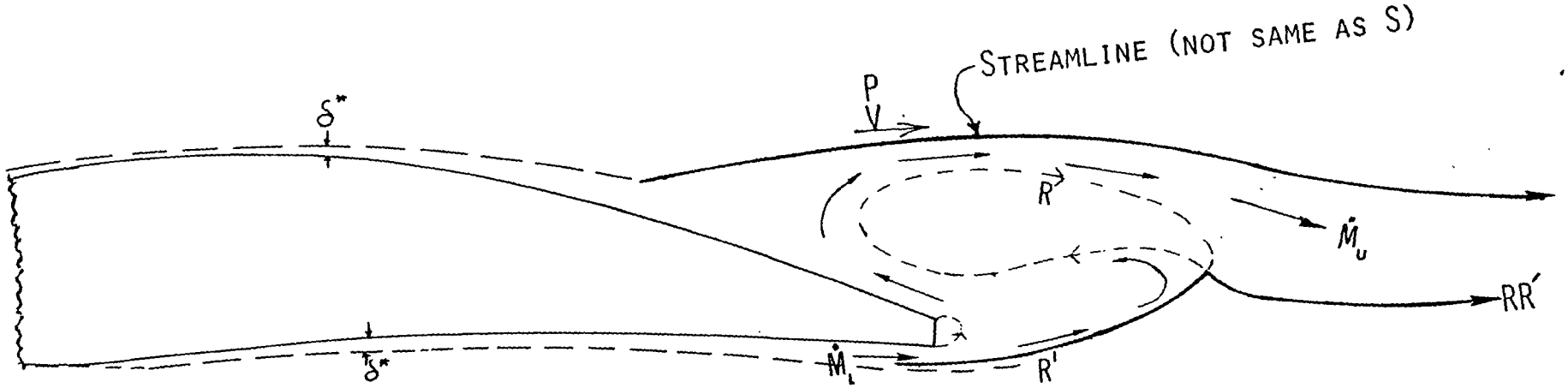

FIGURE 17 GEOMETRY OF THE "OUTSIDE PROBLEM"

MATCH "OUTSIDE PROBLEM":
1. V & P ADJACENT TO MIXING
2. M
3. P AT SADDLE POINT
4. R AND RR'

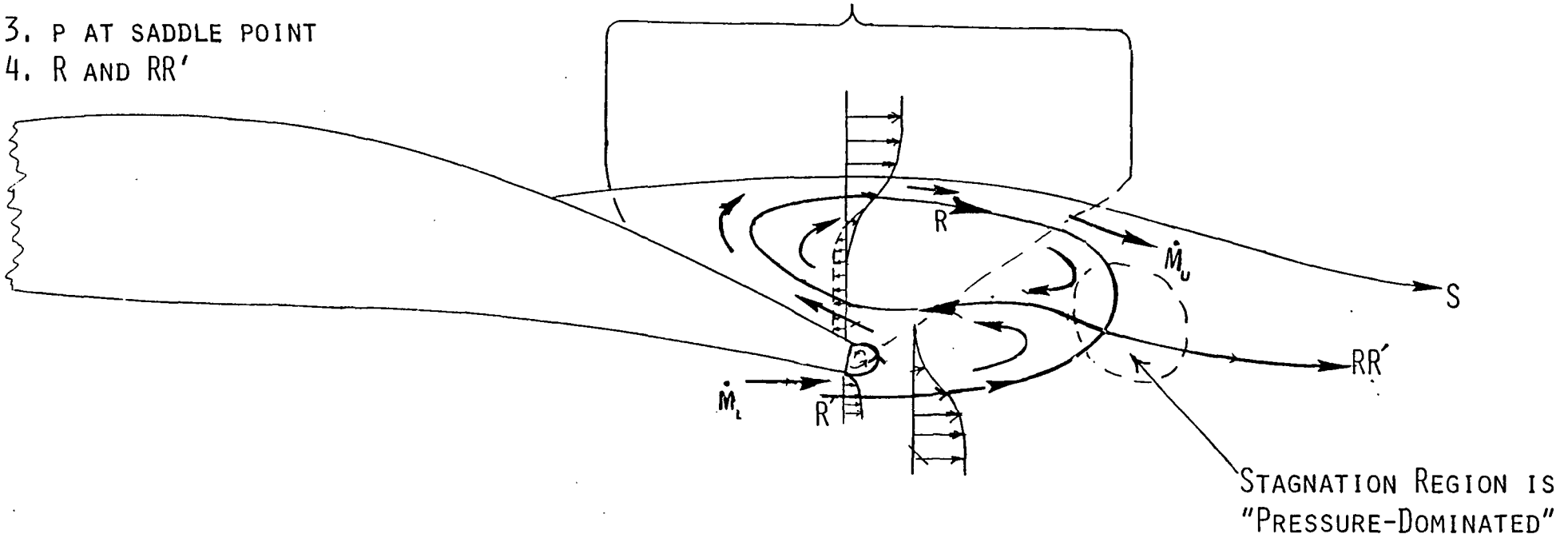

FIGURE 18 GEOMETRY OF THE "INSIDE PROBLEM"

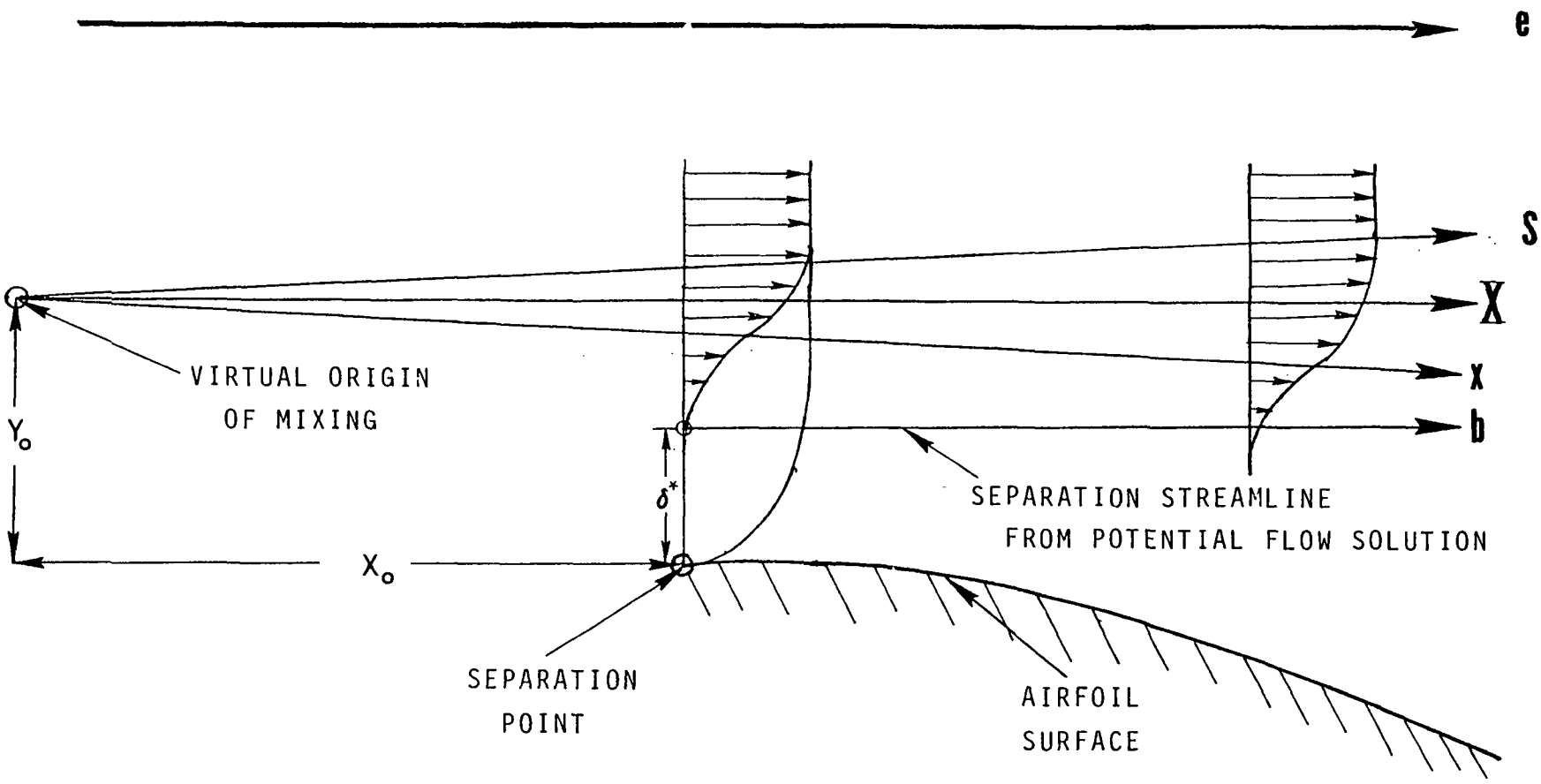

FIGURE 19 MATCHING OF THE EXISTING FLOW WITH KORST'S FLOW AT THE SEPARATION POINT

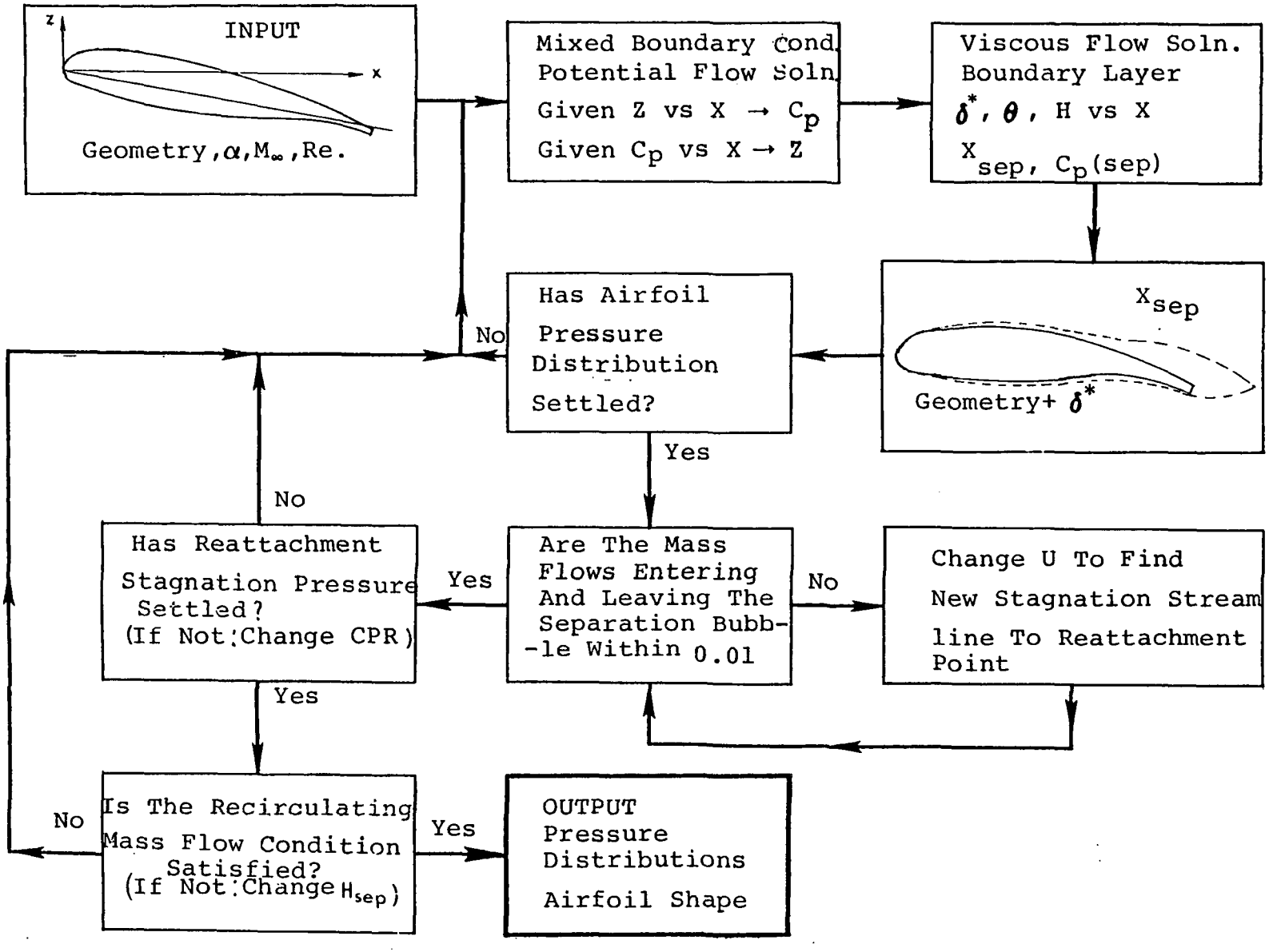

FIGURE 20 COMPUTER PROGRAM FLOW CHART

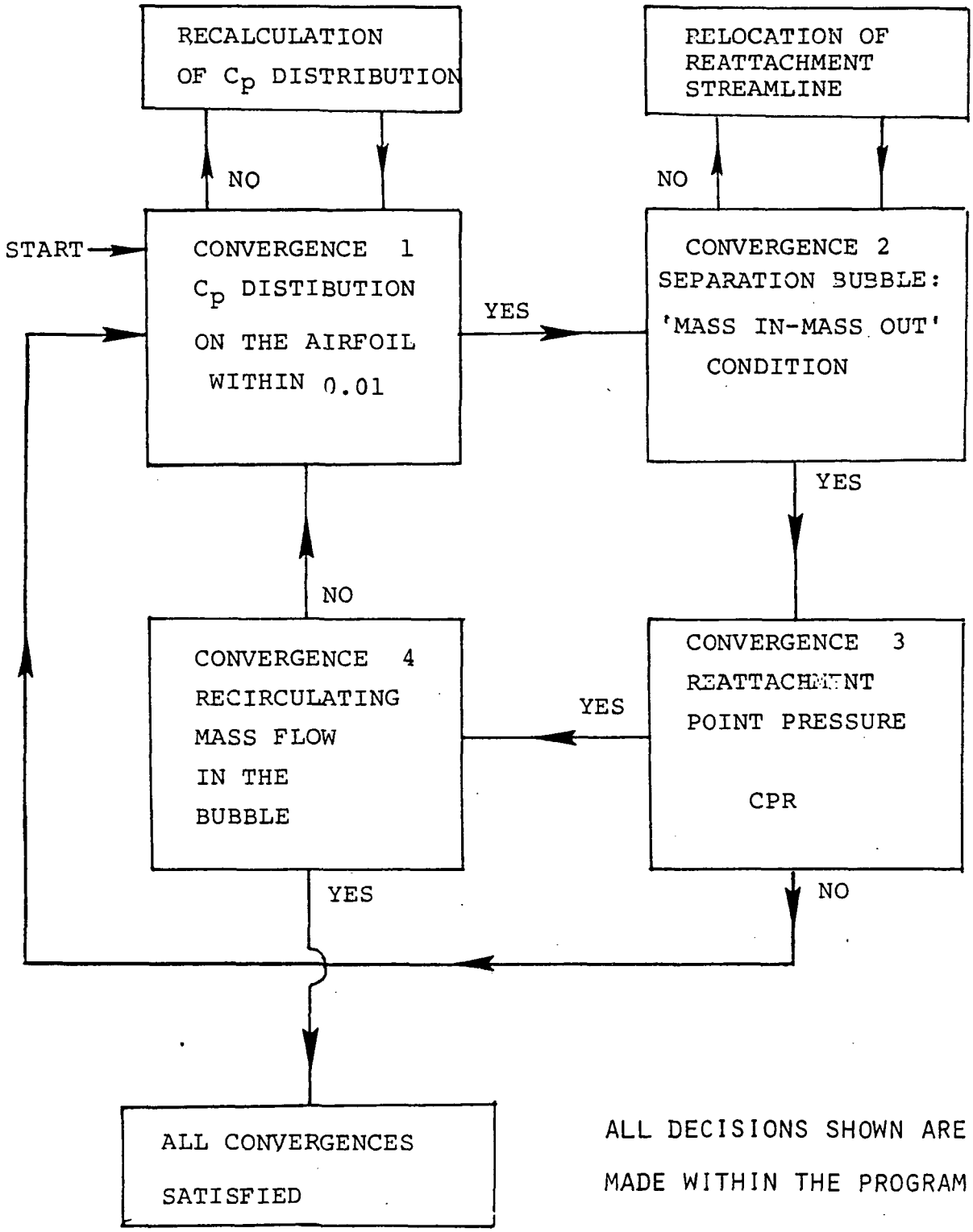

FIGURE 21 COMPUTER PROGRAM CONVERGENCE SCHEME

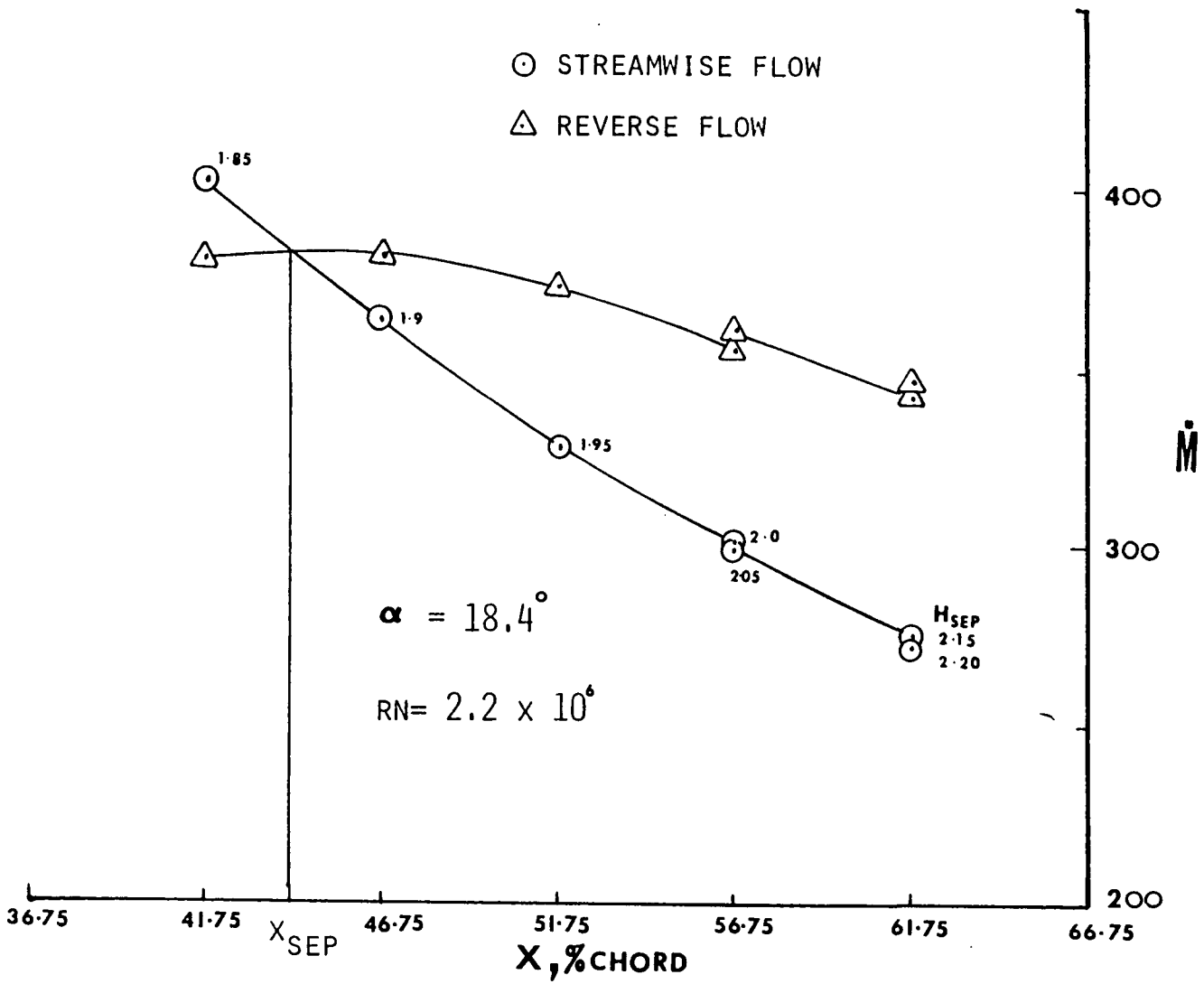

FIGURE 22 TYPICAL PLOT SHOWING BUBBLE MASS FLOW CONVERGENCE (CONVERGENCE 4)

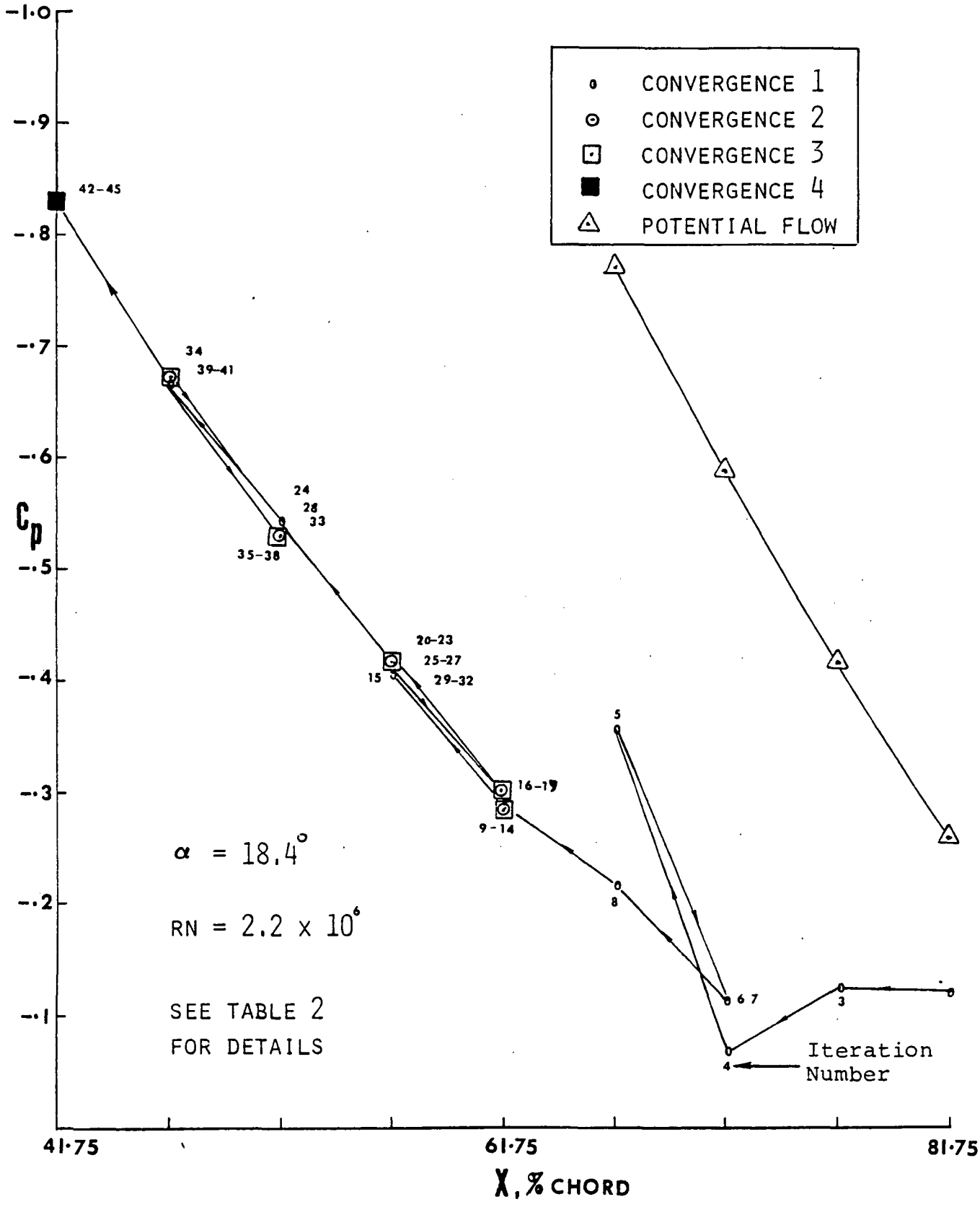

FIGURE 23 SEPARATION C_p VARIATION AND CONVERGENCE

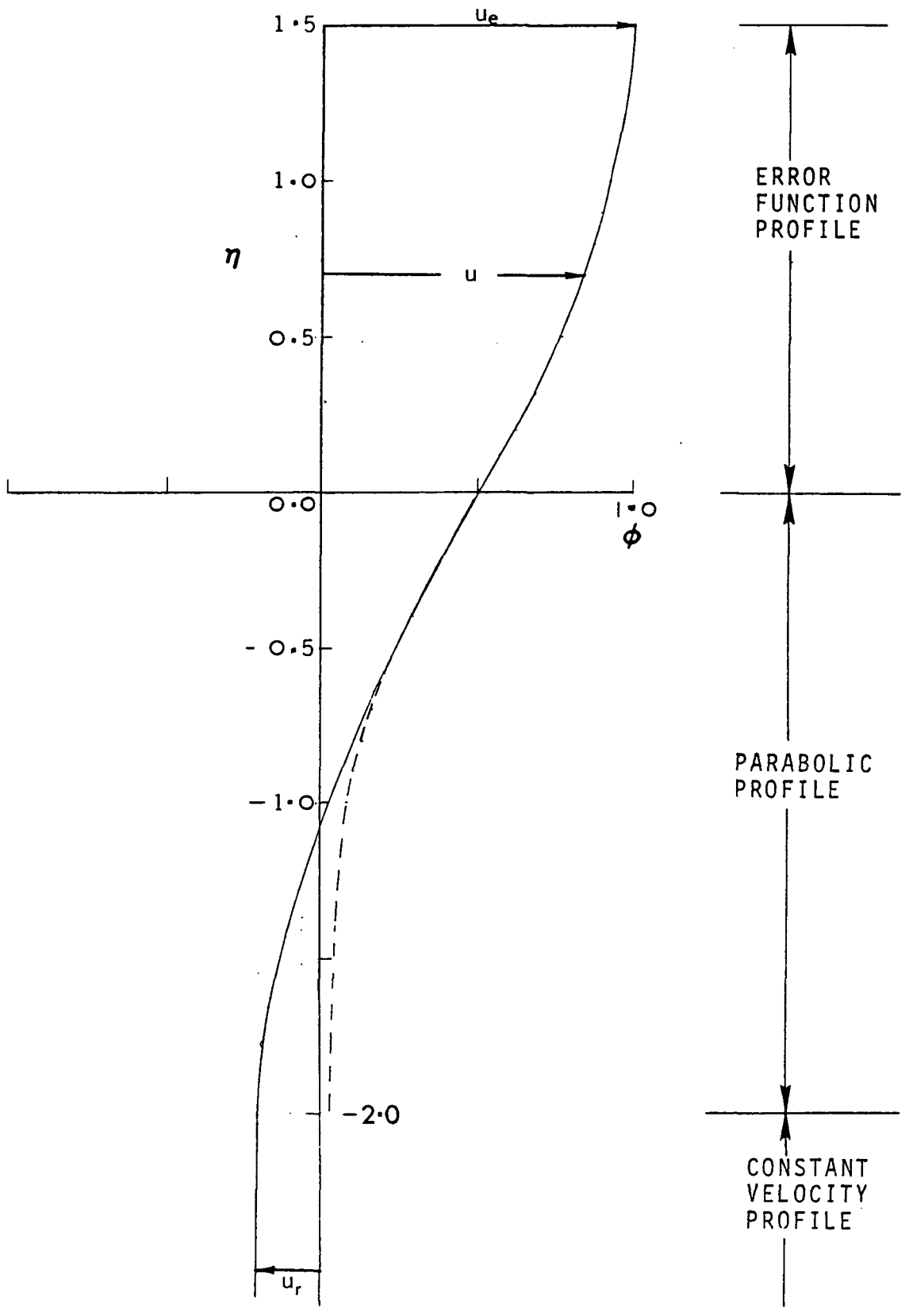

FIGURE 24 VELOCITY PROFILE IN THE SEPARATION BUBBLE ON THE UPPER SURFACE

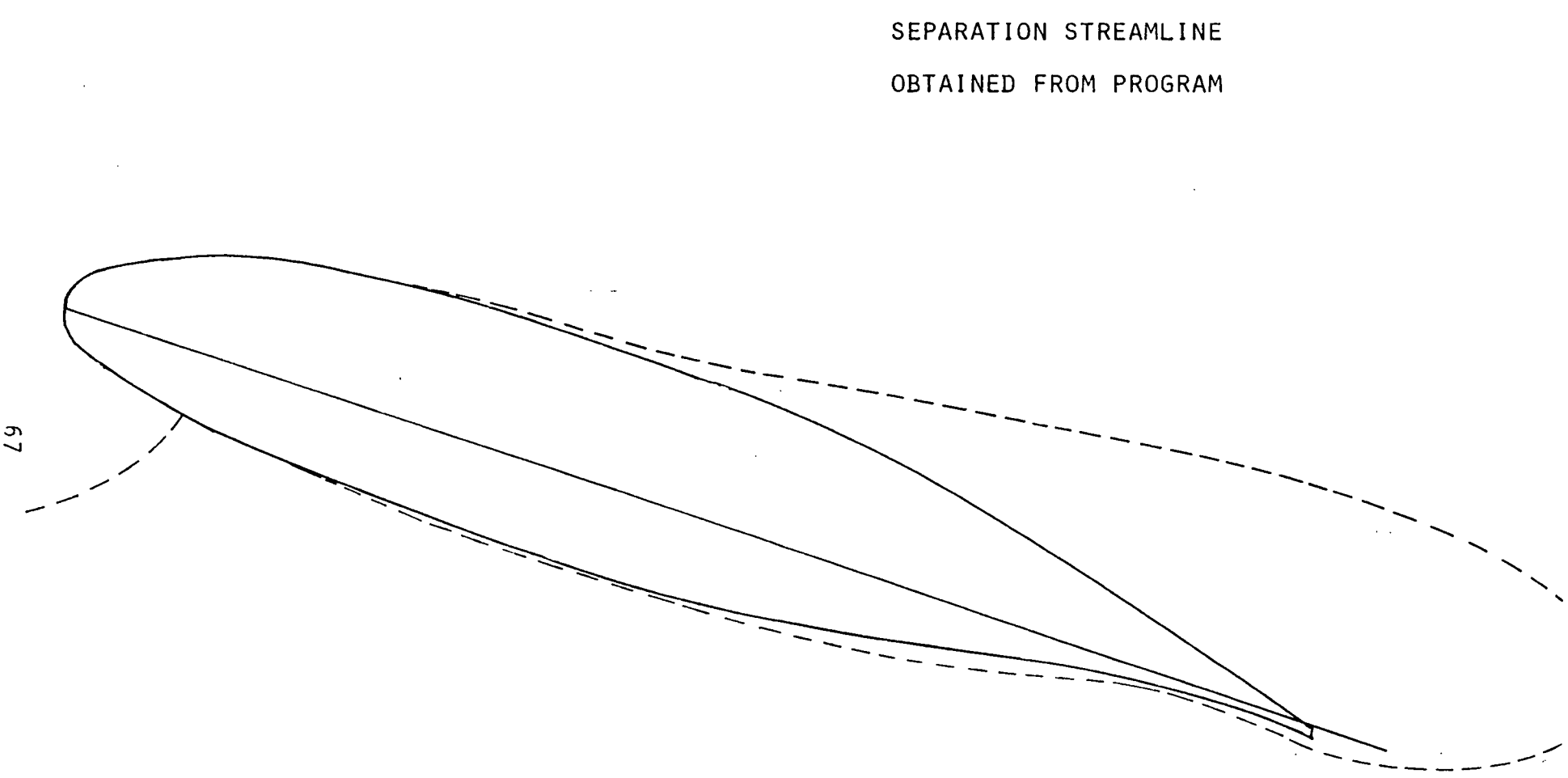

FIGURE 25 GA(W)-1 AIRFOIL AT $\alpha = 18.4^{\circ}$ SHOWING SEPARATION STREAMLINES
RN=2.5×10^{6}

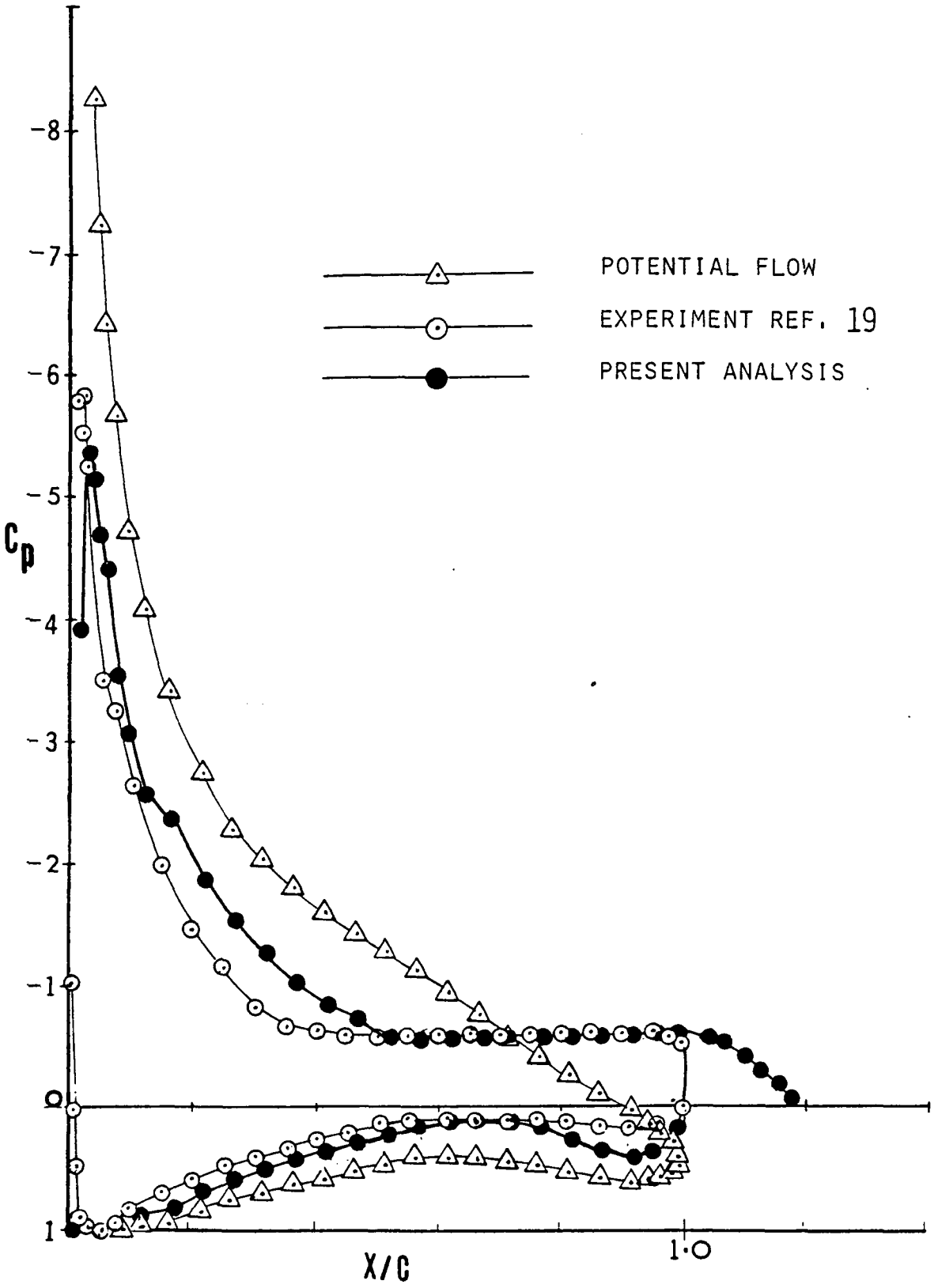

FIGURE 26 PRESSURE DISTRIBUTIONS, GA(W)-1 AIRFOIL
$\alpha = 18.4^{\circ}$, RN = 2.5×10^{6},

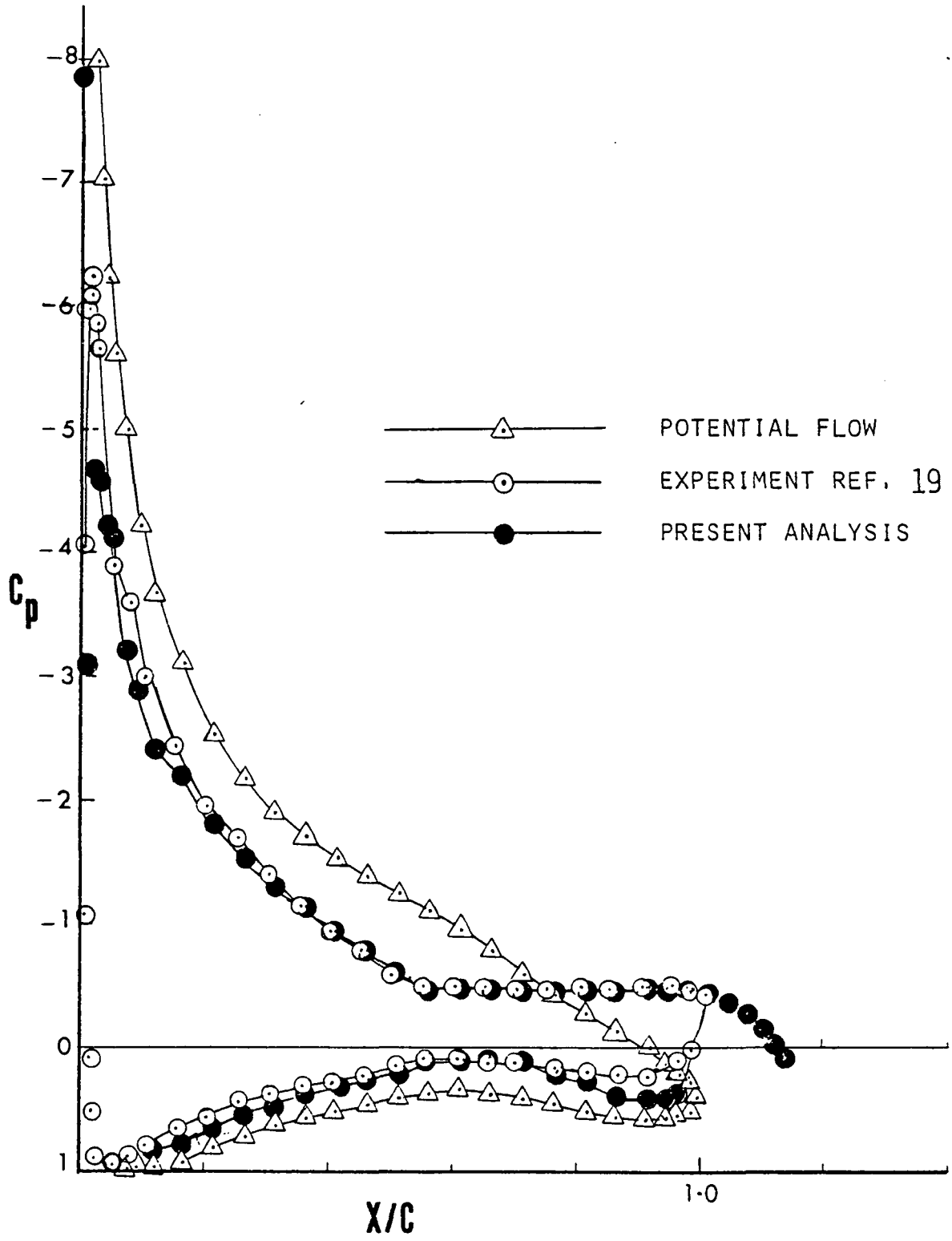

FIGURE 27 PRESSURE DISTRIBUTIONS, GA(W)-1 AIRFOIL

α = 16.4°, RN= 2.9 x 10^6

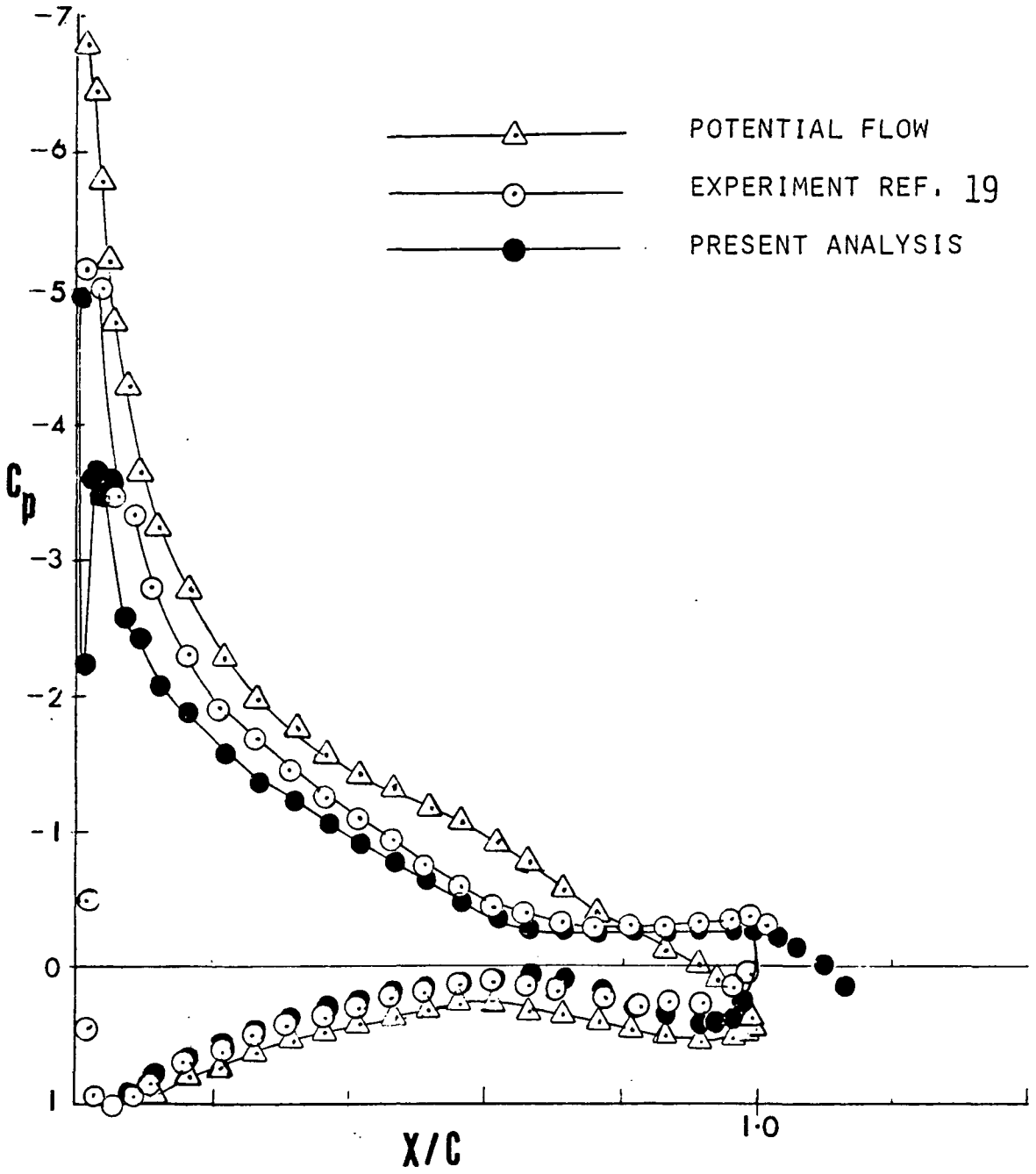

FIGURE 28 PRESSURE DISTRIBUTIONS, GA(W)-1 AIRFOIL
α = 14.4, RN= 2.9 x 10^6,

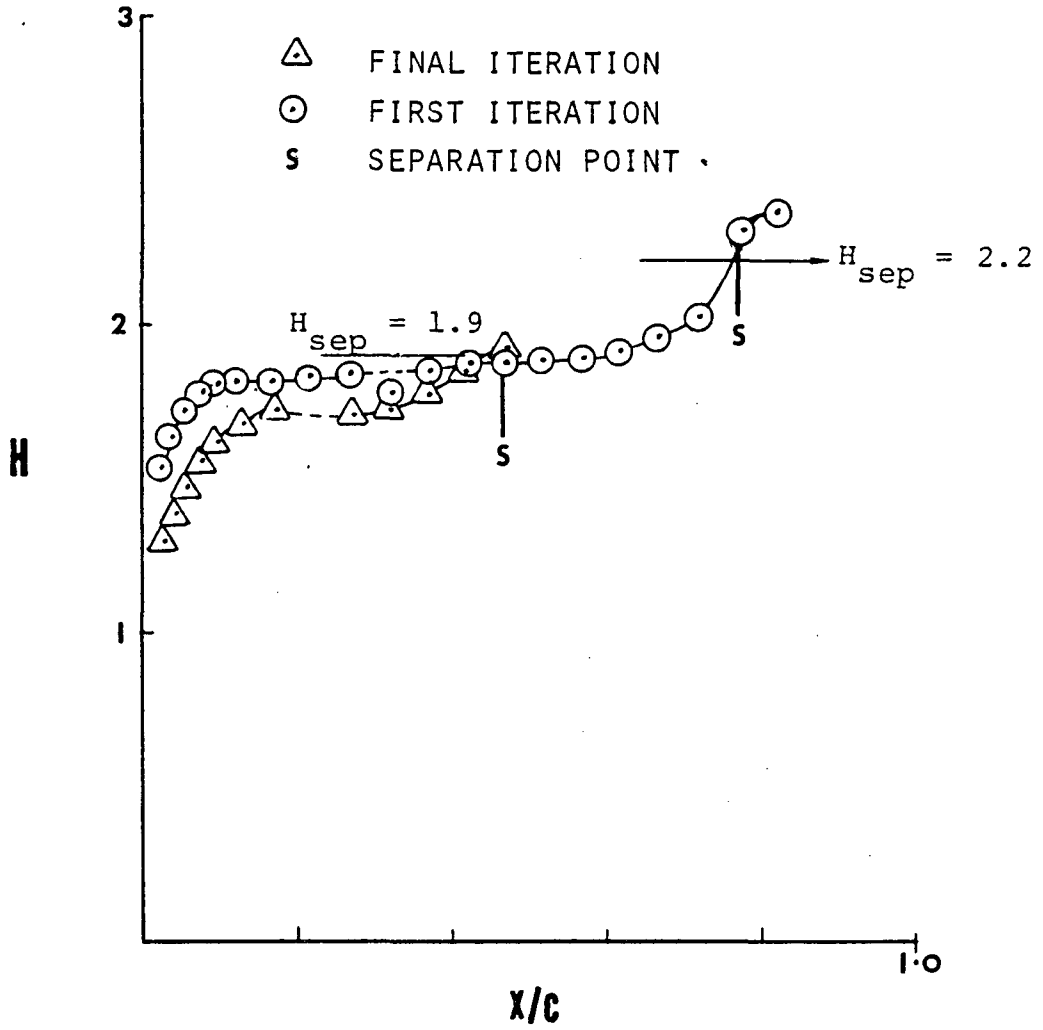

FIGURE 29 TYPICAL H-DISTRIBUTION ON UPPER SURFACE
GA(W)-1, α = 18.4°, RN = 2.5x10^6,

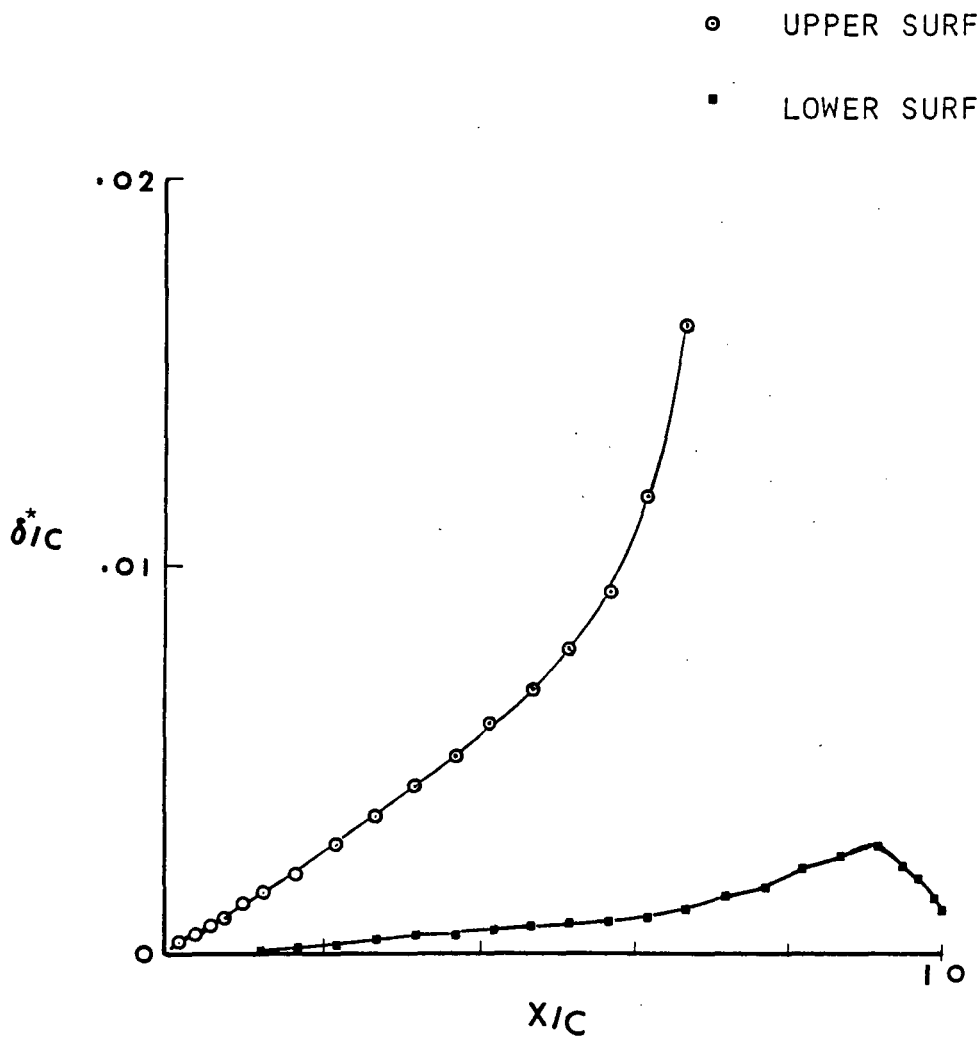

FIGURE 30 TYPICAL DISLACEMENT THICKNESS DISTRIBUTION GA(W)-1 AIRFOIL, $\alpha = 18.4°$, RN= 2.5×10^6,

			X_{SEP}		$C_{P_{SEP}}$		C_{P_R}		H_{SEP}	
α	M_∞	R N	THEORY	EXPT.	THEORY	EIPT.	THEORY	EXPT.	THEORY	EXPT.
18.4°	0.16	2.5×10^6	52%	45%	-0.583	-0.60	-0.076	no data	1.9	no data
16.4°	0.21	2.9×10^6	57%	55%	-0.496	-0.50	+0.0595	no data	1.85	no data
14.4°	0.21	2.9×10^6	65%	70%	-0.285	-0.3	+0.1602	no data	1.8	no data
18.4	0.135	2.2×10^6	44%	45%	-0.640	-0.6	-0.135	≃-0.12	1.85	1.67
14.4	0.135	2.2×10^6	60%	65%	-0.33	-0.4	0.119	≃0.0	1.80	1.81

TABLE 1. RESULTS FROM PRESENT ANALYSIS AND EXPERIMENT (REFS.2 AND 19)

TABLE 2

Typical Convergence History

$\alpha = 18.4°$, M = 0.135, RN = 2.2×10^6

	Iteration at Which Convergence is Achieved			
X_{SEP}	Convergence 1	Convergence 2	Convergence 3	H_{SEP}
91.75				2.2
86.75				2.2
76.75	3			
71.75	4			
66.75	5			
71.75	6			
71.75	7			
66.75	8			
61.75	9			
61.75	10			
61.75	11			
61.75	12	12		
61.75	13	13	13	
61.75	14	14	14	2.15
56.75	15			2.10
61.75	16			
61.75	17			
61.75	18	18		
61.75	19	19	19	
56.75	20			2.05
56.75	21			
56.75	22	22		
56.75	23	23	23	
51.75	24			
56.75	25			2.00
56.75	26			
56.75	27	27		
51.75	28			
56.75	29			
56.75	30			
56.75	31	31		
56.75	32	32	32	
51.75	33			1.95
46.75	34			
51.75	35			
51.75	36			
51.75	37	37		
51.75	38	38	38	
				1.90

TABLE 2 - continued

46.75	39			
46.75	40	40		
46.75	41	41	41	
41.75	42			1.85
41.75	43			
41.75	44	44		
41.75	45	45	45	

COMPUTER PROGRAM FORTRAN VARIABLES

A	Array for coefficients of set of equations
ALFA	Angle of attack, α
ALFB	Tan α
B	Array for coefficients of set of equations
BETA	$\beta = 1 - M_\infty^2$
C	Array for coefficients of set of equations
CF	Coefficient of friction
CPINV	Pressure coefficient of inviscid flow
CPL	Pressure coefficient on lower surface of airfoil
CPR	Pressure coefficient of rear, free, stagnation point
CPU	Pressure coefficient on upper surface of airfoil
DELSL	Displacement thickness - lower surface
DELSU	Displacement thickness - upper surface
DELX	Distance from the jet mixing "virtual origin"
DHDX	dH/dX
DQDX	$d\theta/dX$
DZDX	dZ/dX
EL	Panel width
EN	Exponent of boundary layer profile
ETAM	n_m, non-dimensionalized coordinate in jet mixing
F	Head's entrainment parameter in boundary layer
FID	$\phi_d = u_d/u_e$
FID1	ϕ_d for the previous iteration
FIDL	$\phi_{d_L} = u_d/u_e$ on lower surface

FMDOT	$\dot{M}_F$; streamwise component of recirculating mass flow in the separation bubble
GAM	Vortex strength
HL	Shape factor, H, on lower surface
HSEP	Specified H value for separation
HU	H values for upper surface
I1UD	Korst mass flow integral for the R streamline
I1UJ	Korst mass flow integral for S streamline
IJ,IK, IL,IM, IN	Counters
IPRINT	Printing counter
ISEP	Assumed separation location
ISEPT	True separation location
ITERN	Iteration counter
IU	Counter
KOUNT, KOUNT 2	Counters
MDOTDL	Mass flow into the separation bubble
MDOTDU	Mass flow out of the separation bubble
N	Total number of panels
NA	Number of panels on the airfoil
NJ	Panel number of the location of forward stagnation point on lower surface
NL	Number of panels on lower surface
NT	Number of airfoil points at which ordinates are given
NU	Number of panels on upper surface
NX	Total width of the arrays
Q	Height for reverse flow in separation bubble

R	Recovery factor (not used for low speed flow)
RMDOT	Reverse flow component of recirculating mass
SEPX	The x-coordinate of the separation point
SIGMA	σ, jet spreading rate parameter
TCPR	Temporary storage for CPR
TEMPDL	Temporary storage for DELSC
TEMPDU	Temporary storage for DELSU
TEST TEST 1 TEST 3	Convergence criteria parameters
TGAM	Vortex strengths (obtained from solving the simultaneous equations)
THETAL	Momentum thickness on lower surface
THEATU	Momentum thickness on upper surface
TRIAL 1 TRIAL 2	Convergence criteria parameters
UD	Velocity of the streamline stagnating at the free stagnation point
UINF	Free stream velocity
UL	Lower surface velocity
UNIT	Reynolds number
UU	Upper surface velocity
WL	Slope of the lower surface
WLB	Input slope of lower surface
WTE1	Initial airfoil slope
WU	Slope of the upper surface
WUB	Input slope of the upper surface
XA	X-coordinate of airfoil points
XC	X-coordinate of panel control points

XCPT	X-distance of control point from panel beginning
XE	X-coordinate of a panel beginning points
XF	Final computation point
XM	X-coordinate of panel middle points
XMI	Mach number
XO	X-coordinate of virtual origin (jet mixing)
XR	X-distance of rear stagnation point from trailing edge
XTE	Trailing edge X-coordinate
YO	Z-coordinate of the virtual origin (jet mixing)
ZC	Camber distribution
ZEL	Lower surface Z-ordinates of airfoil at panel beginning points
ZEU	Upper surface Z-ordinates of airfoil at panel beginning points
ZL	Lower surface Z-ordinates at airfoil points
ZT	Thickness distribution
ZU	Upper surface ordinates at airfoil points

COMPUTER PROGRAM INPUT AND OUTPUT DESCRIPTION

A. The program input sequence is given below:

(1) TITLE CARD

The first card contains the title in columns 1-80.

(2) PANEL DETAILS CARD

This gives the total number of panels and its distribution in the field.

N, NA, NT, NU, NL, IK (=1) are read in a (10I5) Format.

(3) FLOW PARAMETERS CARD

This inputs the Mach number, Reynolds number, Recovery Factor (not used for low speeds) and some relevant positions.

XMI, UNIT, R are read in a (3E20.6) Format and XTE, XO, XF, XCPT, WTE1 are read in a (7F10.5) Format.

(4) AIRFOIL COORDINATES CARDS

The airfoil station positions, thickness distribution and the camber distribution are read successively.

XA, ZT, ZC are read in a (7F10.5) Format.

(5) PANEL LENGTH CARD

The panel length on the airfoil as well as in the wake are given by this card.

EL, is read in a (7F10.5) Format.

(6) AIRFOIL INPUT SLOPES CARDS

The airfoil slopes determined by an auxiliary program are provided. The slopes correspond to the airfoil at the prescribed angle of attack.

WUB and WLB are read in successively in a (7F10.5) Format.

(7) ANGLE OF ATTACK CARDS

At present only one angle of attack can be read, but the program is designed so that it can be altered to read different angles of attack to get the results for various angles.

IN (=0) is read in a (I5) Format.

ALFA is read in a (6F10.5) Format.

Note: i) The value of u_r/u_e = 0.2 is included in the program. If convergence is not achieved this value may have to be changed.
ii) The values of ZEU(2) and ZEL(2) have been provided.

B. The program output is as follows:

The first iteration gives the inviscid flow results. The viscous effects are introduced in the second iteration. The value of NPRINT determines the printing sequence. At present the first and second iterations are printed and every iteration corresponding to convergence 3 is printed. The iteration corresponding to convergence 4 is also printed.

The details of the output are as follows:

(1) Station points defining panels.

(2) Ordinates of upper surface of the airfoil at the angle of attack.

(3) Ordinates of the lower surface at the angle of attack.

(4) Station points at panel midpoints.

(5) Pressure coefficients on the upper surface at panel control points of the airfoil, and the wake.

(6) Pressure coefficients on the lower surface at panel control points of the airfoil, and the wake.

(7) Slopes of the upper surface of the airfoil at angle of attack.

(8) Slopes of the lower surface of the airfoil at angle of attack.

(9) Velocity on upper surface of airfoil at panel control points.

(10) Velocity on lower surface of airfoil at panel control points.

```
C      SEPFLOW - A PROGRAM FOR SEPARATED FLOW CALCULATIONS
C                      FOR AIRFOILS AT LOW SPEEDS.
C
C      THIS PROGRAM COMPUTES THE SHAPE AND PRESSURE DISTRIBUTION OF AN
C      AIRFOIL WITH TRAILING EDGE STALL,  INCLUDING THE SEPARATION BUBBLE
C
C      WRITTEN BY SHARAD N. NAIK
C      WICHITA STATE UNIVERSITY
C      APRIL 8, 1977
C
C      THE POTENTIAL FLOW PART CONSISTING OF SUBROUTINES
C      FLSOLV, SETUP, SLOPE, PARINT AND PARINB WAS PROVIDED
C      BY MCDONNELL-DOUGLAS AIRCRAFT COMPANY.
C
C      THE SEQUENCE IN WHICH THE DATA WILL BE READ IS PROVIDED
C      IN REPORT AR77-2, DEPARTMENT OF AERONAUTICAL ENGINEERING,
C      WICHITA STATE UNIVERSITY, WICHITA, KANSAS  67208
C
       COMMON /READ/ ATITLE(20),N,NA,NT,XMI,UNIT,R,XTE,XO,XF,XCPT,WTE1,
     1        XA(51),ZT(51),ZC(51),EL(66),ALFA,WUEND
       COMMON /INT/ IU,IL,IS,ILAM,ISEP,NJ,NL,NP1,NM1,N2,NU1,NL1,IJ,IK
       COMMON /GEOM/ XE(66),XM(66),XC(66),ZUB(51),ZLB(51),ZA(66),ZB(66),
     1        ZEU(66),ZEL(66),ZZ(66),ZU(51),ZL(51)
       COMMON /PAN/ WUB(50),WLB(50),WCB(50),WU(66),WL(66),BETA,ALFB
       COMMON /PAN2/ CPL(66),CPL(66),UU(66),UL(66),ITERN
       COMMON /MAT/ A(66,67),B(66,66),C(132,132)
       COMMON /MATR/ GAM(133),SE(66),TGAM(133)
       COMMON /BLR/ HU(50),HL(50),THETAU(50),THETAL(50),DELSU(50),
     1        DELSL(50),SEPX,HSEP,CPINV(50),NJ
C
       REAL MDOTDU,MDOTDL,I1UJ,I1UU,YBU(66)
C
C      READ IN BASIC AIRFOIL DATA AND SET UP PANELS
C
       READ (5,150) (ATITLE(I),I=1,20)
       READ (5,155) N,NA,NT,NU,NL,IK
       READ (5,160) XMI,UNIT,R,XTE,XO,XF,XCPT,WTE1
C
       CPR=0.1
       HSEP=2.2
       SEPX=100.
       ISEP=NA
       KOUNT2=1
       SIGMA=12
       IPRINT=0
       I1UJ=0.399
       ETAM=0.399
       UINF=0.135*1085.104
       SOH=0.0
       NU1=NU+1
       NL1=NL+1
       NA1=NA+1
       ITERN=1
C
       DO 5 I=1,N
       CPU(I)=0.0
```

```
      CPL(I)=0.0
    5 CONTINUE
C
C     READ IN AIRFOIL COORDINATES AND SLOPES
C
      READ (5,165) (XA(I),I=1,NT)
      READ (5,165) (ZT(I),I=1,NT)
      READ (5,165) (ZC(I),I=1,NT)
      READ (5,165) (EL(I),I=1,N)
      READ (5,165) (WUB(I),I=1,NU)
      READ (5,165) (WLB(I),I=1,NL)
      READ (5,165) (ZU(I),I=1,NT)
      READ (5,165) (ZL(I),I=1,NT)
      READ (5,170,END=145) IN,ALFA
C
      ALFB=ALFA/57.29578
      ALFB=TAN(ALFB)
      XE(1)=0.0
C
      DO 10 I=1,N
      XE(I+1)=XE(I)+EL(I)
      XM(I)=XE(I)+0.5*EL(I)
      XC(I)=XE(I)+XCPT*EL(I)
   10 CONTINUE
C
      KOUNT=1
      CALL SETUP
C
      DO 15 I=1,N
      WU(I)=0.0
      WL(I)=0.0
      UU(I)=0.0
      UL(I)=0.0
      GAM(I)=0.0
   15 CONTINUE
C
      DO 20 I=1,NP1
      ZA(I)=0.0
      ZEU(I)=0.0
      ZEL(I)=0.0
      GAM(N+I)=0.0
      SE(I)=0.0
   20 CONTINUE
C
      ISEP=0
      IU=0
      IL=0
      IM=0
      IJ=0
      CCHEK=0.0
C
C     INITIALIZE THE SLOPE VALUES
C
      CALL SLOPE
      ZA(1)=ZUB(1)
      ZB(1)=ZLB(1)
```

```
C
      DO 25 I=1,NA
      ZA(I+1)=ZUB(I+1)-XE(I+1)*ALFB
      ZB(I+1)=ZLB(I+1)-XE(I+1)*ALFB
   25 CONTINUE
C
      SE(1)=2.0*(WTE1-ALFB)
      N=NA
      ISEP=NA
      IF (ITERN.EQ.1) GO TO 40
   30 CPL(NL)=CPU(ISEP)
C
      DO 35 I=NA1,N
      CPU(I)=CPU(ISEP)+(CPR-CPU(ISEP))*((3.*(XC(I)-100.)/(100.-SEPX))*
     1    *2)
      CPL(I)=CPL(NL)+(CPR-CPL(NL))*((3.*(XC(I)-100.)/(100.-SEPX))**2)
   35 CONTINUE
C
C     COMPUTE AIRFOIL PRESSURE DISTRIBUTION AND BUBBLE SHAPE
C
   40 CALL FLSOLV
      IF (ITERN.GT.1.AND.IL.EQ.1) GO TO 50
C
C     PRINT TITLE AND RESULTS FOR THE PRESENT ITERATION
C
   45 WRITE (6,175) (ATITLE(I),I=1,20),ALFA,ITERN
      WRITE (6,180) (XE(I),I=1,NP1)
      WRITE (6,185) (ZEU(I),I=1,NP1)
      WRITE (6,195) (ZEL(I),I=1,NP1)
      WRITE (6,205) (XM(I),I=1,N)
      WRITE (6,190) (CPU(I),I=1,N)
      WRITE (6,200) (CPL(I),I=1,N)
      WRITE (6,210) (XC(I),I=1,N)
      WRITE (6,215) (WU(I),I=1,N)
      WRITE (6,220) (WL(I),I=1,N)
      WRITE (6,225) (UU(I),I=1,N)
      WRITE (6,230) (UL(I),I=1,N)
C
      IF (IPRINT.EQ.2) STOP
   50 IF (IPRINT.EQ.1) GO TO 135
C
      IF (ITERN.EQ.1) GO TO 55
      GO TO 70
C
   55 DO 60 I=1,NA
      CPINV(I)=CPU(I)
      ZU(I)=ZEU(I)
      ZL(I)=ZEL(I)
   60 CONTINUE
C
      NA1=NA+1
      WRITE (6,180) (XE(I),I=1,NA1)
      WRITE (6,185) (ZEU(I),I=1,NA1)
      WRITE (6,195) (ZEL(I),I=1,NA1)
C
      ISEP=NA-4
```

```
      SEPX=XC(ISEP)
      NU=ISEP
      XR=(100.-SEPX)/3.
      NR=XR+1
      N=NR+NA
      ITERN=ITERN+1
      ISEP1=ISEP+1
C
      DO 65 I=ISEP,NA
   65 CPU(I)=CPU(ISEP)
      GO TO 30
C
C     CALCULATE THE BOUNDARY LAYER CHARACTERISTICS
C
   70 CALL BLAYR
      IF (ITERN.GT.3.AND.IL.EQ.1) GO TO 75
C
C     PRINT BOUNDARY LAYER CHARACTERISTICS FOR THE CURRENT ITERATION
C
      WRITE (6,235) (HU(I),I=1,ISEP)
      WRITE (6,240) (HL(I),I=1,NL)
      WRITE (6,245) (THETAU(I),I=1,ISEP)
      WRITE (6,250) (THETAL(I),I=1,NL)
      WRITE (6,255) (DELSU(I),I=1,ISEP)
      WRITE (6,260) (DELSL(I),I=1,NL)
C
   75 IL=1
      XR=(100.-SEPX)/3.
      NR=XR+1
      N=NR+NA
      IF (N.GT.65) STOP
      IF (KOUNT.EQ.1) GO TO 80
      GO TO 85
C
   80 TRIAL1=CPU(ISEP-3)
      KOUNT=KOUNT+1
      GO TO 30
   85 TRIAL2=CPU(ISEP-3)
C
C     PRINT TRIAL PRESSURE COEFFICIENTS
C
C     WRITE(6,88) TRIAL1,TRIAL2,CPU(ISEP)
C     88 FORMAT(30X,3F10.5)
C
      TEST=TRIAL1-TRIAL2
      IF (ABS(TEST).LT.0.01) GO TO 90
      TRIAL1=CPU(ISEP-3)
      KOUNT=KOUNT+1
      GO TO 30
C
   90 ISEP1=ISEP+1
C
C     SEPARATION BUBBLE "MASS-IN / MASS-OUT" CONDITION
C
      UU(ISEP)=UU(ISEP)*UINF
      UL(NA)=UL(NA)*UINF
```

```
      XO=30.*THETAU(ISEP)
      YO=DELSU(ISEP)+THETAU(ISEP)
C
      DO 95 I=ISEP,N
   95 YBU(I)=DELSU(ISEP)-YO+((XC(I)-SEPX)*ETAM/SIGMA)
C
      EN=2./(HL(NL)-1)
      UO=UINF*SQRT(CPR-CPU(ISEP))
      FID=UO/UU(ISEP)
      FID1=0.612
      TEST1=0.0
C
  100 I1UO=0.11402-0.2045*FID+1.0817*FID*FID
      MDOTDU=(UU(ISEP)*(XE(NA1)-XC(ISEP)+XO)/SIGMA)*(I1UJ-I1UO)
      MDOTDL=UL(NA)*DELSL(NA)*((UO/UL(NA))**(EN+1.))*EN*((EN+1.)**(-1.
     1    /EN))/(EN+1.)
C
C     PRINT THE MASS FLOW IN AND MASS FLOW OUT
C
C     WRITE(6,102) MDOTDU,MDOTDL,UO
C     102 FORMAT(1X,3F15.5)
C
      TEST=MDOTDU-MDOTDL
      IF (ABS(TEST).LE.0.001) GO TO 105
      HOLD=FID
      FID=FID-TEST*(FID1-FID)/(TEST1-TEST)
      FID1=HOLD
      TEST1=TEST
      UO=FID*UU(ISEP)
      GO TO 100
C
C     PRINT REAR ATTACHMENT POINT PRESSURE
C
  105 CPR=CPU(ISEP)+((UO/UINF)**2)
      WRITE (6,265) CPR
      IF (KOUNT2.EQ.1) GO TO 110
      GO TO 115
C
  110 TCPR=CPR
      KOUNT2=KOUNT2+1
      GO TO 30
C
  115 TEST=ABS(TCPR-CPR)
      IF (TEST.LE.0.001) GO TO 120
      TCPR=CPR
      GO TO 30
C
C     BUBBLE VORTEX MASS FLOW CONDITION
C
  120 ZUT=-0.07
      FIDL=UO/UL(NA)
      DELX=XE(NA1)+XO-SEPX
      Q=ZEU(NA)+XC(NA)*ALFB-ZUT+YO)-(2.39893*DELX/SIGMA)-DELSU(ISEP)
     1    -DELSL(NL)*(EN+1)*(FIDL**EN)
      FMDOT=(UU(ISEP)*DELX/SIGMA)*(I1UO-0.2821+0.25054)
      RMDOT=0*0.20*UU(ISEP)+0.0886*UU(ISEP)*DELX/SIGMA
```

```
      TEST3=ABS(RMDOT)-ABS(FMDOT)
C
C     PRINT BUBBLE MASS FLOW VALUES
C
C     WRITE (6,122) RMDOT,FMDOT,HSEP,SEPX,CPU(ISEP)
C     122 FORMAT(1X,5F15.5)
C
      IL=IL+1
      IF (TEST3.GT.0.0) GO TO 125
      GO TO 130
C
  125 HSEP=HSEP-0.05
      QU(ISEP)=QU(ISEP)/QINF
      QL(NA)=QL(NA)/QINF
      GO TO 30
C
C     PRINT SEPARATION POINT SHAPE FACTOR
C
C     125 WRITE(6,126) HSEP
C     126 FORMAT(1X,'HSEP = ',F5.2)
C
  130 IPRINT=1
      GO TO 45
  135 ISEP=ISEP+1
      IPRINT=2
      CPU(ISEP)=2*CPU(ISEP-1)-CPU(ISEP-2)
C
      DO 140 I=ISEP,NA
      CPU(I)=CPU(ISEP)
  140 CONTINUE
      GO TO 30
C
  145 STOP
C
  150 FORMAT (20A4)
  155 FORMAT (10I5)
  160 FORMAT (3E20.6/7F10.5)
  165 FORMAT (7F10.5)
  170 FORMAT (I5,6F10.5)
  175 FORMAT (1H1,25X,'AIRFOIL WITH VISCOUS EFFECTS INCLUDING THE ',
     1         'POSSIBILITY OF TRAILING EDGE STALL'/26X,20A4/1HO,
     2         'ALPHA =',F10.5,' DEGREES',5X,'ITERATION NUMBER =',I3/1HO
  180 FORMAT ('0STATION POINTS DEFINING PANELS'/(1H ,10F12.5))
  185 FORMAT ('0ORDINATES OF UPPER SURFACE'/(1H ,10F12.5))
  190 FORMAT ('0PRESSURE COEFFICIENTS ON UPPER SURFACE'/(1H ,10F12.5))
  195 FORMAT ('0ORDINATES OF LOWER SURFACE'/(1H ,10F12.5))
  200 FORMAT ('0PRESSURE COEFFICIENTS ON LOWER SURFACE'/(1H ,10F12.5))
  205 FORMAT ('0STATION POINTS AT PANEL MIDPOINTS'/(1H ,10F12.5))
  210 FORMAT ('0STATION POINTS AT PANEL CONTROL POINTS'/(1H ,10F12.5))
  215 FORMAT ('0SLOPES OF UPPER SURFACE'/(1H ,10F12.5))
  220 FORMAT ('0SLOPES OF LOWER SURFACE'/(1H ,10F12.5))
  225 FORMAT ('0VELOCITY ON UPPER SURFACE XC'/(1H ,10F12.5))
  230 FORMAT ('0VELOCITY ON LOWER SURFACE XC'/(1H ,10F12.5))
  235 FORMAT (' HU',10F10.5)
  240 FORMAT (' HL',10F10.5)
  245 FORMAT (' THETAU',10F10.5)
```

```
250 FORMAT (' THETAL',10F10.5)
255 FORMAT (' DELSU ',10F10.5)
260 FORMAT (' DELSL ',10F10.5)
265 FORMAT (5X,'CPR = ',F10.5)
    END
```

```
      SUBROUTINE SETUP
C
C     THIS SUBROUTINE READS DATA DEFINING AIRFOIL SHAPE, SETS UP PANELS
C     ALONG THE AIRFOIL CENTERLINE AND FINDS COMPUTING RATIOS OF PANELS
C     THIS HAS TO BE DONE ONLY ONCE FOR EACH AIRFOIL.
C
      COMMON /READ/ ATITLE(20),N,NA,NT,XMI,UNIT,R,XTE,XO,XF,XCPT,WTE1,
     1       XA(51),ZT(51),ZC(51),EL(66),ALFA,WUEND
      COMMON /INT/ IU,IL,IS,ILAM,ISEP,NU,NL,NP1,NM1,N2,NU1,NL1,IJ,IK
      COMMON /GEOM/ XE(66),XM(66),XC(66),ZUB(51),ZLB(51),ZA(66),ZB(66),
     1       ZEU(66),ZEL(66),ZZ(66),ZU(51),ZL(51)
      COMMON /PAN/ WUB(50),WLB(50),WCB(50),WU(66),WL(66),BETA,ALFB
      COMMON /PAN2/ CPU(66),CPL(66),UU(66),UL(66),ITERN
      COMMON /MAT/ A(66,67),B(66,66),C(132,132)
C
C
C     INDICATOR IK = 0   VISCOUS SOLUTIONS AT VARIOUS ALPHA
C              IK = 1   INVISCID SOLUTIONS AT VARIOUS ALPHA
C              IK = 2   VARIOUS INVISCID SOLUTIONS
C
C     IF NU OR NL IS LESS THAN NA, SOLUTION WILL BE FOUND FOR THE MIXED
C     BOUNDARY CONDITIONS OF GEOMETRY SPECIFIED UP TO PANEL NU OR NL
C     AND PRESSURE COEFFICIENTS ON SUBSEQUENT PANELS.
C
    5 WRITE (6,30) (ATITLE(I),I=1,20)
      WRITE (6,35) N,NA,NT
      WRITE (6,40) XMI,UNIT,R,XTE,XO,XF,XCPT,WTE1
      WRITE (6,45) (XA(I),I=1,NT)
      WRITE (6,50) (ZT(I),I=1,NT)
      WRITE (6,55) (ZC(I),I=1,NT)
      WRITE (6,60) (WUB(I),I=1,NU)
      WRITE (6,65) (WLB(I),I=1,NL)
C
      PI=3.1415927
      TPI=2.0*PI
      XM2=XMI*XMI
      BETA=SQRT(1.0-XM2)
      NP1=N+1
      NM1=N-1
      N2=2.0*N
C
C     FIND COMPUTING RATIOS OF PANELS
C
      DO 10 I=1,N
      A(I,NP1)=0.0
      DO 10 J=1,N
      A(I,J)=0.0
      B(I,J)=(1.0/TPI)*(ALOG(ABS((XC(I)-XE(J+1))/(XC(I)-XE(J)))))
   10 CONTINUE
C
      DO 15 I=1,N
      DO 15 J=1,N
      T1=ALOG(ABS((XM(I)-XE(J+1))/(XM(I)-XE(J))))
      A(I,J)=(T1-1.0)/PI-T1*(XM(I)-XE(J))/(PI*EL(J))+A(I,J)
      A(I,J+1)=1.0/PI+T1*(XM(I)-XE(J))/(PI*EL(J))+A(I,J+1)
   15 CONTINUE
```

```
C
      DO 20 I=1,N
      DO 20 J=1,NP1
      A(I,J)=A(I,J)/DETA
   20 CONTINUE
C
      ZUB(1)=ZT(1)
      ZLB(1)=ZT(1)
C
C     CALCULATE SLOPE AT THE CONTROL POINTS
C     INTEGRATE THE SLOPES TO OBTAIN AIRFOIL ORDINATES
C
      DO 25 I=1,NA
      XX=XC(I)
      CALL PARINT (XA,ZC,1,NT,XX,XX,Z,W1,ZI)
      WCB(I)=W1
      XX=XE(I+1)
      CALL PARINB (XA,ZT,1,NT,XX,XX,Z,W,ZI,I)
      IF (I.EQ.1) Z=ZT(2)*SQRT(XE(2)/XA(2))
      CALL PARINT (XA,ZC,1,NT,XX,XX,Z1,W,ZI)
      ZUB(I+1)=Z+Z1
      ZLB(I+1)=-Z+Z1
   25 CONTINUE
C
      RETURN
C
   30 FORMAT (1H1,25X,'AIRFOIL WITH VISCOUS EFFECTS INCLUDING THE ',
     1          'POSSIBILITY OF TRAILING EDGE STALL'/26X,20A4/1H0)
   35 FORMAT (1H0,17X,'TOTAL NUMBER OF PANELS =',I4/
     1        13X,'NUMBER OF PANELS IN AIRFOIL =',I4/
     2        7X,'NUMBER OF POINTS DEFINING AIRFOIL =',I4)
   40 FORMAT (29X,'MACH NUMBER =',E12.5/
     1        24X,'UNIT REYNOLDS NO =',E12.5/
     2        25X,'RECOVERY FACTOR =',E12.5/
     3        19X,'TRAILING EDGE STATION =',E12.5/
     4        4X,'DISTANCE FROM T.E. TO BUBBLE CLOSURE =',E12.5/
     5        15X,'FINAL COMPUTATION STATION =',E12.5/
     6        9X,'DISTANCE TO PANEL CONTROL POINT =',E12.5/
     7        13X,'INITIAL AIRFOIL SLOPE =',E12.5/1H0)
   45 FORMAT ('0STATION POINTS DEFINING AIRFOIL'/(1H0,10F12.5))
   50 FORMAT ('0ORDINATES OF THICKNESS DISTRIBUTION'/(1H0,10F12.5))
   55 FORMAT ('0ORDINATES OF CAMBER DISTRIBUTION'/(1H0,10F12.5))
   60 FORMAT ('0SPECIFIED UPPER SURFACE SLOPES'/(1H0,10F12.5))
   65 FORMAT ('0SPECIFIED LOWER SURFACE SLOPES'/(1H0,10F12.5))
      END
```

```
      SUBROUTINE SLOPE
C
C     INITIALIZE THE SLOPE VALUES
C
      COMMON /READ/ ATITLE(20),N,NA,NT,XMI,UNIT,R,XTE,XO,XF,XCPT,WTEL,
     1       XA(51),ZT(51),ZC(51),EL(66),ALFA,WUEND
      COMMON /INT/ IU,IL,IS,ILAM,ISEP,NJ,NL,NP1,NM1,N2,NU1,NL1,IJ,IK
      COMMON /GEOM/ XE(66),XM(66),XC(66),ZUB(51),ZLB(51),ZA(66),ZB(66),
     1       ZEU(66),ZEL(66),ZZ(66),ZU(51),ZL(51)
      COMMON /PAN/ WUB(50),WLB(50),WCB(50),WU(66),WL(66),BETA,ALFB
      COMMON /PAN2/ CPU(66),CPL(66),UU(66),UL(66),ITERN
      COMMON /MAT/ A(66,67),B(66,66),C(132,132)
C
      ZEU(1)=ZT(1)
      DO 5 I=2,NU1
      ZEU(I)=ZUB(I)
    5 CONTINUE
C
      ZEL(1)=ZT(1)
      DO 10 I=2,NL1
      ZEL(I)=ZLB(I)
   10 CONTINUE
C
      DO 15 I=1,NU
      WU(I)=WUB(I)
   15 CONTINUE
C
      DO 20 I=1,NL
      WL(I)=WLB(I)
   20 CONTINUE
C
      RETURN
      END
```

```
      SUBROUTINE FLSOLV
C
C     THIS SUBROUTINE TAKES GEOMETRY, ESTABLISHES PRESSURES ON SPECIFIE
C     PANELS AND THEN SOLVES FOR PRESSURES OR GEOMETRY AS APPROPRIATE.
C     THE SHAPE AND PRESSURE DISTRIBUTION IS PRINTED OUT.
C
      COMMON /READ/ ATITLE(20),N,NA,NT,XMI,UNIT,R,XTE,XO,XF,XCPT,WTE1,
     1       XA(51),ZT(51),ZC(51),EL(66),ALFA,WUEND
      COMMON /INT/ IU,IL,IS,ILAM,ISEP,NU,NL,NP1,NM1,N2,NU1,NL1,IJ,IK
      COMMON /GEOM/ XE(66),XM(66),XC(66),ZUB(51),ZLB(51),ZA(66),ZB(66),
     1       ZEU(66),ZEL(66),ZZ(66),ZU(51),ZL(51)
      COMMON /PAN/ WUB(50),WLB(50),WCB(50),WU(66),WL(66),BETA,ALFB
      COMMON /PAN2/ CPU(66),CPL(66),UU(66),UL(66),ITERN
      COMMON /MAT/ A(66,67),B(66,66),C(132,132)
      COMMON /MATR/ GAM(133),SE(66),TGAM(133)
C
      DIMENSION WUI(66), WLI(66), XCI(66), CPT(66)
      DIMENSION WC(66)
C
      NX=132
      DO 5 I=1,N
      GAM(I)=0.0
      GAM(N+I)=0.0
      SE(I)=0.0
    5 CONTINUE
C
      N2P1=2*N+1
      GAM(N2P1)=0.0
      SE(NP1)=0.0
C
C     ESTABLISH BOUNDARY CONDITIONS ON APPROPRIATE PANELS
C
      T2=0.5*XCPT
      T3=0.5*(1.0-XCPT)
      N2=2.0*N
      NP1=N+1
C
      DO 10 I=1,N2
      DO 10 J=1,N2
      C(I,J)=0.0
   10 CONTINUE
C
      DO 45 I=1,N
      IF (ITERN.EQ.1) GO TO 15
      GO TO 20
   15 IF (I.GT.NU) GO TO 35
      GO TO 25
   20 IF (I.GE.NU) GO TO 35
   25 GAM(I)=WU(I)
      IF (I.EQ.1) GAM(1)=GAM(1)-T3*SE(1)
C
      DO 30 J=1,N
      C(I,J)=B(I,J)
   30 CONTINUE
C
      C(I,N+I)=T2
```

```
      IF (I.NE.1) C(I,N+I-1)=T3
      GO TO 45
C
   35 CPU(I)=2.*(1.0-SQRT(1.0-CPU(I)))
      GAM(I)=CPU(I)-A(I,1)*SE(1)
      C(I,I)=-1.0/BETA
C
      DO 40 J1=2,NP1
      J=N+J1-1
      C(I,J)=A(I,J1)
   40 CONTINUE
   45 CONTINUE
C
      DO 80 I=1,N
      IF (ITERN.EQ.1) GO TO 50
      GO TO 55
   50 IF (I.GT.NL) GO TO 70
      GO TO 60
   55 IF (I.GE.NL) GO TO 70
   60 GAM(N+I)=WL(I)
      IF (I.EQ.1) GAM(N+1)=GAM(N+1)+T3*SE(1)
C
      DO 65 J=1,N
   65 C(N+I,J)=B(I,J)
C
      C(N+I,N+I)=-T2
      IF (I.NE.1) C(N+I,N+I-1)=-T3
      GO TO 80
C
   70 CPL(I)=2.*(1.0-SQRT(1.0-CPL(I)))
      GAM(N+I)=CPL(I)-A(I,1)*SE(1)
      C(N+I,I)=1.0/BETA
C
      DO 75 J1=2,NP1
      J=N+J1-1
      C(N+I,J)=A(I,J1)
   75 CONTINUE
   80 CONTINUE
C
C     SOLVE FOR SOURCE AND VORTEX STRENGTHS
C
      CALL SIMEQ (C,GAM,TGAM,N2,NX)
C
      DO 85 I=2,NP1
      SE(I)=TGAM(N+I-1)
   85 CONTINUE
C
      DO 115 I=1,N
      VC(I)=0.0
      CPT(I)=A(I,NP1)*SE(NP1)
C
      DO 90 J=1,N
      CPT(I)=CPT(I)+A(I,J)*SE(J)
   90 VC(I)=VC(I)+B(I,J)*TGAM(J)
C
      TL=(SE(I)+XCPT*(SE(I+1)-SE(I)))/2.0
```

```
      WU(I)=WC(I)+T1
      WL(I)=WC(I)-T1
      UU(I)=1.0-0.5*(CPT(I)-TGAM(I)/BETA)
      IF (ITERN.NE.1) GO TO 95
      IF (I.LE.NU) UU(I)=UU(I)/SQRT(1.0+WU(I)**2)
      GO TO 100
C
   95 IF (I.LT.NU) UU(I)=UU(I)/SQRT(1.0+WU(I)**2)
  100 CPU(I)=1.0-UU(I)**3/ABS(UU(I))
      UL(I)=1.0-0.5*(CPT(I)+TGAM(I)/BETA)
      IF (ITERN.NE.1) GO TO 105
      IF (I.LE.NL) UL(I)=UL(I)/SQRT(1.0+WL(I)**2)
      GO TO 110
  105 IF (I.LT.NL) UL(I)=UL(I)/SQRT(1.0+WL(I)**2)
  110 CPL(I)=1.0-UL(I)**3/ABS(UL(I))
  115 CONTINUE
C
C     THE AIRFOIL SLOPES CAN NOW BE INTEGRATED TO FIND
C     THE SHAPE OF THE AIRFOIL AND SEPARATION BUBBLE.
C
      ZEU(1)=ZT(1)
      WUI(1)=SE(1)/2.0
      ZEL(1)=ZT(1)
      WLI(1)=-SE(1)/2.0
      XCI(1)=0.0
C
      DO 120 I=2,NP1
      WUI(I)=WU(I-1)
      WLI(I)=WL(I-1)
  120 XCI(I)=XC(I-1)
C
      ZEU(2)=1.325
      ZEL(2)=-2.25
C
      DO 125 I=3,NP1
      XX=XE(I)
      XO=XE(I-1)
      CALL PARINT (XCI,WUI,1,NP1,XO,XX,Z,W,ZI)
      ZEU(I)=ZEU(I-1)+ZI
      CALL PARINT (XCI,WLI,1,NP1,XO,XX,Z,W,ZI)
  125 ZEL(I)=ZEL(I-1)+ZI
      RETURN
      END
```

```
      SUBROUTINE BLAYR
C
C     THIS ROUTINE COMPUTES THE BOUNDARY LAYER CHARACTERISTICS
C           USING THE VELOCITIES FROM FLSOLV.
C
      COMMON /READ/ ATITLE(20),N,NA,NT,XMI,UNIT,R,XTE,XO,XF,XCPT,NTE1,
     1      XA(51),ZT(51),ZC(51),EL(66),ALFA,WUEND
      COMMON /INT/ IU,IL,IS,ILAM,ISEP,NU,NL,NP1,NM1,N2,NU1,NL1,IJ,IK
      COMMON /GEOM/ XE(66),XM(66),XC(66),ZUB(51),ZLB(51),ZA(66),ZB(66),
     1      ZEU(66),ZEL(66),ZZ(66),ZU(51),ZL(51)
      COMMON /PAN/ WUB(50),WLB(50),WCB(50),WU(66),WL(66),BETA,ALFB
      COMMON /PAN2/ CPU(66),CPL(66),UU(66),UL(66),ITERN
      COMMON /BLR/ HU(50),HL(50),THETAU(50),THETAL(50),DELSU(50),
     1      DELSL(50),SEPX,HSEP,CPINV(50),NJ
      DIMENSION TEMPDU(50), TEMPDL(50)
C
      ALFAR=ALFA/57.29578
      CALL CONV
      THETAU(1)=0.005
      THETAL(1)=0.005
      HU(1)=1.5
      HL(1)=1.5
      UINF=0.135*1085.104
      I=1
C
    5 I=I+1
      IF (I.GT.NA) GO TO 25
      HUB=HU(I-1)
      THETAB=THETAU(I-1)
      F=0.025*HU(I-1)-0.022
      CF=0.058*((0.93-1.95*ALOG10(HU(I-1)))**1.705)*((22000.*THETAU(I
     1    -1))**(-0.268))
      DUDX=0.5*CF-(THETAU(I-1)*(UU(I)-UU(I-1))*(HU(I-1)+2.))/(UU(I)
     1    *(XC(I)-XC(I-1)))
      DHDX=(0.5*HU(I-1)*(HU(I-1)-1.)/THETAU(I-1))*(CF-(F*(HU(I-1)-1.)
     1    /HU(I-1))-(2.*THETAU(I-1)*(UU(I)-UU(I-1))*(HU(I-1.)+1.)
     2    /(UU(I)*(XC(I)-XC(I-1)))))
      THETAU(I)=THETAB+DUDX*(XC(I)-XC(I-1))
      IF (THETAU(I).LE.0.0) THETAU(I)=THETAU(I-1)/2.0
      HU(I)=HUB+DHDX*(XC(I)-XC(I-1))
C
C     PRINT H-VALUE
C
C     WRITE(6,8) HU(I)
C     8  FORMAT(1X,F10.5)
C
      IF (HU(2).GT.1.6) HU(2)=1.45
      IF (HU(I).LE.1.0) HU(I)=1.05
      IF (HU(I).GE.3.0) HU(I)=HSEP-.3
      IF (XC(I).LE.15) GO TO 5
      IF (HU(I).GT.HSEP) GO TO 10
      IF (I.EQ.ISEP) GO TO 15
      GO TO 5
C
   10 IF (I.LT.ISEP) ISEP=ISEP-1
      ISEPT=I
```

```
      CPUP=CPU(ISEP+1)
      GO TO 20
C
   15 ISEP=ISEP+1
      CPU(ISEP)=2.*CPU(ISEP-1)-CPU(ISEP-2)
      CPU(ISEP)=(CPU(ISEP)+CPUP)/2.
      ISEPT=I
C
   20 SEPX=XC(ISEP)
   25 J=2
      IF (CPL(J-1).GT.1.0) CPL(J-1)=1.0
   30 J=J+1
      IF (CPL(J-1).GT.1.0) CPL(J-1)=1.0
      IF ((CPL(J-1)-CPL(J-2)).GE.0.0) GO TO 30
      NJ=J
C
C     PRINT LOCATION OF THE AIRFOIL FRONT STAGNATION POINT
C
C     WRITE(6,33) NJ
C     33 FORMAT(10X,I3)
C
      HL(NJ-1)=1.4
      THETAL(NJ-1)=0.005
C
      DO 35 I=NJ,NL
      THETAB=THETAL(I-1)
      HLB=HL(I-1)
      F=0.025*HL(I-1)-0.022
      CF=0.058*((0.93-1.95*ALOG10(HL(I-1)))**1.705)*((22000.*THETAL(I
     1    -1))**(-0.268))
      DODX=0.5*CF-(THETAL(I-1)*(UL(I)-UL(I-1))*(HL(I-1)+2.))/(LL(I)
     1    *(XC(I)-XC(I-1)))
      DHDX=(0.5*HL(I-1)*(HL(I-1)-1.)/THETAL(I-1))*(CF-(F*(HL(I-1)-1.)
     1    /HL(I-1))-(2.*THETAL(I-1)*(UL(I)-UL(I-1))*(HL(I-1.)+1.)
     2    /(UL(I)*(XC(I)-XC(I-1)))))
      THETAL(I)=THETAB+DODX*(XC(I)-XC(I-1))
      IF (THETAL(I).LE.0.0) THETAL(I)=THETAL(I-1)/2.0
      HL(I)=HLB+DHDX*(XC(I)-XC(I-1))
      IF (HL(NJ).GT.1.6) HL(NJ)=1.45
      IF (HL(I).LE.1.0) HL(I)=1.05
      IF (HL(I).GE.3.0) HL(I)=HSEP-0.3
   35 CONTINUE
C
      THETAL(NL)=THETAL(NL-1)+(THETAL(NL-1)-THETAL(NL-2))*(XC(NL)-XC(NL
     1    -1))/(XC(NL-1)-XC(NL-2))
      HL(NL)=HL(NL-1)+(HL(NL-1)-HL(NL-2))*(XC(NL)-XC(NL-1))/(XC(NL-1)
     1    -XC(NL-2))
C
      DO 40 I=1,ISEPT
   40 DELSU(I)=HU(I)*THETAU(I)
C
      ISEPT1=ISEPT+1
      DO 45 I=ISEPT1,N
   45 DELSU(I)=DELSU(ISEPT)
C
      DO 50 I=NJ,NL
```

```
   50 DELSL(I)=HL(I)*THETAL(I)
      NSU=NA/2
C
      DO 55 I=1,NSU
   55 IF (DELSU(I).GT.DELSU(I+1)) DELSU(I)=DELSU(I+1)
      NSL=(NA+NJ)/2
C
      DO 60 I=NJ,NSL
   60 IF (DELSL(I).GT.DELSL(I+1)) DELSL(I)=DELSL(I+1)
C
      IF (ITERN.LT.4) GO TO 75
      IF (ISEP.GT.ISEPG) TEMPDU(ISEP)=DELSU(ISEP)
C
      DO 65 I=1,ISEP
   65 DELSU(I)=(DELSU(I)+TEMPDU(I))/2.
C
      IF (NJ.LT.NJO) TEMPDL(NJ)=DELSL(NJ)
      DO 70 I=NJ,NL
   70 DELSL(I)=(DELSL(I)+TEMPDL(I))/2.
C
   75 DO 80 I=1,ISEPT
   80 ZEU(I)=ZU(I)+DELSU(I)
C
      DO 85 I=ISEPT1,ISEP
   85 ZEU(I)=ZU(I)+DELSU(ISEPT)
C
      ISEP1=ISEP+1
      DO 90 I=ISEP1,N
   90 ZEU(I)=ZEU(I)+DELSU(ISEPT)
C
      DELSL(NJ)=0.005
      DELSL(NJ+1)=0.01
      DELSL(NJ+2)=0.015
C
      DO 95 I=NJ,NL
   95 ZEL(I)=ZL(I)-DELSL(I)
C
      NL1=NL+1
      IF (N.LE.NL) GO TO 105
C
      DO 100 I=NL1,N
  100 ZEL(I)=ZEL(I)-DELSL(NL)
C
  105 NU=ISEP
      NU1=NU+1
C
      DO 110 I=NU,NA
  110 CPU(I)=CPU(ISEP)
C
      DO 115 I=1,NU
  115 TEMPDU(I)=DELSU(I)
C
      DO 120 I=NJ,NL
  120 TEMPDL(I)=DELSL(I)
C
      ISEPG=ISEP
```

```
      NJG=NJ
C
C     CALCULATE NEW SLOPES
C
      CALL AFSL
      WL(9)=(WL(10)+WL(8))/2.
C
C     SMOOTH OUT LAST TEN PANEL SLOPES
C
      CALL LEASQ
      ITERN=ITERN+1
C
      RETURN
      END
```

```
      SUBROUTINE CONV
C
C     FIND THE ORDINATES AT THE CONTROL POINTS
C
      COMMON /READ/ ATITLE(20),N,NA,NT,XMI,UNIT,R,XTE,XO,XF,XCPT,WTE1,
     1       XA(51),ZT(51),ZC(51),EL(66),ALFA,WUEND
      COMMON /INT/ IU,IL,IS,ILAM,ISEP,NU,NL,NP1,NM1,N2,NU1,NL1,IJ,IK
      COMMON /GEOM/ XE(66),XM(66),XC(66),ZUB(51),ZLB(51),ZA(66),ZB(66),
     1       ZEU(66),ZEL(66),ZZ(66),ZU(51),ZL(51)
      COMMON /PAN/ WUB(50),WLB(50),WCB(50),WU(66),WL(66),BETA,ALFB
      COMMON /PAN2/ CPU(66),CPL(66),UU(66),UL(66),ITERN
C
      DO 5 J=1,N
    5 ZZ(J)=ZEU(J)
C
      MUCH=N-2
      K=1
   10 L=1
      I=0
   15 I=I+1
      IF (I.GT.MUCH) GO TO 35
C
   20 TERM1=(ZZ(I+1)-ZZ(I))/(XE(I+1)-XE(I))
      TERM2=(ZZ(I+2)-ZZ(I+1))/(XE(I+2)-XE(I+1))
      C=(TERM2-TERM1)/(XE(I+2)-XE(I))
      B=TERM1-C*(XE(I)+XE(I+1))
      A=ZZ(I)-B*XE(I)-C*XE(I)*XE(I)
C
   25 XI=XC(L)
      IF (XI.LT.XE(I)) GO TO 30
      IF (XI.EQ.XE(I)) GO TO 50
      IF (XI.GT.XE(I+1)) GO TO 15
      GO TO 35
C
   30 I=I-1
      IF (I.GT.0) GO TO 20
      ZI=0.0
      GO TO 40
C
   35 ZI=A+B*XI+C*XI*XI
   40 IF (K.EQ.1) GO TO 65
      IF (K.EQ.2) GO TO 70
C
   45 IF (L.GE.N) GO TO 55
      L=L+1
      GO TO 25
   50 ZI=ZZ(I)
      GO TO 40
   55 IF (K.EQ.2) GO TO 75
      K=K+1
C
      DO 60 J=1,N
   60 ZZ(J)=ZEL(J)
      GO TO 10
C
   65 ZEU(L)=ZI
```

```
      GO TO 45
   70 ZEL(L)=ZI
      GO TO 45
C
   75 IF (ITERN.EQ.1) GO TO 80
      GO TO 90
C
   80 DO 85 I=1,NA
      ZU(I)=ZEU(I)
      ZL(I)=ZEL(I)
   85 CONTINUE
C
   90 RETURN
      END
```

```
      SUBROUTINE LEASQ
C
C     SMOOTH OUT THE LAST TEN PANEL SLOPES ON THE LOWER SURFACE
C
      COMMON /INT/ IU,IL,IS,ILAN,ISEP,NU,NL,NP1,NM1,N2,NU1,NL1,IJ,IK
      COMMON /GEOM/ XE(66),XM(66),XC(66),ZUB(51),ZLB(51),ZA(66),ZB(66),
     1       ZEU(66),ZEL(66),ZZ(66),ZU(51),ZL(51)
      COMMON /PAN/ WUB(50),WLB(50),WCB(50),WU(66),WL(66),BETA,ALFB
      COMMON /BLR/ HU(50),HL(50),THETAU(50),THETAL(50),DELSU(50),
     1       DELSL(50),SEPX,HSEP,CPINV(50),NJ
      DIMENSION AA(30,30), BB(30,30), CC(30,30), BC(30), TL(30), X(30),
     1          Y(30)
C
      NN=NL
      NS=NL-9
      M=2
      L=1
C
      DO 5 I=NS,NN
      X(I)=XC(I)-XC(NS)
    5 Y(I)=WL(I)-WL(NS)
C
      DO 10 I=NS,NN
   10 CC(I,1)=X(I)
C
      DO 15 J=2,M
      DO 15 I=NS,NN
   15 CC(I,J)=CC(I,J-1)*X(I)
C
      DO 20 J=1,M
      DO 20 I=1,M
      AA(I,J)=0.0
      DO 20 K=NS,NN
   20 AA(I,J)=AA(I,J)+CC(K,I)*CC(K,J)
C
      DO 25 J=1,L
      DO 25 I=1,M
      BB(I,J)=0.0
      DO 25 K=NS,NN
   25 BB(I,J)=BB(I,J)+CC(K,I)*Y(K)
C
C     SOLVE FOR SLOPE COEFFICIENTS
C
      CALL SIMEQ (AA,BB,BC,M,30)
C
      DO 35 J=NS,NN
      TL(1)=X(J)
      SUM=BC(1)*TL(1)
C
      DO 30 I=2,M
      TL(I)=TL(I-1)*X(J)
      SUMT=BC(I)*TL(I)
   30 SUM=SUM+SUMT
   35 Y(J)=SUM
C
      DO 40 I=NS,NN
   40 WL(I)=Y(I)+WL(NS)
C
      RETURN
      END
```

```
      SUBROUTINE AFSL
C
C     CALCULATE THE SLOPE OF THE AIRFOIL FROM ITS ORDINATES
C
      COMMON /READ/ ATITLE(20),N,NA,NT,XMI,UNIT,R,XTE,XO,XF,XCPT,WTEL,
     1       XA(51),ZT(51),ZC(51),EL(66),ALFA,WUEND
      COMMON /INT/ IU,IL,IS,ILAM,ISEP,NU,NL,NP1,NM1,N2,NU1,NL1,IJ,IK
      COMMON /GEOM/ XE(66),XM(66),XC(66),ZUB(51),ZLB(51),ZA(66),ZB(66),
     1       ZEU(66),ZEL(66),ZZ(66),ZU(51),ZL(51)
      COMMON /PAN/ WUB(50),WLB(50),WCB(50),WU(66),WL(66),BETA,ALFB
      COMMON /PAN2/ CPU(66),CPL(66),UU(66),UL(66),ITERN
      COMMON /BLR/ HU(50),HL(50),THETAU(50),THETAL(50),DELSU(50),
     1       DELSL(50),SEPX,HSEP,CPINV(50),NJ
      DIMENSION DZDX(50)
C
      ALPHR=ALFA*3.14159/180.
      DO 5 J=1,NU
    5 ZZ(J)=ZEU(J)
C
      K=1
      MUCH=NU-2
      I=0
   10 I=I+1
      IF (I.GT.MUCH) GO TO 15
C
      TERM1=(ZZ(I+1)-ZZ(I))/(XC(I+1)-XC(I))
      TERM2=(ZZ(I+2)-ZZ(I+1))/(XC(I+2)-XC(I+1))
      C=(TERM2-TERM1)/(XC(I+2)-XC(I))
      B=TERM1-C*(XC(I)+XC(I+1))
      A=ZZ(I)-B*XC(I)-C*XC(I)*XC(I)
C
   15 ZI=A+B*XC(I)+C*XC(I)*XC(I)
      DZDX(I)=B+2.*C*XC(I)
      IF (K.NE.1) GO TO 20
      IF (I.GE.NU) GO TO 25
      GO TO 10
   20 IF (I.GE.NL) GO TO 40
      GO TO 10
   25 IF (K.EQ.2) GO TO 40
C
      DO 30 I=2,NU
   30 WU(I)=DZDX(I)
C
      K=K+1
      DO 35 J=NJ,NL
   35 ZZ(J)=ZEL(J)
C
      MUCH=NL-2
      I=NJ-1
      GO TO 10
C
   40 DO 45 I=NJ,NL
   45 WL(I)=DZDX(I)
C
      RETURN
      END
```

```
      SUBROUTINE PARINB (X,Y,I1,I2,XO,XIN,YOUT,DYOUT,YIOUT,IXXX)
C
C     THIS SUBROUTINE INTERPOLATES BETWEEN POINTS BY PASSING A PARABOLA
C     THROUGH THREE ADJACENT POINTS WITH THE DESIRED POINT IN THE SECON
C     INTERVAL OR COINCIDING WITH THE MIDPOINT.  INTEGRATION OCCURS OVE
C     THE INTERVAL BETWEEN XO AND XIN.  BOTH XO AND XIN MUST LIE WITHIN
C     THE TABLE VALUES X(I1) AND X(I2).
C
      DIMENSION X(1), Y(1)
C
      I=IXXX
      YOUT=0.0
      DYOUT=0.0
      YIOUT=0.0
      IF (I1.EQ.I2) GO TO 45
      IF (I2-I1.EQ.1) GO TO 50
      IF (X(I1).GT.X(I1+1)) GO TO 10
      IF (X(I)-XIN) 5,20,20
    5 CONTINUE
      GO TO 20
C
   10 DO 15 I=I1,I2
      IF (X(I)-XIN) 20,20,15
   15 CONTINUE
C
   20 I=I
      IF (XIN.NE.X(I)) I=I-1
      IF (I.LE.I1) I=I1+1
      IF (I.GE.I2) I=I2-1
      IF (Y(I+1).EQ.Y(I).OR.Y(I).EQ.Y(I-1)) GO TO 55
      IF (Y(I+1).EQ.Y(I-1)) GO TO 55
C
      A=(X(I+1)-X(I))/(Y(I+1)-Y(I))-(X(I)-X(I-1))/(Y(I)-Y(I-1))
      A=A/(Y(I+1)-Y(I-1))
      B=(X(I)-X(I-1))/(Y(I)-Y(I-1))-A*(Y(I)+Y(I-1))
      C=X(I)-B*Y(I)-A*Y(I)*Y(I)
      IF (A.EQ.0.0) GO TO 55
C
      D=-B/(2.0*A)
      IF (B.EQ.0.0) GO TO 25
      E=4.0*A/(B*B)
      F=1.0-E*(C-XIN)
      G=1.0-E*(C-XO)
      IF (G.LT.0.0.OR.F.LT.0.0) GO TO 55
C
      Y1=D*(1.0-SQRT(F))
      Y2=D*(1.0+SQRT(F))
      IF (Y(I).LT.Y(I-1)) GO TO 40
      IF (Y1.GE.Y(I-1).AND.Y1.LE.Y(I+1)) GO TO 30
      IF (Y2.GE.Y(I-1).AND.Y2.LE.Y(I+1)) GO TO 35
      GO TO 55
C
   25 D=2.0/(3.0*A)
      E=XIN-C
      F=XO-C
      IF (E.LT.0.0.OR.F.LT.0.0) GO TO 55
```

```
      YOUT=SQRT(E/A)
      DYOUT=1.0/(2.0*A*YOUT)
      YIOUT=D*(SQRT(E*E*E)-SQRT(F*F*F))
      GO TO 60
C
   30 YOUT=Y1
      DYOUT=1.0/(2.0*A*Y1+B)
      YIOUT=D*(XIN-X0-2.0*(SQRT(F*F*F)-SQRT(G*G*G))/(3.0*E))
      GO TO 60
C
   35 YOUT=Y2
      DYOUT=1.0/(2.0*A*Y2+B)
      YIOUT=D*(XIN-X0+2.0*(SQRT(F*F*F)-SQRT(G*G*G))/(3.0*E))
      GO TO 60
C
   40 IF (Y1.LE.Y(I-1).AND.Y1.GE.Y(I+1)) GO TO 30
      IF (Y2.LE.Y(I-1).AND.Y2.GE.Y(I+1)) GO TO 35
      GO TO 55
C
   45 DYOUT=0.0
      YOUT=Y(I1)
      YIOUT=Y(I1)*(XIN-X0)
      GO TO 60
C
   50 DYOUT=(Y(I2)-Y(I1))/(X(I2)-X(I1))
      YOUT=Y(I1)+DYOUT*(XIN-X(I1))
      Y0=Y(I1)+DYOUT*(X0-X(I1))
      YIOUT=0.5*(Y0+YOUT)*(XIN-X0)
      GO TO 60
C
   55 CALL PARINT (X,Y,I1,I2,XC,XIN,YOUT,DYOUT,YIOUT)
   60 RETURN
C
      END
```

```
      SUBROUTINE PARINT (X,Y,I1,I2,XO,XIN,YOUT,DYOUT,YIOUT)
C
C     THIS SUBROUTINE INTERPOLATES BETWEEN POINTS BY PASSING A PARABOLA
C     THROUGH THREE ADJACENT POINTS WITH THE DESIRED POINT IN THE SECON
C     INTERVAL OR COINCIDING WITH THE MIDPOINT.  INTEGRATION OCCURS IN
C     THE INTERVAL BETWEEN XO AND XIN.
C
      DIMENSION X(1), Y(1)
C
      IF (I1.EQ.I2) GO TO 55
      IF (I2-I1.EQ.1) GO TO 50
      IF (X(I1).GT.X(I1+1)) GO TO 10
C
      DO 5 I=I1,I2
      IF (X(I)-XIN) 5,20,25
    5 CONTINUE
      GO TO 60
C
   10 DO 15 I=I1,I2
      IF (X(I)-XIN) 25,20,15
   15 CONTINUE
      GO TO 60
C
   20 I=I
      IF (I.EQ.I2) GO TO 25
      GO TO 30
C
   25 I=I-1
   30 IF (I-I1) 50,35,40
   35 A=(Y(I+2)-Y(I+1))/((X(I+2)-X(I+1))*(X(I+2)-X(I)))-(Y(I+1)-Y(I))
     1     /((X(I+1)-X(I))*(X(I+2)-X(I)))
      GO TO 45
C
   40 A=(Y(I+1)-Y(I))/((X(I+1)-X(I))*(X(I+1)-X(I-1)))-(Y(I)-Y(I-1))
     1     /((X(I)-X(I-1))*(X(I+1)-X(I-1)))
   45 B=(Y(I+1)-Y(I))/(X(I+1)-X(I))-A*(X(I+1)+X(I))
      C=Y(I)-A*X(I)*X(I)-B*X(I)
C
      YOUT=A*XIN*XIN+B*XIN+C
      DYOUT=2.0*A*XIN+B
      YIOUT=(XIN**3-XO**3)*A/3.0+(XIN**2-XO**2)*B/2.0+C*(XIN-XO)
      GO TO 65
C
   50 DYOUT=(Y(I1+1)-Y(I1))/(X(I1+1)-X(I1))
      YOUT=Y(I1)+DYOUT*(XIN-X(I1))
      YO=Y(I1)+DYOUT*(XO-X(I1))
      YIOUT=(YOUT+YO)*(XIN-XO)/2.0
      GO TO 65
C
   55 DYOUT=0.0
      YOUT=Y(I1)
      YIOUT=Y(I1)*(XIN-XO)
      GO TO 65
C
   60 DYOUT=(Y(I2)-Y(I2-1))/(X(I2)-X(I2-1))
      YOUT=Y(I2)+DYOUT*(XIN-X(I2))
      YO=Y(I2)+DYOUT*(XO-X(I2))
      YIOUT=(YOUT+YO)*(XIN-XO)/2.0
C
   65 RETURN
      END
```

```
      SUBROUTINE SIMEQ (A,Y,X,N,NMAX)
C
C     THIS IS THE STANDARD IBM ROUTINE TO SOLVE SIMULTANEOUS EQUATIONS
C
      DIMENSION A(NMAX,1), Y(1), X(1)
C
      M=N-1
      DO 15 I=1,M
      AII=A(I,I)
      L=I+1
      DO 15 J=L,N
      AJI=A(J,I)
      IF (AJI) 5,15,5
    5 DO 10 K=L,N
   10 A(J,K)=A(J,K)-A(I,K)*AJI/AII
      Y(J)=Y(J)-Y(I)*AJI/AII
   15 CONTINUE
C
      X(N)=Y(N)/A(N,N)
      DO 25 I=1,M
      K=N-I
      L=K+1
      DO 20 J=L,N
   20 Y(K)=Y(K)-X(J)*A(K,J)
   25 X(K)=Y(K)/A(K,K)
      RETURN
      END
```